TMJ
MT
X-39(N)

NS/mk

U. S. NAVAL TECHNICAL MISSION TO JAPAN
CARE OF FLEET POST OFFICE
SAN FRANCISCO, CALIFORNIA

21 February 1946

RESTRICTED

From: Chief, Naval Technical Mission to Japan.
To : Chief of Naval Operations.

Subject: Target Report - Miscellaneous Reports of Various Japanese Naval Research Activities.

Reference: (a)"Intelligence Targets Japan" (DNI) of 4 Sept. 1945.

1. Subject report, covering Target X-39(N) of Fascicle X-1 of reference (a), is submitted herewith.

2. The report was compiled by Comdr. M. C. Mains, USN, Ret.

C. G. GRIMES
Captain, USN

31765

RESTRICTED

X-39(N)

# MISCELLANEOUS REPORTS OF VARIOUS JAPANESE NAVAL RESEARCH ACTIVITIES

"INTELLIGENCE TARGETS JAPAN" (DNI) OF 4 SEPT. 1945

FASCICLE X-1, TARGET X-39(N)

FEBRUARY 1946

U.S. NAVAL TECHNICAL MISSION TO JAPAN

# SUMMARY

MISCELLANEOUS TARGETS

MISCELLANEOUS REPORTS OF VARIOUS
JAPANESE NAVAL RESEARCH ACTIVITIES

Many reports on the research projects underway in Japan at the time of the surrender have been submitted by various Japanese research activities. The reports contained herein constitute those which were either received too late to include in the target reports to which they logically pertain or were not pertinent to any specific target.

To obtain these reports, a list of all research programs underway when the Japanese surrendered was ordered to be submitted to the Occupation Forces, and from the list were chosen those subjects upon which full reports were desired. The Japanese government was ordered to arrange for their preparation. To do this they created the Central Laboratory of the Home Ministry located at Meguro Ku, TOKYO, which laboratory replaced specifically the First and Second Naval Technical Institutes but in practice represented all naval research organizations in Japan and acted as a clearing house for the majority of the reports obtained. The Central Laboratory assembled the key technicians that had been participating in those programs on which reports were desired and produced the reports which are presented here.

# TABLE OF CONTENTS



# LIST OF ENCLOSURES

REPORTS OF THE CENTRAL LABORATORY OF THE HOME MINISTRY



REPORTS OF THE FIRST NAVAL TECHNICAL INSTITUTE



REPORTS OF EXPERIMENTAL DEPARTMENTS OF NAVY YARDS AND ARSENALS

# LIST OF ILLUSTRATIONS

# ENCLOSURE (A) 1

## RESEARCH ON HEAT-PROOF STEEL FOR TURBINE ROCKETS

By Lt. Comdr. (Eng.) Y. YASUDA

### I. INTRODUCTION

In turbine rockets, the higher the fuel combustion temperature and the rotating velocity of the turbine the better its efficiency. So, to increase the efficiency of the rocket, the material of the turbine must endure great stress at high temperature, that is, the creep limit of the steel used has to be very high. Although the current high Mn, high Cr and V steel has a creep limit of 20 kg/mm$^2$ at 600°C, we have attempted to get the same strength at 650°C. (Figure 1(A)1 shows the rotor of a rocket turbine and Figure 2(A)1 a turbine blade.)

### II. NATURE OF THE STEEL USED

When we began the study, the steel used for the material of the turbine (both rotor and blades) was high Mn, high Cr and V steel (so-called A-309 by the Japanese Aeroengineering Standard) whose percentage composition is as follows:

| | |
|---|---|
| C | 0.20-0.25 |
| Si | 0.8 -1.2 |
| Mn | 15 -17 |
| Cr | 10 -12 |
| V | 0.6 -1.0 |

This steel is melted by a basic high frequency induction furnace, forged at 1050-1150°C, quenched in water from 1100-1200° C and tempered for three hours at 750-850° C. Steel thus manufactured generally satisfies the following standards of strength at ordinary temperatures:

| | |
|---|---|
| Tensile strength | >85 kg/mm$^2$ |
| Elongation | >30% |
| Contraction | >40% |
| Impact value | >6 kg-m |
| BHN | 238-321 |

The creep limit of this steel measured by the short time method at the First Naval Technical Institute is:

| | |
|---|---|
| 23 kg/mm$^2$ | at 550°C |
| 18 kg/mm$^2$ | at 600 |
| 14 kg/mm$^2$ | at 650 |
| 11 kg/mm$^2$ | at 700 |

It is also found that the creep limits are very regularly proportional to BHN at ordinary temperature, so hardness testing is very important to insure mechanical strength at high temperatures.

The fatigue limit tested by the rotary-bending method (Ono type machine) is 36 kg/mm$^2$ at room temperature, 25 kg/mm$^2$ at 600°C and the one measured by the tension-compression method (Haigh type machine) is 15 kg/mm$^2$ at 600°C under a mean stress of 15 kg/mm$^2$. The weldability of this steel is a serious problem, because the welded part between the rotor and the blades sometimes cracks while rotating from internal stress. For this reason the carbon content is

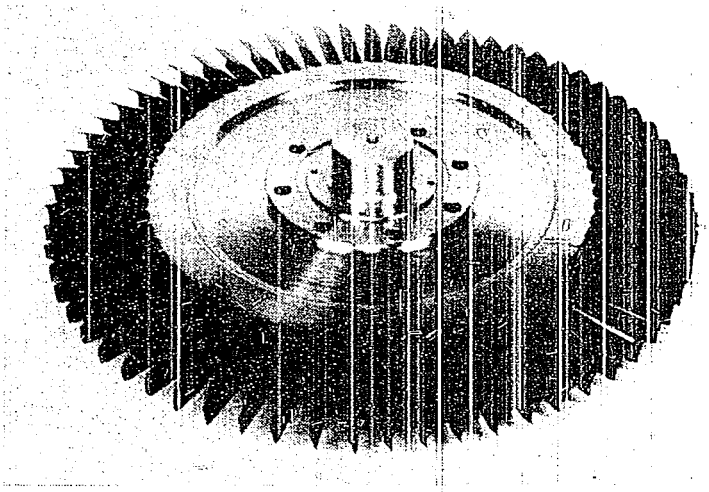

*Figure 1(A)1*
*ROCKET TURBINE ROTOR*

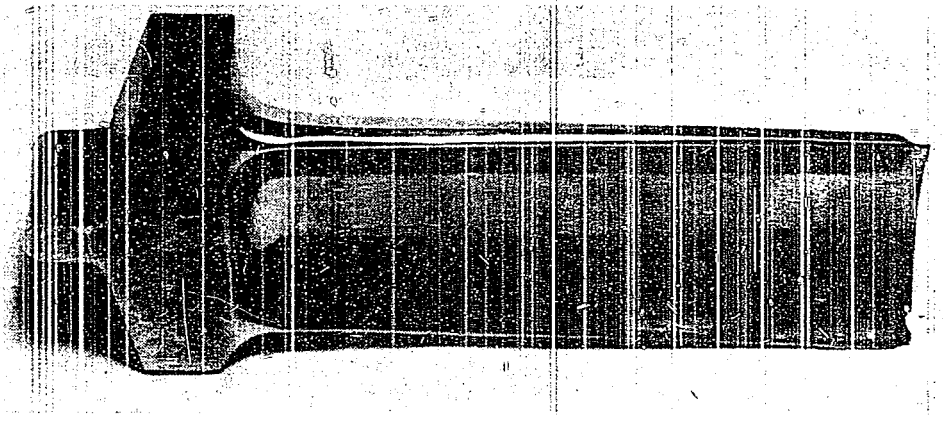

*Figure 2(A)1*
*BLADE OF ROCKET TURBINE ROTOR*

this steel is strictly limited to 0.25% and a lower limit of 0.20% is necessary to insure strength.

III. RESEARCH PLANS

To improve the qualities of this steel, various methods were considered, viz- the addition of about 10-20% Ni, which is believed to be useful to strengthen austenite, or, increase of C content in A-309. But the latter cannot be used because the weldability is greatly decreased and the former is impossible in view of the scarcity of nickel in Japan. So we have selected another method: as a substitute for C we add nitrogen, a part of which dissolves in austenite and strengthens it and the other part of which is thought to form nitrides with V or Cr and to facilitate the so-called precipitation hardening. At that time we heard that our ideas were adopted in Germany to improve the materials for turbine rockets and this news encouraged us to continue our plan.

IV. MELTING AND ADDITION OF NITROGEN

From various fundamental researches about the stability of austenite we determined the percentage composition of the new steel as follows:

| | | | |
|---|---|---|---|
| C ..... | 0.10-0.20 | Cr ..... | 10-12 |
| Si ..... | 0.8 -1.2 | V ..... | 0.6-1.0 |
| Mn ..... | 13-15 | N ..... | 0.10-0.20 |

It was melted in a basic induction furnace and cast in 50 kg ingots. For nitrogen we used nitrised manganese, which was made by nitrising the powder (40-100 mesh) of electrolytic manganese in ammonia gas at 600° C for two hours using a specially made nitrising box. The nitrised manganese contains 10-20% of N and is added to the molten steel just before tapping. The yield of nitrogen is about 50%. The nitrising of manganese has been greatly simplified by subsequent research, namely, the process is continued only long enough to heat in air for two hours at 700-900° C the manganese powder scattered in 10-15mm thickness. Oxygen in the air is caught by the surface of the layer but only nitrogen penetrates into the layer and combines with the manganese. The manganese made by this method contains only 3-5% N, but the yield is better than by the former method. Another method for the addition of nitrogen, for example, nitrising of ferro-chromium, was not adopted because it was impracticable.

V. HEAT TREATMENT

The ingot thus manufactured is forged to billets of 50mm square section and rolled to bars of 25mm diameter. Turbine forging practices have been studied at the Material Department of the First Naval Technical Institute. We studied heat treatment with small pieces of this steel. The mechanical strength of steel of this kind is believed to depend chiefly on precipitation hardening. It is, therefore, of prime importance that the constituents to be precipitated be dissolved in austenite. We plotted the relation between the hardness and quenching temperature (Figure 3(A)1) and determined that to obtain a perfect solid solution, heating at 1150° C for 15 minutes is sufficient. This supersaturated solid solution softens to about 210-230 BHN, but, by tempering, hardness, accompanied by precipitation is recovered. The increase in hardness varies with tempering temperature and time. Figure 4(A)1 shows this variation of hardness. From these curves it is obvious that the highest hardness is attained by tempering for three hours at 700-800° C. Thus the most suitable conditions for heat treatment of the new steel are determined as follows:

Quenching : from 1100-1200° C (for 15 min.) into water
Tempering : at 700-800° C for 3 hours.

*ENCLOSURE (A)1, continued*

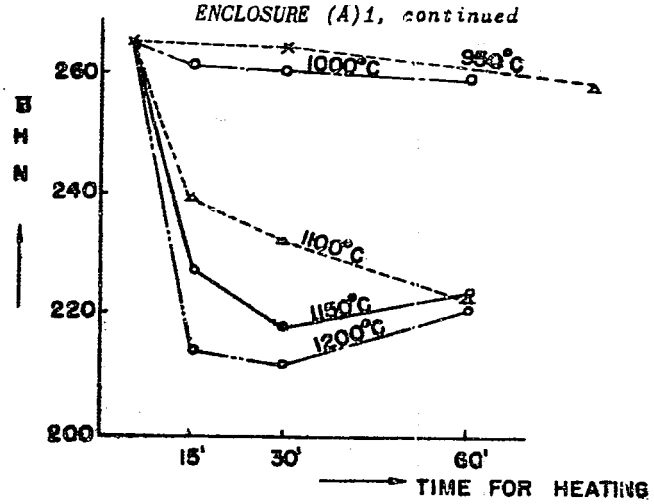


*Figure 3(A)1*
*PRECIPITATION HARDENING CURVES*
*FOR Mn, Cr, V, AND N STEEL (HEATING)*

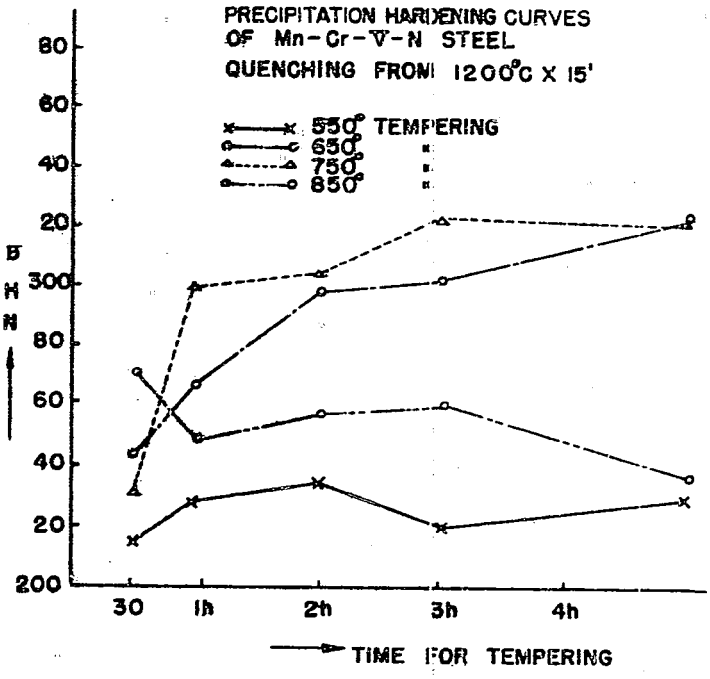


*Figure 4(A)1*
*PRECIPITATION HARDENING CURVES*
*FOR Mn, Cr, V, AND N STEEL (TEMPERING)*

Quenching from such a high temperature is practically very difficult for material the size of a turbine rotor (about 700mm in dia. and 100mm in thickness). Subsequent research showed that quenching was not necessary, and tempering immediately after forging is sufficient to obtain the required strength. The loss of hardness caused by elimination of quenching is very small. (This method is applicable to A-309 containing no nitrogen.)

The mechanical properties of the new steel are:

| | |
|---|---|
| Tensile strength ..... | 105 kg/mm (>95) |
| Elongation ..... | 17% (>20) |
| Contraction ..... | 20% (>20) |
| Impact value ..... | 3.6 kg/m (>3) |
| BHN ..... | 334 (270-350) |

The numerals in parentheses show our temporary standards for the new steel.

The creep limit of this steel, measured at First Naval Technical Institute, is 22-24 $kg/mm^2$ at 650° C.

Thus we have attained our first purpose, to make steel whose creep limit is over 20 $kg/mm^2$ at 650°C. But manufacturing turbines with this steel has not been executed up to the present time, so the machinability, the weldability and other properties have not yet been examined. (Machinability was partly tested when we prepared tension test pieces; in this test the new steel machined as well as A-309 or Ni-Cr steel.)

## VI. ANALYSIS OF NITROGEN IN STEEL

The quantity of nitrogen in this steel is determined by the combustion method. The sample is drilled and washed and, after weighing, is burned together with metallic tin in a porcelain boat under $CO_2$ gas. This is absorbed by a KOH solution leaving nitrogen gas. (Same as Dumas' method in organic chemistry.) The distillation method (for measuring nitrogen as $NH_3$) is not suitable for this steel, because the insoluble residue is apt to be the cause of error. We established our method as the standard analysis of nitrogen in this steel.

# ENCLOSURE (A) 2

## RESEARCH ON THUNDER-CLOUD DETECTORS (Atmospheric Recorder)

By YOSHINARI

### A. Purpose

By means of this apparatus, the position of thunder and atmospheric electricity is found and recorded as a function of time. By this process, the positions and transitions of discontinuity lines, typhoons, snow, hail, thunder, etc. are measured in order to assist meteorological observations.

### B. Operation

The apparatus consists of a frame-aerial, receiver and recorder. The frame-aerial consists of two simple frame-antennas which are arranged 90° to each other. The recorder is fixed under this frame-aerial and recording paper is arranged on the main rotating shaft of the frame-aerial. Atmospheric electricity with respect to its direction and time is recorded on the recording paper. The receiver first amplifies the atmospheric electricity induced in the frame-aerial and supplies it to the recorder after rectifying. The receiver consists of two individual receivers and the input side of each receiver is connected to one of the crossed frame antennae. The output side of each receiver is connected to the recorder and, by utilizing the combination of the figure of eight as well as the cardioid characteristics of the antennae, sharp directivity is obtained. For rotating the frame-aerial, a clock-work and weight wind-up device is provided. The aerial can also be rotated by hand, if necessary. Some technical data follow:

1. Speed of rotation of the frame-aerial: One rotation in 12 minutes.
2. Minimum field strength which can be measured: 2 millivolts/meter.
3. Amplification of the receiver: 120 db.
4. Directivity: 5-30°.
5. Time for continuous recording: 25 hours.

### C. Progress of Trial Manufacturing

Engineers of the Navy Technical Research Institute, Imperial Nagoya University, Technical Research Institute of Broadcast Association, and Nihon Musen Co. were assembled at the beginning of June 1943 in the Navy Technical Research Institute and a plan for the trial manufacturing of the apparatus for observing thunder clouds was determined. For the first trial, two sets were to be manufactured in Nihon Musen Co. in three months between July and September. They were actually completed at the beginning of October.

These trial sets were tested during October, November and December in 01 Air Fleet of the Navy, Yokosuka Naval Navigation School, as well as in the Navy Technical Research Institute and it was proved that they were suitable for actual use. Improvements on these first sets was investigated in January and February of 1944 and it was decided to start a second trial manufacturing. Between February and March the design of the equipment and the preparation for manufacturing were finished and during March the manu-

*ENCLOSURE (A)2, continued*

facture of a total of 25 sets started. From June to October, five sets were manufactured per month. Operators for these equipments were trained in August and September. Experiments for investigating the characteristics of the second trial sets and for preventing errors in direction-finding due to outside disturbances were made by the engineers of Imperial Nagoya University, Kowa Air Fleet of the Navy, and Sakawa Metecrological School between December 1944 and January 1945. It was intended to start with the third trial manufacturing, but this scheme was not realized up to the end of the war.

# ENCLOSURE (A) 3

## COPPER COLUMNS FOR PRESSURE MEASUREMENT

By T. OYAMA

### I. INTRODUCTION

Hitherto all copper columns for pressure measurement in guns and machine guns used in Japan were manufactured only at Osaka Army Arsenal. Then we were instructed to make studies for manufacturing them at our arsenal or at the civilian foundries. The foundries we used were Hitachi Electric Wire Co. and Sumitomo Electric Wire Co.

We melted, rolled, drew, machined, and annealed the proof-making copper columns in our foundry. We also machined and annealed columns from ordinary electric copper wire which was manufactured by the two foundries named above.

The kinds of columns which were proof-made were as follows: 10mm diameter, 15mm length; 8mm diameter, 13mm length; and 4mm diameter, 7mm length.

Several proof-made columns were tested and then all columns were brought into the Second Navy Gun Powder Arsenal at HIRATSUKA and given tests for practical use. The result was quite satisfactory and we knew that the columns which were manufactured by our process were suitable for practical use.

### II. EXPERIMENTAL DATA

#### A. Manufacturing Process

1. At the Army Arsenal: The method of melting and dimensions of the ingot are shown in Figure 1(A)3.

After blowing for about 20 minutes, the molten copper is carried into the ladle, the upper case is removed, the molten metal covered with the charcoal, and, after a little while poured very slowly into the ingot case. Casting temperature is approximately 1150°C. The ingot is quartered as shown in Figure 1(A)3 and each block rolled and drawn. During the rolling and drawing the material is annealed frequently and then machined carefully.

2. Process at Our Foundry: Fifty kilograms of electrolytic copper were charged with charcoal into two graphite crucibles and melted in a natural draft type coke furnace. As soon as the melting began the charcoal carried up and covered the surface of the molten metal. Thus we were able to keep the metal surface free from the atmosphere After the two charges melted down we poured them into the ingot case which has the same dimensions as the one shown in Figure 1(A)3.

The most satisfactory melting temperature and casting temperature were 1450-1470°C and 1170-1200°C, respectively. The ingot was quartered and each block was machined to remove the surface shortage. The blocks were forged at 920°C to 34mm, hot rolled to 14mm and then cold drawn to 11mm (for 10mm column), 9.2mm (for 8mm column) and 5.8mm (for 4mm column).

Of course, during these treatments machining for removing cracks, annealing and pickling took place several times. The annealing temperature was 600°C (1 hr.) and pickling reagent was a 5% $H_2SO_4$ solu-

tion.

After machining, the columns which were within the required range (± 0.015mm for diameter and length) were selected. The final annealing took place at 580° C (2 hrs.) in a vacuum furnace.

3. Process at Hitachi Co. and Sumitomo Co: The process of Hitachi Co. and Sumitomo is the same as the ordinary mass production methods for high conductivity electric wire.

Fifty tons of electrolytic copper were melted in a reflecting gas furnace and poured into an ingot case (length 1300mm, height 95mm, upper width 95mm and lower width 70mm). The weight of an ingot is about 90 kgs. After hot rolling at 900-950° C, they were cold drawn to 12, 10, 6mm (for 10, 8, and 4mm columns) and carried to our foundry. The treatment after that was the same as the above description.

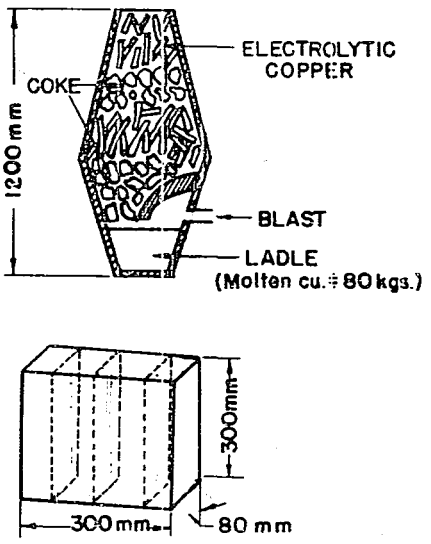


*Figure 1(A)3*
*PRESSURE TEST COLUMNS-MELTING METHOD AND INGOT DIMENSIONS*

B. Tests

1. Chemical Analysis: The result of chemical analysis is shown in Table I(A)3.

Table I(A)3
CHEMICAL COMPOSITION OF COPPER USED FOR CRUSHER GAUGES

| Foundry | | Composition (%) | | | | | |
|---|---|---|---|---|---|---|---|
| | Cu | Fe | Si | S | As | Sb | Pb |
| Our Foundry | 99.980 | 0.0029 | 0.0029 | 0.010 | --- | --- | --- |
| Hitachi Co. | 99.974 | 0.0210 | 0.0070 | --- | --- | --- | --- |
| Sumitomo Co. | 99.950 | 0.0036 | 0.0011 | 0.0053 | 0.0015 | 0.0038 | 0.0015 |

2. Hardness Test: The result of Vickers hardness tests is shown in Table II(A)3.

*ENCLOSURE (A)3, continued*

Table II(A)3
HARDNESS OF COPPER USED FOR CRUSHER GAUGES

| Column dia./length (mm) | Vickers Hardness | | | |
|---|---|---|---|---|
| | Army | Our Foundry | Hitachi | Sumitomo |
| 10/15 | 40.0 | 39.6 | 42.6 | 44.2 |
| 8/13 | 39.2 | 39.3 | 42.5 | 42.3 |
| 4/7 | 38.6 | 39.0 | 43.4 | 45.7 |

3. Compression Test by Amsler Universal Testing Machine:

(Note: Seven figures and 29 tables covering this subject have been forwarded to Washington Document Center, as NavTechJap Document No. ND50-5500.)

C. Practical Experiment

On the basis of these tests, we thought the proof-made columns suitable for practical use. Then all manufacture was shifted to the Second Navy Gun Powder Arsenal at Hiratsuka and the practical experiments were carried out. Two kinds of test were made at the Arsenal, namely, compression by mercury manometer and bomb erosion.

The results of test on columns which were made by our foundry are shown in ... (tables sent to Washington Document Center as explained above).

We also studied the manufacturing of copper columns by the Army's method and the results were as good as in the case described above.

III. CONCLUSION

We studied methods of manufacturing copper columns for pressure measurements in guns and machine guns, and we found that columns which were manufactured in our foundry were about as good as the columns which were made in the Army arsenal.

Columns manufactured from material for ordinary mass-production high electric conductivity wire were also suitable for practical use.

# ENCLOSURE (A) 4

## STUDY OF ZIRCONIUM STEELS

By T. OYAMA

### I. INTRODUCTION

Hitherto it has been said that zirconium is a useful element as a scavenger and as an alloying element for steels.

To ascertain its effect on the mechanical properties of special steels and to obtain superior materials for ordnance equipment, we added a few kinds of ferro-zirconiums to molten steels.

Over one hundred ingots were cast, forged, heat-treated and tested. The results were not satisfactory as the mechanical properties of the steels to which zirconium was added were the same as the ones to which none was added.

### II. EXPERIMENTAL DATA

#### A. Ferro-Zirconium

The Fe-Zr used chiefly in our experiments is manufactured by the Research Department of Mitsubishi Mining Industry and has approximately the following composition: 10-12% Zr, 20-30% Si and 70-58% Fe.

We also used silico-zirconium (50% Si, 50% Zr) and found that this alloy was easier to melt than Fe-Zr.

#### B. Adding Process

One hundred kgs of steels were melted in the high frequency electric induction furnance and poured continuously into three ladles. Fe-Zr was not added in the first ladle; we added a small percentage of it to the second ladle and more of it to the third ladle.

Thus we had steels which contained varying amounts of Zr. The percentage of Zr used in this experiment was 0-0.9%.

#### C. Preparation of Specimens

The kinds of steel experimented upon were as follows:

C steels (0.1-0.5% C),
Ni steels (3-5% Ni)
Ni-Cr or Ni-Cr-Mo steels (special ordnance steels)
Mn-Cr-Mo steels

Specimens for gas analysis ($O_2$, $H_2$, $N_2$) were extracted from each 33 kg ingot. The remainder of the ingot was forged, heat-treated, machined and given mechanical tests (tension, impact and hardness).

#### D. Results of Tests

According to the gas analysis the steel which included Zr showed no different result compared to the other steels. Similarly we could not establish any variation in mechanical properties between the two cases.

We lost the details of this test by the fire. We can not describe it in more detail.

*ENCLOSURE (A)4 Continued*

III. CONCLUSION

We studied several zirconium steels, and found in this experiment that zirconium adds no desirable properties to steels.

# ENCLOSURE (A) 5

## STUDIES ON THE MECHANISM OF CAVITATION EROSION

By T. NAGAKURA

### A. Purpose

The purpose of these experiments was to find a method to prevent cavitation erosion which appears in centrifugal or axial pumps, and propellers of battleships.

### B. Experimental Methods

We have studied these problems with two methods as follows:

1. Vibration method: We used a strong ultrasonic-wave generator of about 10,000 cycles. The vibration bar was a nickel tube about 20cm long and 1.5cm in diameter and the test piece was attached to one end of this tube. (See Figures 1(A)5 and 2(A)5). Input power was 500 watts.

   If we close the electric circuit of the apparatus, extreme cavitation phenomena take place in front of the test piece and after about one or two hours quite extreme erosion appears in the test piece.

2. Water hammer method: The apparatus is shown in Figure 3(A)5. To the lower part of the cone-shaped cylinder "a", the piston "b" is attached. The piston is moved up and down by lever "c". The test piece "d" is placed on the top of the cylinder and the cylinder is filled with water when the piston is at the upper position. By up and down motion of the the piston, pressure is applied to the test piece. Figure 4(A)5 is a record of the pressure thus applied to a test piece.

### C. Results and Discussion

1. Vibration method: We studied test pieces made from brass, iron, aluminum, etc. In one or two hours we could observe quite extreme erosion. The surface was fresh and bright so that we could not observe that any chemical reaction had taken place.

2. Water hammer method: We adjusted the spring (e) so that the static pressure at the test piece was about 100 $kg/cm^2$ and ran the apparatus for few hours. We obtained erosion as shown in Figure 5(A)5.

   As we wanted to study what type of erosion may take place by mechanical action, we used aluminum test pieces of various shapes. The relation between the type of erosion and the shape of the test piece is shown in Figure 6(A)5 and we can conclude as follows:

   a. The bottom of the concave part is extremely affected.

   b. The inner edges are as badly affected as in (a).

   c. The hole and wedge-shaped clearance are eroded more and more deeply, and, as the result of the combination of these phenomena even on the flat surface, once erosion starts, it may develop by mechanical action and growth to sponge-like erosion.

### D. Conclusions

From the above experimental data we can conclude that:

*ENCLOSURE (A)5 Continued*

1. The process of erosion induced by cavitation is not a chemical reaction, but a mechanical destructive process due to impact pressure induced by the collapse of cavities in the water.

2. If once pin-holes or shallow holes are formed, the center or corner part of them may be bored more and more deeply and sponge-like erosion may be formed.

From these points of view the methods of preventing erosion by cavitation are to use dynamically strong materials and to shape moving parts of pumps so as to make them as little liable to cavitation as possible.

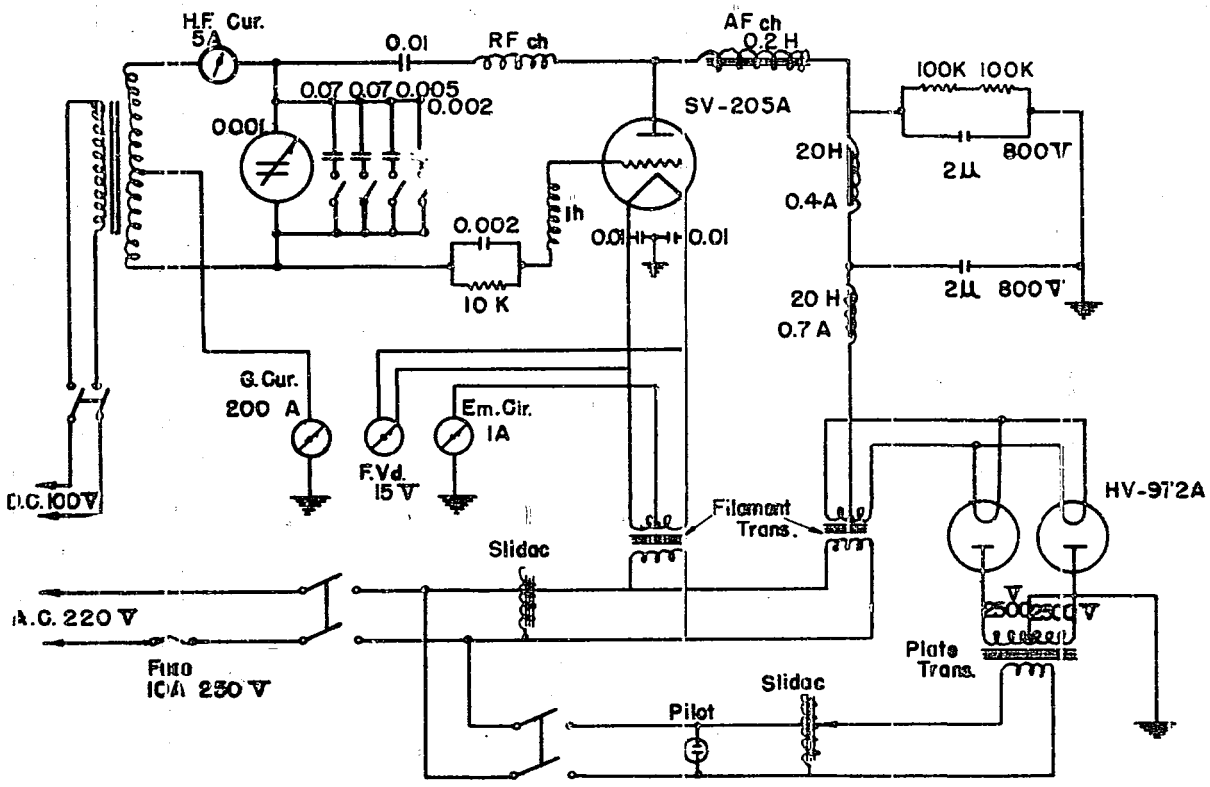


*Figure 1(A)5*
*CIRCUIT OF THE ULTRASONIC WAVE GENERATOR*

*ENCLOSURE (A)5 Continued*

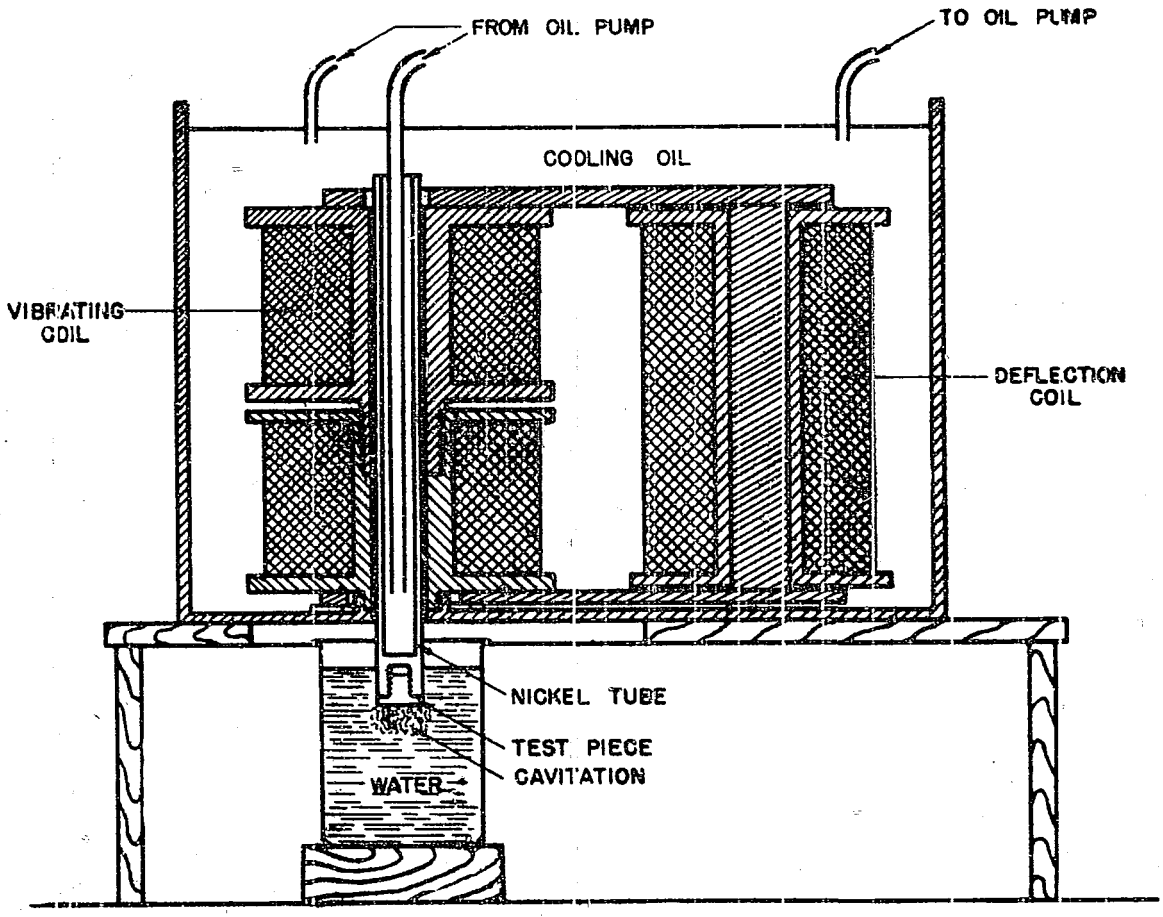


*Figure 2(A)5*
*ULTRASONIC VIBRATOR*

*ENCLOSURE (A)5 Continued*

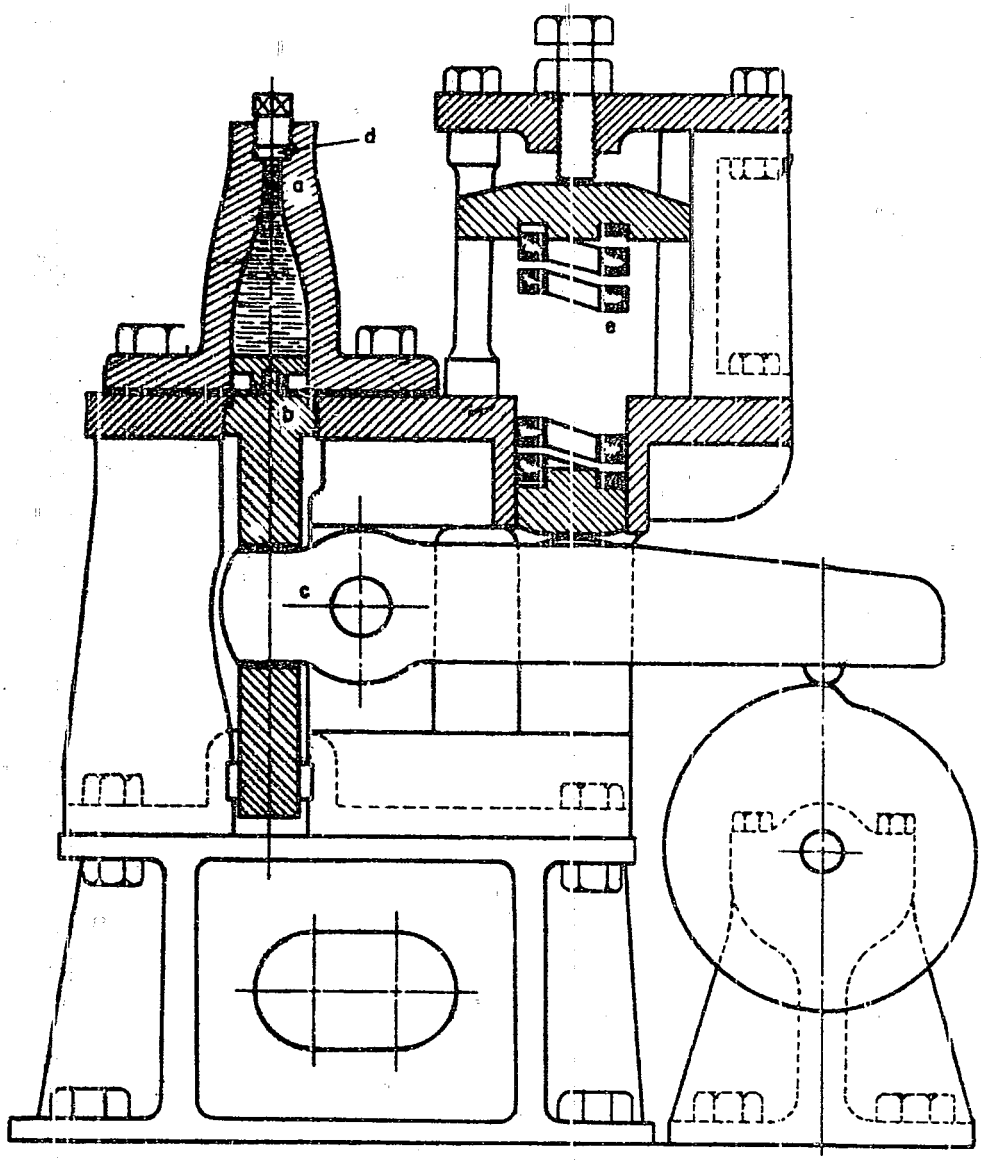


*Figure 3(A)5*
*WATER HAMMER TEST APPARATUS*

*ENCLOSURE (A)5 Continued*

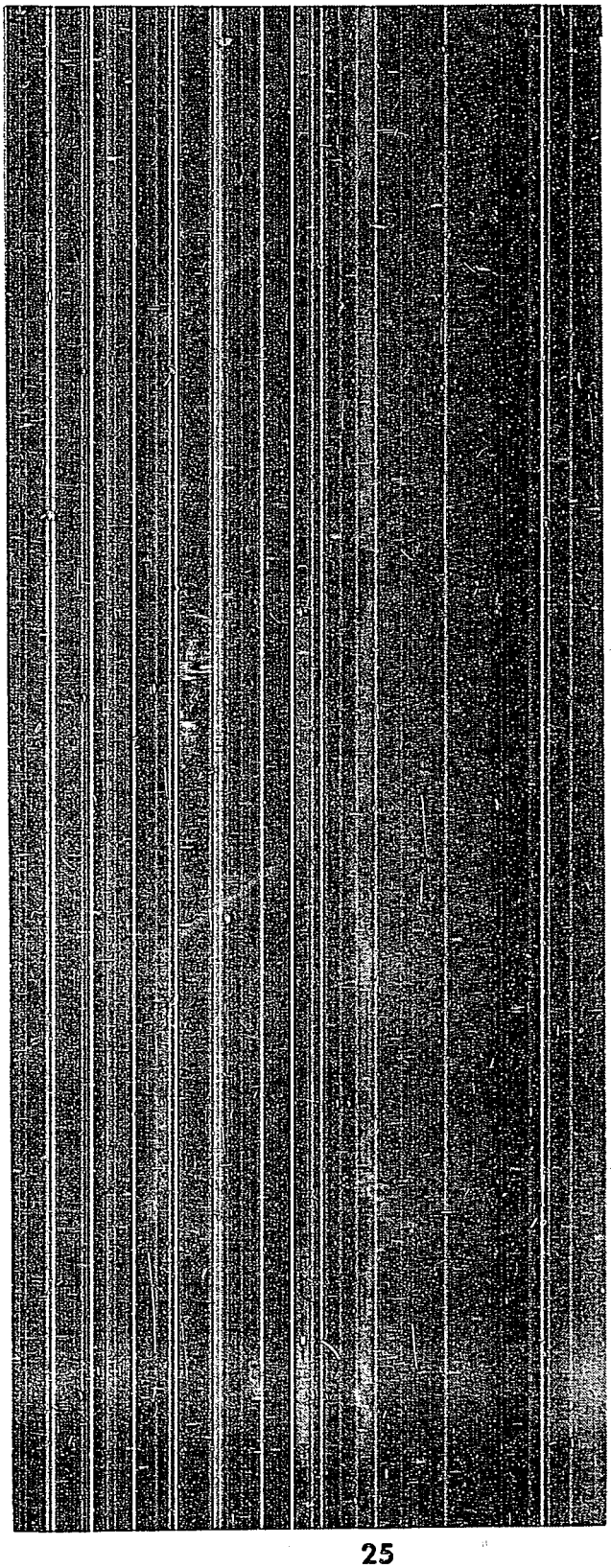

*Figure 4(A)5*
*EXPERIMENTAL PRESSURE CURVE FROM WATER HAMMER TEST*

*ENCLOSURE (A)5 Continued*

*No. of strokes ..... 8020*
*Static pressure ..... 116 kg/cm$^2$*
*Impact pressure ..... 280 kg/cm$^2$*

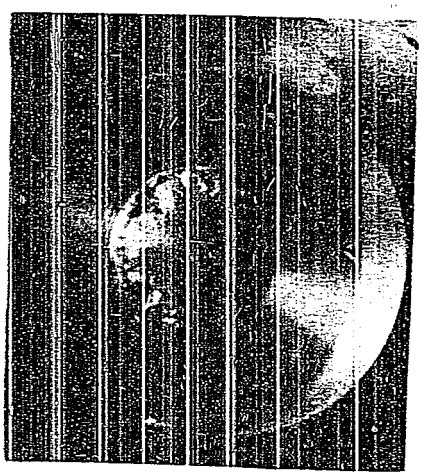

*No. of strokes ..... 1650*
*Static pressure ..... 116 kg/cm$^2$*
*Impact pressure ..... 280 kg/cm$^2$*

*Figure 5(A)5*
*EXAMPLES OF EROSION FROM WATER HAMMER TEST*

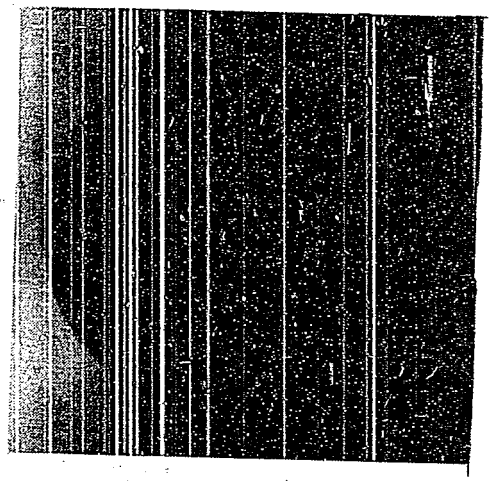

*No. of strokes ..... 39000*
*Static pressure ..... 67 kg/cm$^2$*
*Impact pressure ..... 195 kg/cm$^2$*

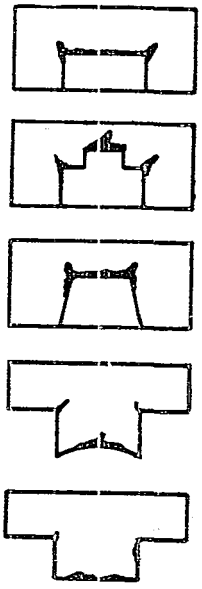

*Figure 6(A)5*
*EROSION BY WATER HAMMER TEST OF VARIOUS SHAPES OF TEST PIECES*

# ENCLOSURE (A) 6

## ELECTRICAL INSULATING PAINT DERIVED FROM SARDINE OIL

By S. HYODO

The object of this investigation was to obtain an electrical insulating paint with high stability against heat and humidity. For this purpose we investigated a high unsaturated fatty acid abstracted from sardine oil.

Sardine oil is constructed chemically from a few glycerides of unsaturated fatty acids, and the main part of them is glyceride of clupanodonic acid. This acid is one of the highest unsaturated fatty acids, and its molecular formula is as follows:

$$CH_3 \cdot CH_2 \left[CH : CH(CH_2)_2\right]_3 \left[CH \cdot CH\,CH_2\right]_2 CH_2 \cdot COOH$$

It has five unsaturated double bonds. The iodine value of this acid is 335.

We prepared this unsaturated fatty acid from sardine oil by using the acetone soda process.

Under suitable conditions, this high unsaturated fatty acid polymerizes to black resin when heated with a small percentage of benzoic peroxide as catalyzer. This polymer is a kind of black pitch and soluble in naphtha. We prepared an electrical insulating paint from this solution containing 10-20% of this polymer. However, the industrial application of this process was very difficult, because the acetone soda process is difficult on an industrial scale.

### Properties of Sardine Oil Insulating Paint

Color.....Black or deep brown liquid
Fixing temperature.....150-180°, more than 30 min.
Stability for heating.....180-200°

Electrical properties:

Specific resistivity.....$2.3 \times 10^{15}$ ohm/cm
Dielectric strength.....1000-1500 volt per 0.01mm
Dielectric loss factor (tan $\delta$)....$100 \times 10^{-4}$ (at 1000 cycles)

Stability of specific resistivity against humidity:

Dry air.....$10^{15}$ ohm/cm
50% humidity.....$10^{14}$ ohm/cm
85% humidity.....$10^{13}$ ohm/cm

# ENCLOSURE (A) 7

## MODEL EXPERIMENTS ON THE STABILITY OF THE BATTLESHIP "NAGATO" UNDER DAMAGED CONDITIONS

By M. SATO

The effects on transverse stability of flooding and counter-flooding BB NAGATO have been experimentarily investigated by the use of a 1/25 scale model. The model is subdivided into 39 watertight compartments above and 38 below the water line. Each compartment is loaded with wooden cylinders in order to adjust the permeability. There are ten 100mm diameter holes with lids, (corresponding to 2.5m in the actual ship) at one-half draft below the water line; the lids are taken off according to desired conditions.

Particulars of NAGATO

| | |
|---|---|
| Displacement | 44,672 tons |
| Draft (even keel) | 9.708 m |
| Center of buoyancy above base line (KB) | 5.084 m |
| Metacentric radius (BM) | 6.870 m |
| Center of gravity above base line (KG) | 9.634 m |
| Metacentric height (GM) | 2.320 m |
| Complete period of rolling | 15.0 sec |

According to desired conditions, various compartments were opened to the sea and the weight of flooding water, angle of heel, statical stability, etc. were measured. Compartments on the opposite side were then counter-flooded until the ship became upright and on an even keel, and the weight of flooding water, statical stability, etc. were measured. Judging from the results thus obtained, possible limits of flooding on one side and counter-flooding on the opposite side have been deduced as shown in the following table.

DAMAGE CONTROL STUDIES - BB NAGATO
(1/25 scale model)

Original reserve buoyancy.....26,009 tons
Draft.....9.7m

| Side Gun Compartments | Initial Conditions: Living Spaces above Water | | Initial Conditions: Loss of Reserve Buoyancy | | Ship will lose transverse stability when: Flooding on One Side Amounts to | | | Flooding and Counter-Flooding Amounts to | | | Flooding at Bow Amounts to | | | Flooding at Stern Amounts to | | |
|---|---|---|---|---|---|---|---|---|---|---|---|---|---|---|---|---|
| | fore | aft | tons | %* | tons | %* | heel | tons | %* | draft | tons | %* | trim bow | tons | %* | trim stern |
| Water-Tight | S*** | S | 0 | 0 | 7600 | 29.2 | 40° | 23,980 | 92.2 | 15.3m | | | | | | |
| | D** | S | 2767 | 10.6 | | | | | | | 13,733 | 52.8 | 3m | | | |
| | S | D | 2267 | 8.7 | | | | | | | | | | 11,233 | 43.2 | 33m |
| Non-Water-Tight | S | S | 5484 | 21.1 | 2020 | 7.8 | 30° | 14,660 | 56.4 | 10.0m | | | | | | |
| | D | S | 8251 | 31.7 | 1750 | 6.7 | 15° | 14,550 | 56.0 | 12.9m | 7249 | 27.9 | 9.8m | | | |
| | S | D | 7751 | 29.8 | 1700 | 6.5 | 14° | 12,650 | 48.7 | 12.5m | | | | 7000 | 26.9 | 13.3m |
| | D | D | 10,519 | 40.4 | 1680 | 6.5 | 14° | 12,980 | 49.9 | 12.7m | | | | | | |

*Percentage of the original reserve buoyancy.
**D-Damaged.
***S-Safe.

# ENCLOSURE (A) 8

## EFFECTS OF ANTI-ROLLING TANKS

By M. SATO

### I. INTRODUCTION

In 1942, a new icebreaker was projected and it was expected that it would be laid down in 1945. This ship was to have a round bottom and broad beam for its main duty--icebreaking. The metacentric height was to be large and as a result, the period of rolling would be necessarily very short. In winter she would be engaged in icebreaking duty and this was not thought to be serious. However, in the summer, on ordinary cruises, it was feared that she would roll heavily by synchronizing with the comparatively short waves which might be encountered frequently. It was thought undesirable, however, to fit larger bilge keels as a counter-measure.

Anti-rolling tanks came under consideration. At first, some of a passive type were designed for simplicity of construction and we experimentally investigated their effectiveness. Next, investigations on effects of bilge keels, number of air escapes, depth of communication trunk, change of displacement, freezing of water in the tank and obstacles in the trunk were undertaken.

On the other hand, studies on an anti-rolling tank of an active type were conducted by Professors Y. WATANABE and K. NODA, Kyushu Imperial University. A definite plan was obtained and experiments in the laboratory were accomplished successfully.

A. Particulars of the Projected Icebreaker were:

| | |
|---|---|
| Length between perpendiculars | 107.000m |
| Length over all | 115.800m |
| Length on load waterline | 112.000m |
| Maximum breadth | 20.500m |
| Breadth on load waterline | 19.500m |
| Depth | 11.460m |
| Draft (even keel) | 7.360m |
| Displacement (with appendages) | 8,667 tons |
| Center of buoyance above base line (KB) | 4.206m |
| Metacentric radius (BM) | 4.246m |
| Center of gravity above base line (KG) | 6.232m |
| Metacentric height (GM) | 2.220m |
| Complete period of rolling | 9.50 sec |

B. Plans of Passive Type Anti-Rolling Tanks

Three plans based on the method proposed by Professor Y. WATANABE* were proposed.

Generally, the resonance curve of a ship fitted with anti-rolling tanks has two peaks. In planning the tanks, their form and dimensions were so selected that the resonance curves with and without the tank would intersect each other at the peak.

In view of the results of the experiments, some modifications in the form of the communication trunk were tried, and three more proposals were added. Particulars of these six tanks are shown in Figure 1(A)8.

---

*Journal of the Society of Naval Architects of Japan, Vol. 46, 1930.

*ENCLOSURE (A)8 Continued*

C. Results of Experiments

Each type of anti-rolling tank (No. 1 to No. 6) was tried in regular waves of a height of 4.14m and below, length from 70m to 240m and period from 6.5 seconds to 12.5 seconds. Number 6 proved the most effective of the six.

Next, effects of various factors mentioned above, were investigated on Tank No. 6.

D. Effect of Bilge Keels

Comparing bilge keel designs (as shown in Table I (A)8, it was proved that their effects were roughly proportional to the area, but that even the largest could not be expected to be sufficiently effective by itself. On the other hand, it was also found that any one of the tanks alone was not effective enough. When tank and bilge keels are used jointly, excellent results can be obtained. In this case, even the smallest bilge keels, No. 4, are sufficiently effective.

Table I(A)8
PARTICULARS OF BILGE KEELS USED WITH ANTI-ROLLING TANKS

| | No. 1 | No. 2 | No. 3 | No. 4 |
|---|---|---|---|---|
| Length (m) | 35.900 | 28.000 | 35.900 | 28.000 |
| Breadth (m) | 1.650 | 1.650 | 1.500 | 1.500 |
| Area (both sides) ($m^2$) | 110.48 | 84.40 | 99.71 | 76.01 |
| Ratio of Area to That of No. 1 | 1.000 | 0.764 | 0.902 | 0.688 |

E. Effect of the Number of Air Escapes

The effect of the number of air escapes (0, 2, 4, 6, 8, on one side and completely opened) were investigated. As a result, six or eight on each side (3-4% of the total free surface of the tank) were found most suitable.

F. Effect of Depth of the Communication Trunk

Depths of the communication trunk tried were 1.00m, 1.15m and 1.30m. The first one, 1.00m, proved most effective.

G. Effect of Change of Displacement

Displacement was changed to 8,644 tons, 6,944 tons and 7,345 tons, but effects of the changes were scarcely noticeable.

H. Effect of Freezing of Water in the Tank

If the water in No. 6 tank freezes, the center of gravity of the ship will be 0.094m higher, but there is no danger that the ship will roll more heavily than she does without the tank.

*ENCLOSURE (A)8 Continued*

## I. Effect of Obstacles in the Communication Trunk

In the actual ship, there must be some obstacles in the trunk owing to the construction of the ship. The area of the trunk was reduced to half by a slotted plate at the center line of the ship, but the effect was not important.

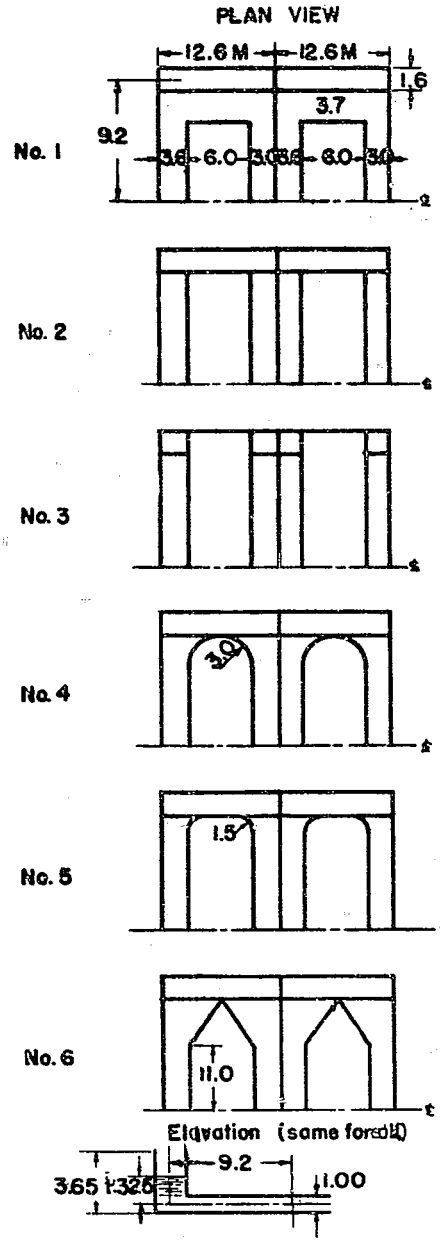


| | Area of free surface | Weigh of water (% of displacement) | Natural period of oscillation of water |
|---|---|---|---|
| No. 1 | 40.32 M$^2$ | 431 tons (5.1%) | 9.57 sec. |
| No. 2 | 40.32 M$^2$ | 363 tons (4.3%) | 10.52 sec. |
| No. 3 | 21.12 M$^2$ | 295 tons (3.5%) | 7.33 sec. |
| No. 4 | 40.32 M$^2$ | 378 tons (4.4%) | 10.16 sec. |
| No. 5 | 40.32 M$^2$ | 367 tons (4.3%) | 10.63 sec. |
| No. 6 | 40.32 M$^2$ | 401 tons (4.7%) | 9.88 sec. |

*Figure 1(A)8*
*DETAIL OF ANTI-ROLLING TANKS*

# ENCLOSURE (A) 9

## STRESS DISTRIBUTION ON SHIPS IN ROUGH SEAS

By M. SATO

(This research is unfinished)

In order to get a conception of the relation between stresses on a ship voyaging in rough seas and its motion, we made experiments with a brass model ship, 7.667m long at the water line. Strain developed on the ship, ship's motion, wave form etc., were all simultaneously recorded by means of an electromagnetic oscillograph. Analysis of the data has not yet been completed, but the following tendencies have been observed:

1. When a ship is at anchor among uniform waves, stresses are approximately proportional to wave height.

2. When a ship is being towed, stresses change with ship's speed, and near that speed at which the period of encounter resonates with the natural periods of pitching and rolling, compressive stresses on deck near midships increase remarkably and amount to almost twice what they are when speed is zero.

# ENCLOSURE (B) 1

TURBO-ROCKET

1. Purpose of Research

The purpose of this research was to obtain a small, high capacity jet engine, suitable for installation in small, high speed planes. The airplanes on which installation that had been actually planned were:

KIKKA.....Twin engine, small type bomber
OOKA-43.....Single engine, small type bomber

Large type engines which were to be installed in interceptor fighters were under research. At first, these were planned to be used as auxiliary rockets for medium bombers, but the effect was so small in relation to the difficulties of assembly that this plan was suspended.

2. Results of Research and Experiments

a. For KIKKA and OOKA, trial manufacture of Ne-20 was completed, and in Naval Air Arsenals and Naval Yards preparations for mass production were started in full scale and production was partially begun. In the Branch Arsenal of the First Naval Air Technical Arsenal, experimental models had been completed; six were used for endurance improving tests, two were installed in a KIKKA. That plane flew its first test flight on 7 August and its second on 11 August, when it landed in the sea owing to a pilot fault in the control of take-off.

In Yokosuka Naval Yard, ten production-type engines had been completed, but their performance was not sufficient and four were sent to Koizumi Manufacturing Plant of Nakajima Airplane Company for KIKKA.

b. Ne-12 was manufactured experimentally as the prototype of Ne-20. Since the performance of both was very poor trial manufacture was suspended.

c. For fighters, we ordered three civilian companies to build jet engines that would have performances equal or superior to the German BMW 109-003 rocket engine. Shibaura Plant of Ishikawazima Co. Ltd. was to manufacture Ne-130, Nakajima Airplane Co. Ltd. Ne-230, and Nagoya Engine Plant of Mitsubishi which cooperated with Kobe Dockyard, Ne-330, respectively. None of them completed their experimental work.

The first Ne-130 produced were damaged one after another in tests. Of the experimental engines at Mitsubishi, work was suspended owing to air raid damage.

d. General performance of each type:

| TYPE | Static Thrust (kg) | RPM | Diam. (mm) | Length (mm) | Dry Weight (kg) |
|---|---|---|---|---|---|
| Ne-12 | 320 | 15,000 | 855 | 1800 | 315 |
| Ne-20 | 475-500 | 11,000 | 620 | 3000 | 450 |
| Ne-130 | 900 | 9000 | 767 | 3850 | 900 |
| Ne-230 | 885 | 9000 | 762 | 3430 | 810 |
| Ne-330 | 1320 | 7600 | 842 | 4000 | 1200 |

*ENCLOSURE (B)1, continued*

e. General description of the construction of each type:

(1) Ne-10

Air compressor: Centrifugal fan (duralumin forging, outer diameter - 500 mm), one stage, compression ratio - 3.5.

Combustion chamber: Triple, concentric drum type. (Made of stainless steel or surface treated with Al-diffusion mild steel plates); sixteen fuel injection valves located equi-distant to each other on the circumference.

Turbine: Fifty percent reactionary turbine, one stage. (Forged special steel blades attached by welding, height of blade - 50 mm, PCD - 500 mm).

(2) Ne-12

Air compressor: One-stage axial blower added at fan entrance of Ne-10.

Combustion chamber: Same as Ne-10

Turbine: Same as Ne-10 except for the reinforcement of the blades by 20% of the reactionary degree.

(3) Ne-20

Air compressor: Eight stage axial blower, outer diameter 480 mm, compression ratio - 3.4.

Combustion chamber: BMW 109 Type, concentric drum type, 12 fuel injection valves.

Turbine: Reactionary degree - 7%, height of blade - 80 mm, PCD - 475 mm, one stage. (Forged special steel blades attached by welding.)

(4) Ne-130, Ne-230, and Ne-330

All had a seven stage axial blower, a modified type of the BMW 109. Ne-230 only had air-cooled, hollow turbine blades.

f. Trial manufacture: In February 1942, for installation in large type, higher-altitude airplanes, a large type exhaust gas turbine named YT 15 had been manufactured experimentally. Experiments were completed, but owing to the low strength of the turbine blades it was not adopted.

In February 1943 we began to modify YT 15 as a turbine jet and named it TR 10. The first one was completed in June of the same year. (Made by Ebara Mfg. Co. Ltd.)

In July 1944 tests had been finished using the first three engines, but combustion was not good and the strength of the turbine blades was not sufficient. Therefore, we attempted to remedy these defects and manufactured Ne-10. In September of the same year, the work on Ne-20 was finished but improvements were not entirely satisfactory. We began to plan

Ne-12 and together with this, we ordered the civilian companies to manufacture Ne-230 and Ne-330, after referring to the data about BMW 109 that had been sent from Germany in May.

*ENCLOSURE (B)1, continued*

In November 1944 the first Ne-12 was completed. But performance and endurance were not satisfactory and we continued improvements. After December, we began the basic plan of Ne-20 and by February 1945 this plan was completed and Ne-12 B (modified type of Ne-12) was finished. Again performance was insufficient and we pushed the manufacture of Ne-20. By 26 March 1945 the first Ne-20 was finished. Six Ne-12 were manufactured in the First Air Technical Arsenal and the other six in Yokosuka Naval Yard. Thereafter, trial manufacture was suspended.

In May 1945, after measures to correct the cracking of turbine blades and to improve the performance of the axial blower, and after adopting a ball-bearing to partially absorb thrust, the Ne-20 was given an endurance test (maximum speed for 5 hours, 10,000 RPM for 1 minute). Some further improvements appeared necessary. In the same month, the first Ne-130 and Ne-230 engines were tested with poor results. Damage occurred to the blades of the axial blowers and to the bearing.

Deliberate tests of Ne-20 had been completed on 22 June 1945 and on 27 June 1945 Ne-20 was installed in a land-based torpedo-bomber. Preparations for a test flight were completed.

On 29 June 1945 the first KIKKA was completed and on 7 August 1945 was flight-tested for the first time with good results, but on 11 August 1945 at the second flight test, the pilot lost control on take-off and the plane sank.

g. Special materials: At first, we used 18-8 Cr-Ni stainless steel (I-306) turbine wheels and blades, but changed to Cr-Mn stainless steel (I-307) to conserve nickel. The next time we intended to use a material (I-309) that had vanadium added to the former. Adding nitrogen to this material, we found, had some effect but production was not carried out practically.

For welding rods we used 18-8 stainless steel at first and then shifted to Cr-Mn (I-307).

| | Percent Composition | | | | | | | |
|---|---|---|---|---|---|---|---|---|
| Name of Material | C | Si | Mn | Cr | Ni | Mo | W | V |
| I-306 | 1.5 | 1.0-1.4 | 1.6 | 1.7-2.0 | 7-0.7 | 0.3-0.7 | 1.0 | - |
| I-307 | 0.1-0.2 | 0.8-1.2 | 15-17 | 10-12 | - | 0.5 | 1.8-2.2 | - |
| I-309 | 0.15-0.25 | 0.8-1.2 | 15-17 | 10-12 | - | - | - | 0.5-1.0 |

For the combustion chamber, we used 18-8 stainless steel. As the result of this, work was done easily and no deficiencies in endurance were encountered.

h. Method of test: For the test of the complete turbine rocket, we used a common performance test-running bed for the engine and a thrust gauge (remote control indicator using magnetic hysteresis) for a hydraulic brake.

We tested by ordinary methods the vibration of turbine and blower blades and the strength of the materials that were to be used at high temperature.

# ENCLOSURE (B) 2

RESEARCH ON LIQUID-FUEL ROCKET MOTORS

by Ukon FUJIHIRA

25 December 1945

## I. Object of the Research

To develop a liquid-fuel rocket motor which would be fully reliable for use in combat planes.

## II. Results

Hydrogen Peroxide System (Mark Ro, B Fuel). The reliability and performance of this fuel were proven by bench tests, in a rocket motor. Subsequently, success was obtained in maintaining continuous combustion of this fuel for four minutes, after which it was submitted to an actual flight test in a SHUSUI pursuit plane. This preliminary test showed good results, but further flight tests were not undertaken.

Nitric Acid System (Mark Ro, C Fuel). Fundamental combustion tests on these liquids were completed, but an actual motor using this type of fuel was never designed.

## III. Methods and Materials

### A. Hydrogen peroxide system

A rocket motor using hydrogen peroxide fuel was designed from German data as the main motor of the SHUSUI. It was called "TOKURO No. 2" or "KURO" and placed in the tail of the plane.

In operation, two liquids, A and B, were withdrawn from the fuselage fuel tanks and raised to a pressure of thirty atmospheres by means of centrifugal pumps. They next passed through a device which controlled both quantity and mixture ratio and were injected into combustion chamber through injection valves. In this chamber the liquids were mixed and reacted to form gases having a temperature of 1900°C. This gas expanded through a Laval nozzle from a pressure of 19 atmospheres to atmospheric pressure, and high velocity, obtained at the exit port of the nozzle, gave the propelling thrust. The pumps were driven by a steam turbine, which, in turn, was driven be the decomposition products (at 500°C) of the A Liquid (hydrogen peroxide). In order to obtain safe starting and steady combustion at a low thrust rate, injection pressure and the number of acting injection valves were regulated according to the desired conditions.

Two types of liquids (A Liquid and B Liquid) and a steam producing catalyst were used.

The A Liquid -- hydrogen peroxide (80% solution) -- is also known by its German name, T-Stoff, has a specific gravity of 1.36 at 15°C. and is colorless. Its degree of concentration is determined by its specific gravity. Impurities or warm temperatures cause it to decompose. Contact with organic materials cause it to ignite spontaneously and contact with the skin causes a painful burn. As it reacts with common metals it must be stored in glass or porcelain vessels, or in tin-lined tanks in a dark,

*ENCLOSURE (B)2, continued*

cool place. If it is not stored and handled carefully, it is liable to explode spontaneously. Therefore, it must be handled with great care and protective clothing must be worn by those working with it.

(For details of the methods of manufacturing A Liquid (hydrogen peroxide) and B Liquid (hydrazine hydrate) and Japanese naval research thereon, refer to NavTechJap Report, "Japanese Fuels and Lubricants, Article 5 - Research on Rocket Fuels of the Hydrogen Peroxide-Hydrazine Type," Index No. X-38(N)-5. Rocket fuel stabilizers and catalysts are also discussed in the above-referenced report.)

The B Liquid -- a hydrazine hydrate mixture -- was based on data from Germany and is composed as follows:

| | Ratio First Used | Ratio Later Used |
|---|---|---|
| Hydrazine hydrate ($N_2N_4N_2O$) | 30% | 30% |
| Methyl alcohol | 62% | 58% |
| Water | 8% | 12% |

Injection mixture ratio of A Liquid and B Liquid is given as follows (weight):

| | Ratio First Used | Ratio Later Used |
|---|---|---|
| A Liquid | 10 | 10 |
| B Liquid | 3.3 | 3.6 |

The calculated change of performance with change of injection mixture ratio is plotted in Figure 1 (B) 2.

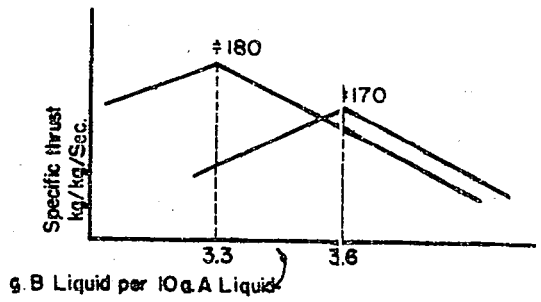


*Figure 1(B)2*
*CHANGE IN PERFORMANCE OF LIQUID FUEL ENGINES WITH CHANGE IN INJECTION MIXTURE RATIO*

Specific thrust is one of the indices of performance of a rocket motor and it is the thrust per total liquid flow rate (kg/kg/sec)

The catalyst, hydrazine, is a mixture of potassium permanganate, sodium hydroxide, portland cement, etc., kneaded and solidified into blocks 8 mm square.

The rocket motor designed to be installed in the SHUSUI plane consisted

*ENCLOSURE (B)2, continued*

of six main parts (see Figure 2 (B)2): pump, quantity controller, pressure controller, combustion device, frame, and piping.

For a description of the operation of the motor refer to Figure 3 (B)2. When the turbine shaft is revolved at 600 RPM by the starter motor, the pressure of A Liquid rises to 6 atm, and then, if the low speed valve of the pressure controller is opened, the flow of A Liquid to the steam producer reaches 7 liters per minute. Thereafter, the pump system continues automatic operation when the switch is off.

The start and stop valve is then opened by the controlling gear, and by opening the distributing valve, B Liquid is led to the inner space of the distributing valve through the cooling mantle space of the combustion device of the quantity controller. This is the starting condition. Next by revolving the controller gear, the main flow path in the pressure controller is opened simultaneously with the first speed, second speed, and third speed in the quantity controller (first stage, second stage, and third stage). Corresponding to these speeds, the number of injection nozzles used increases from 2 to 6, and to 12, and combustion is continued. In this time the injection pressure of A Liquid is balanced to the pressure of B Liquid by the balance piston of the quantity controller. By means of this mechanism, the correct mixture ratios of the two liquids may be regulated and good combustion conditions obtained. The purpose of the safety valve of the pressure controller is to prevent the overspeeding of the turbine.

Principal data are as follows:

1. Principal dimensions

| | |
|---|---|
| Total weight | 180 kg |
| Total length | about 2500mm |
| Total width | about 900mm |
| Total height | about 600mm |

2. Main values at maximum thrust

| | |
|---|---|
| Thrust | 1500 kg |
| Rotary speed of turbine | 14500 RPM |
| Pressure of combustion chamber | 19 atm |
| Delivery pressure of pump (both A and B Liquid) | 30 atm |
| Flow rate of A Liquid | 5.9 kg/sec (6.2 kg/sec) |
| Flow rate of B Liquid | 2.0 kg/sec (2.2 kg/sec) |
| Flow rate of A Liquid to steam producer | 0.4 kg/sec |
| Specific thrust | 180 kg/kg/sec (170 kg/kg/sec) |

Note: The values in parentheses indicate values based on later data.

3. Starter motor

| | |
|---|---|
| Voltage | 24 V |
| Rated power | 1 kw |
| Gear ratio to turbine shaft | 1:1 |

*ENCLOSURE (B)2, continued*

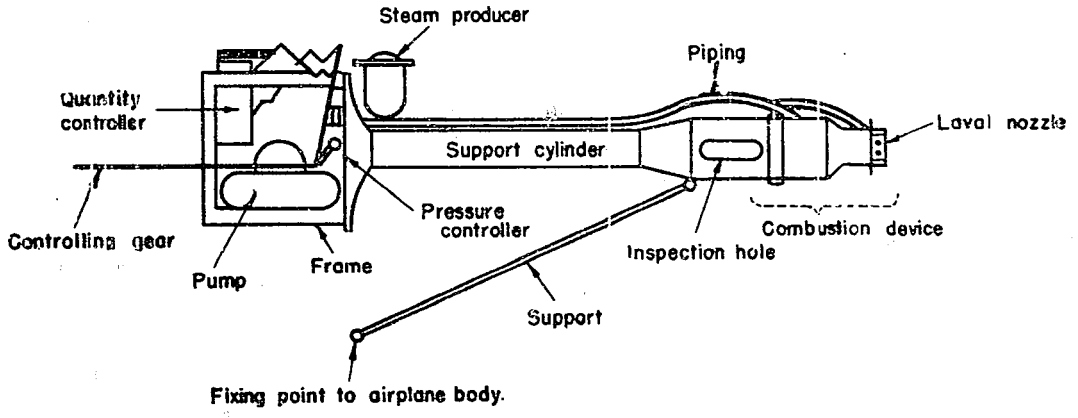


*Figure 2(B)2*
*SIDE VIEW OF LIQUID FUEL MOTOR*

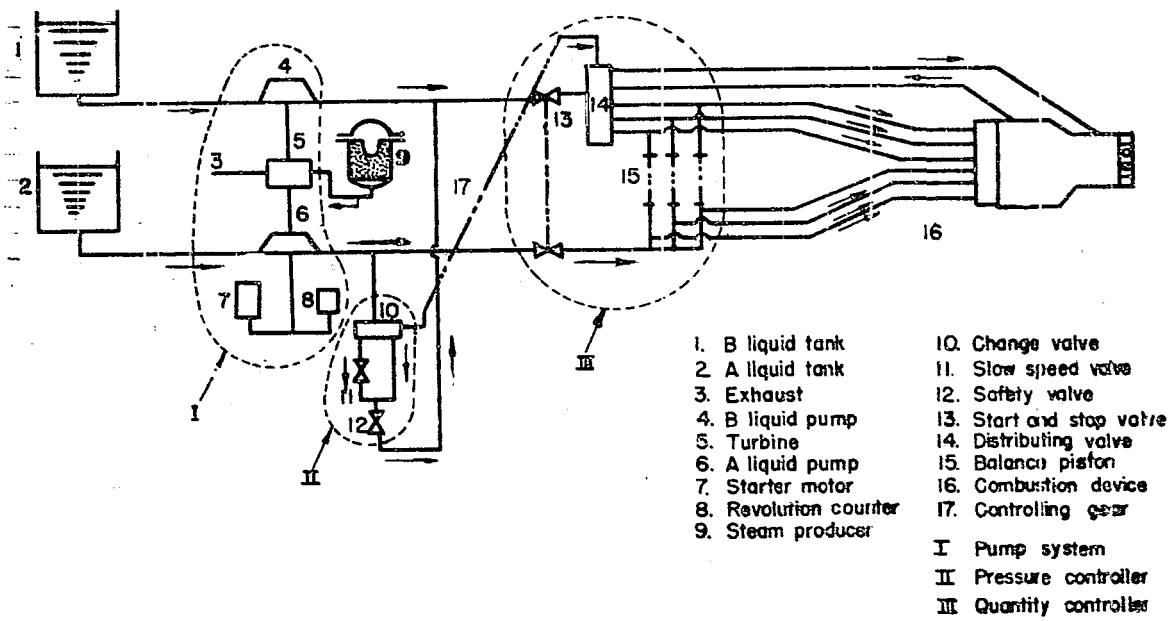


*Figure 3(B)2*
*SCHEMATIC DIAGRAM OF LIQUID FUEL ROCKET MOTOR*

4. Revolution counter

Type.....electric
Gear ratio to turbine shaft.....1:10

The pump system is shown in the diagram in Figure 4 (B)2. Both the A Liquid pump and the B Liquid pump consist of a 2-stage booster (first stage with two blades and second stage with three blades) and a main pump (centrifugal) of six blades. The entrance passage of the main pump is wide enough to prevent pitting. For liquid packing, bellows, springs, and a carbon ring system are used. The carbon ring, which is divided into three pieces, is kept in contact with the shaft by spring force.

The turbine has impulse-type blades and a simple secondary steam nozzle.

Material used in the pump system are as follows:

Turbine blades: 18-8 stainless steel.
Turbine shaft: At first, 18-8 stainless steel; later, 18 Cr stainless steel.
Pump impellers and casing: Silumin.
Turbine case: Cast iron.
Bellows: Phosphor bronze plated with tin.

The start and stop valve consists of a pair of poppet valves for A Liquid and B Liquid. They are opened and shut by a driving piston using B Liquid delivery pressure.

The distribution of B Liquid is accomplished by the distribution valve as shown in Figure 5 (B)2. The sleeve valve rotates and its surface has several hollow spaces in the liner with several holes oppositely situated.

The combustion chamber is shown in the diagram in Figure 6 (B)2. The inner wall was made from special steel by cutting out of a forged block. However, making it by pressing steel plate was also being investigated.

Details of the injection nozzle are shown in Figure 7 (B)2, and data below.

Valve lift (A Liquid).....1.8 mm
Pressure loll in this nozzle...about 4 atm (both ...liquids)
Flow rate of A Liquid...0.9 kg/sec (0.52 kg/sec)
Flow rate of B Liquid..0.17 kg/sec (0.18 kg/sec)
Material.....18-8 stainless steel

(Values in parenthesis are based on later data)

There was a total of twelve injection nozzles distributed as follows:

1st stage.....2
2nd stage.....4
3rd stage.....6

The arrangement of nozzles is shown in Figure 8 (B)2.

*ENCLOSURE (B)2, continued*

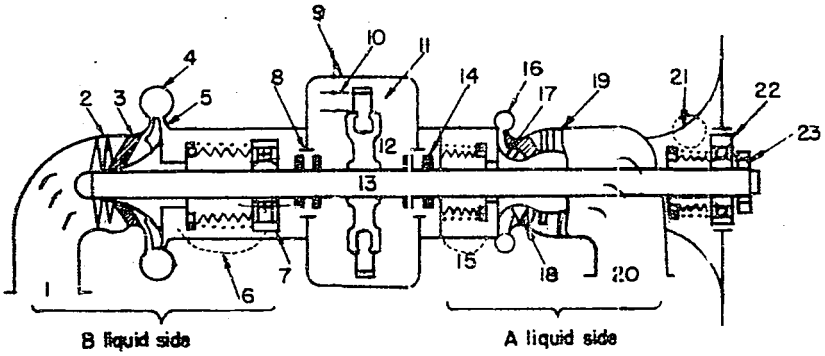


1. Suction port
2. Booster (2stage)
3. Guide vane
4. Pump casing
5. Main pump
6. Liquid packing
7. Roller bearing
8. Steam packing
9. Turbine case
10. Secondary steam nozzle
11. Turbine blade
12. Turbine disc
13. Turbine shaft
14. Steam packing
15. Liquid packing
16. Pump casing
17. Main pump
18. Guide vane
19. Booster
20. Suction port
21. Liquid packing
22. Ball bearing
23. Gear

*Figure 4(B)2*

*SKETCH OF PUMP SYSTEM*

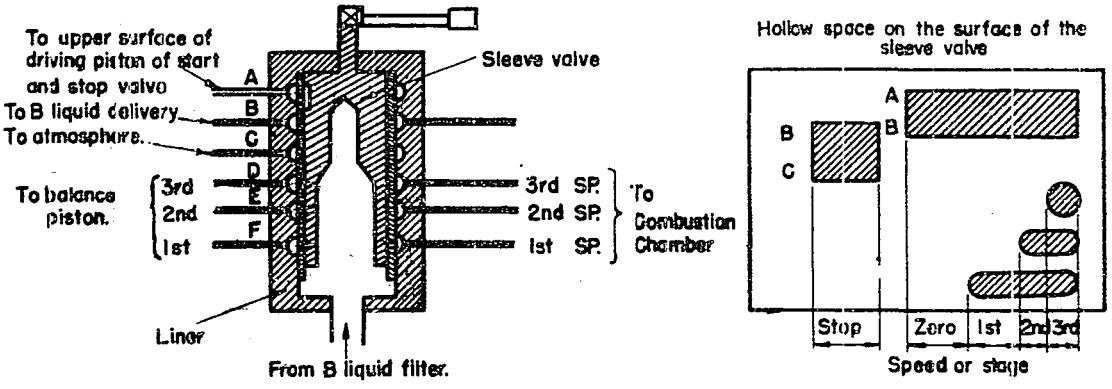


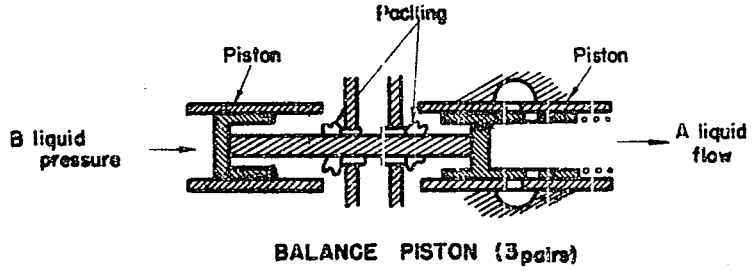


*Figure 5(B)2*

*SKETCH OF FUEL DISTRIBUTING VALVE FOR ROCKET ENGINE*

*ENCLOSURE (B)2, continued*

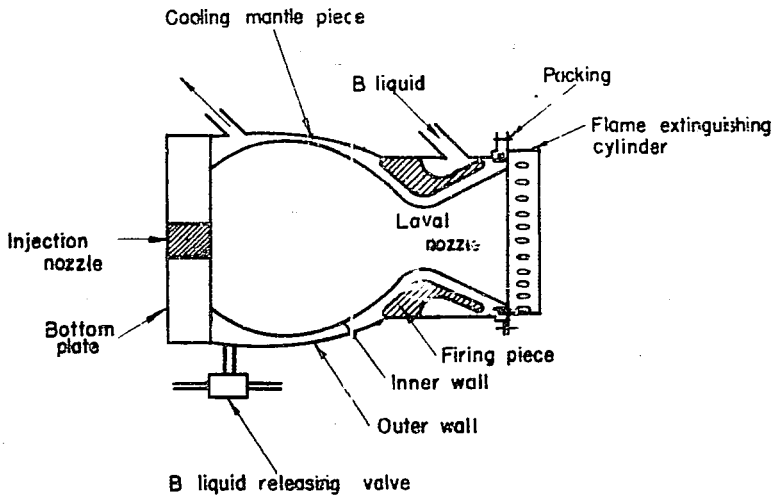


*Figure 6(B)2*
*COMBUSTION CHAMBER FOR ROCKET ENGINE*

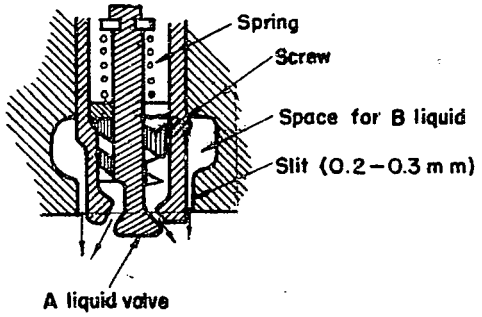


*Figure 7(B)2*
*INJECTION NOZZLE FOR ROCKET ENGINE*

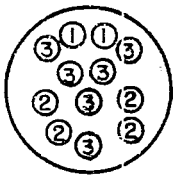


*Figure 8(3)2*
*ARRANGEMENT OF INJECTION NOZZLES*

*ENCLOSURE (B)2, continued*

The release valve for B Liquid is shown in Figure 9 (B)2. In case of a sudden stop, the pressure in the cooling mantle space becomes very high compared with B part pressure of the distributing valve and residual B Liquid in the cooling mantle space is released. Thus after-burning in the combustion chamber is prevented.

The pressure controller is shown in Figure 10 (B)2. In the sleeve valve are drilled passages for slow speed and full speed, and by revolving this sleeve valve, we can change from slow to full speed.

The passage formed by the piston and liner holes is throttled by the pressure rise of the liquid, and therefore flow of liquid can be limited to the desired amount.

When turbine shaft speed becomes too great, the safety valve reacts to this high pressure, and stops the flow to the steam producer.

Characteristics of pressure controller are shown in Figure 11 (B)2.

Note: $\triangle P$ is the pressure difference between the pressure at the steam producer and at the front of the pressure controller.

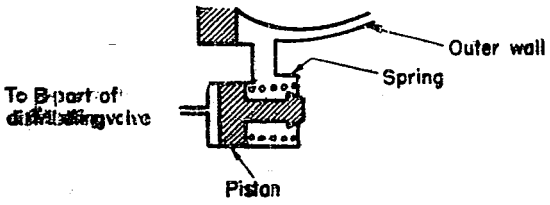


*Figure 9(B)2*
*RELEASE VALVE FOR B LIQUID*

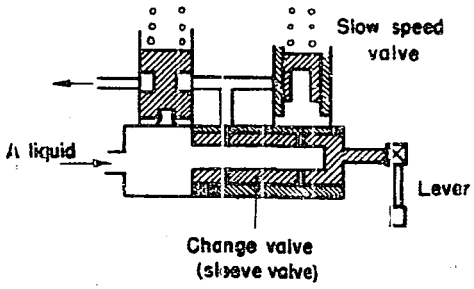


*Figure 10(B)2*
*PRESSURE CONTROLLER*

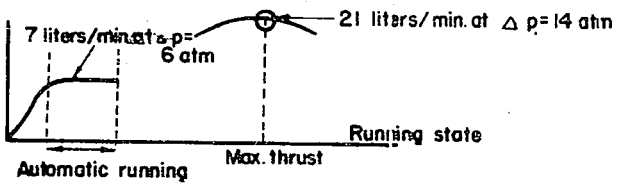


*Figure 11(B)2*
*CHARACTERISTICS OF PRESSURE CONTROLLER*

*ENCLOSURE (B)2, continued*

For combustion tests (see Figure 12 (B)2) the rocket motor was placed on a thrust measuring table and the two liquids were pumped from their storage tanks through flexible suction pipe. Controlling gear was led to the meter room. In this room, the controlling lever, revolution indicator, pressure gauge thrust meter, secondary battery for the starter motor, switches, and electric meters, etc., were located.

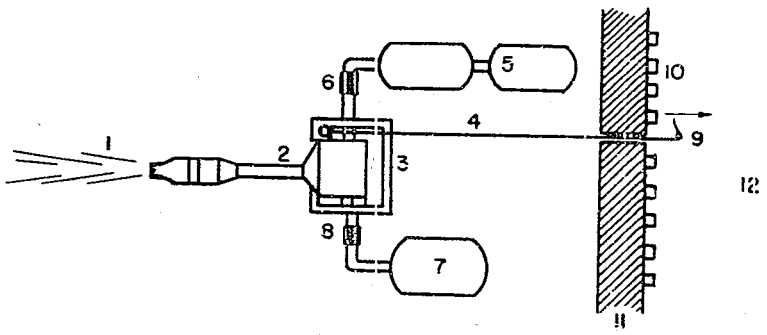


*Figure 12(B)2*
*COMBUSTION TESTS ARRANGEMENTS*

1. *Jet of burnt gas*
2. *Rocket motor*
3. *Thrust measuring table*
4. *Controlling gear*
5. *A liquid tank*
6. *Flexible joint*
7. *B Liquid tank*
8. *Flexible joint*
9. *Controlling lever*
10. *Meters*
11. *Protecting wall*
12. *Meter room*

After the rocket was installed and the thrust meter and piping were connected, the two kinds of liquids were put into their respective tanks. Next the starter motor was switched on and the controlling lever opened to the position of L speed (automatic running or no-load running, Leerlauf.) When the turbine revolutions reached 6000 RPM (in about 40 sec.) the starter motor switch was cut off, and the turbine and pump system continued automatic running. According to the steam temperature, after about 20 seconds, the lever was opened to first speed and then to second and third speeds. At the start of combustion the noise of burning had to be listened to carefully.

Several cautions to be observed while running are as follows:

1. Is the temperature rise of steam enough?

*ENCLOSURE (B)2, continued*

2. Is the burning sound at the start smooth?
3. Is there variation of pressure and rotation speed?
4. Is the colour of combustion flame good?
5. Is the residual amount of liquid enough?
6. Is there firing due to leakage of liquids?

B. $HNO_3$ System

In this rocket concentrated nitric acid and ethyl alcohol were used as the liquids. By means of compressed air, the two kinds of liquids in the pressure tanks were pushed out and injected into the combustion chamber where they mixed together and combustion began. For igniting this mixture, chemicals or ignition plugs were used. Due to the results of the fundamental research on combustion, it was known that if the correct mixture ratio was used, the performance would be very good but the combustion temperature too high. By lowering the combustion temperature to that of the $H_2O_2$ system with the use of an over-rich mixture ratio of alcohol, performance was obtained which was slightly inferior to that of the $H_2O_2$ system. The special advantage of this system was that the production, storing and handling of the liquids were easy and safe. Fundamental research on the combustion in this rocket was completed at the Sagami Navy Yards. However, at the First Naval Technical Institute several experiments on combustion were carried out so this rocket will be described briefly. It was reported that this system was successful as an energy source in torpedoes.

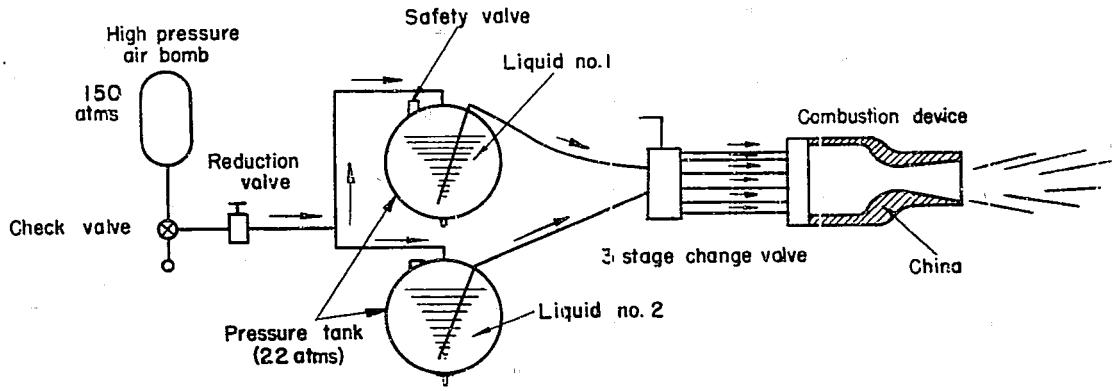


*Figure 13(E)2*

*SKETCH OF THE ENGINE USING NITRIC ACID*

*ENCLOSURE (B)2, continued*

Three liquids were used as follows:

Liquid No. 1. - $HNO_3$ 95%, water solution

Liquid No. 2. - $C_2H_5OH$ 85-90% (ethyl alcohol)

Liquid No. 3. - igniting substance consisting of:

$Pb(C_2H_5)4$ (Tetra ethyl lead)

Mixture of $C_6H_4(OH)CH_3$ (creosol) and $(C_2H_5)2NH$ (diethylamine)

Ignition plug using burning substance.

The injected mixture was in the proportion of

Liquid No 1 : Liquid No. 2 :: 2.3 : 1 (weight ratio)

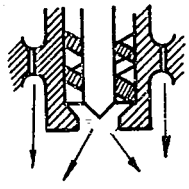

*Figure 14(B)2*
*INJECTION NOZZLE*

In the $H_2O_2$ system, combustion is good when the injection liquids form a film, but in this system the injected liquids must form a mist. (See Figure 13 (B)2 for sketch of this engine and Figure 14 (B)2 diagram of injection nozzle).

It is known that in this system the burning velocity of the liquids is slower than that of the $H_2O_2$ system.

IV Test and Experimental Data. ($H_2O_2$ System)

Concerning the fire resistance capacity of the combustion chamber inner wall, it was found that using a mixture ratio based on old data, the inner wall was burnt after one minute, but, as the number of tests were inadequate, it cannot be decided whether the mixture ratio based on old data is suitable or not.

Experiments on the performance of the pump were done at the Hiro Naval Yards. As a result of experiments, a pump was obtained which produced 30 atm at 14500 RPM at atmospheric pressure, but at an altitude of 8000 cavitation phenomena occurs, pump delivery pressure greatly decreases and vibration occurs. To prevent cavitation, a jet pump booster was used. Using this booster, cavitation does not occur at altitudes of 12000-13000m.

Some of the experimental problems encountered and their solutions are tabulated below:

| Item | Trouble | Solution or Plan |
|---|---|---|
| Pump System | Insufficiency of pump delivery pressure. | Improvement of the design of booster and main pump. |
| | Whirling of two bearing turbine axis. | First: Adoption of three bearings. Next: Two bearings with small interval and a large shaft. |
| | Damage to bellows: | Stop the whirling of shaft. |
| | Explosion of the pump of three bearings | First: Improvement of A Liquid drain space. Next: Adoption of two bearings. |

*ENCLOSURE (B)2, continued*

| | | |
|---|---|---|
| Pump System (Continued) | Insufficiency of starter motor power. | Increase power up from 0.75kw to 1.0kw. |
| | Separation of carbon ring from bellows. | Improvement of fixing substance. |
| Quantity Controller | Attachment of balance piston connecting rod to its guide. (Because of this trouble, explosion of combustion chamber occurred.) | Improvement of material of rod with 18-8 stainless steel plated with chrome. Guide with 18-8 stainless steel. Use of pure water. |
| Pressure Controller | Breathing or hunting combustion due to weak safety valve. Damage of volute chamber of pump due to strong safety valve. | Adjustment of acting pressure of safety valve (38 atm). |
| Combustion Device | Explosion of combustion chamber. Damage and burning of injection nozzle. | Connected the passages of the quantity controller to each other by the narrow passages through the casing. The liquids leak to the nozzles when these are not used. |
| | Damage and leakage at the pipes distributing to injection nozzle. | Adoption of flexible pipes and improvement of setting. |
| Piping | Firing due to leakage of liquids. | Improvement of setting. |

# ENCLOSURE (B) 3

## ROCKET PROJECTION OF BOMBS

The intention in this research was to combine a rocket with an aerial bomb for use in land warfare. It is comparatively easy to project bombs with a simply constructed wooden projector, but dispersion is somewhat extensive.

The projector is made of wood and covered with iron plate, as is shown in Figure 1 (B) 3. The rocket and the bomb are combined by a simple wooden piece upon the projector, as shown in Figure 2 (B) 3. The rocket, ignited electrically, projects the bomb. The desired range is attained by adjusting the angle of departure according to tables compiled from previous experiments.

Some of the essential particulars of these devices are as follows:

1. No. 6 Bomb-Projector

Weight of bomb.....60 kg
Output of rocket (kg x sec).....500 kg x 2 sec
Weight of propellant.....5.5 kg
Total weight of rocket.....28 kg
Range.....no entry

2. No. 25 Bomb-Projector

Weight of bomb.....250 kg
Output of rocket (kg x sec).....4500 kg x 3 sec
Weight of propellant.....78 kg
Total weight of rocket.....130 kg
Range.....1,000 meters

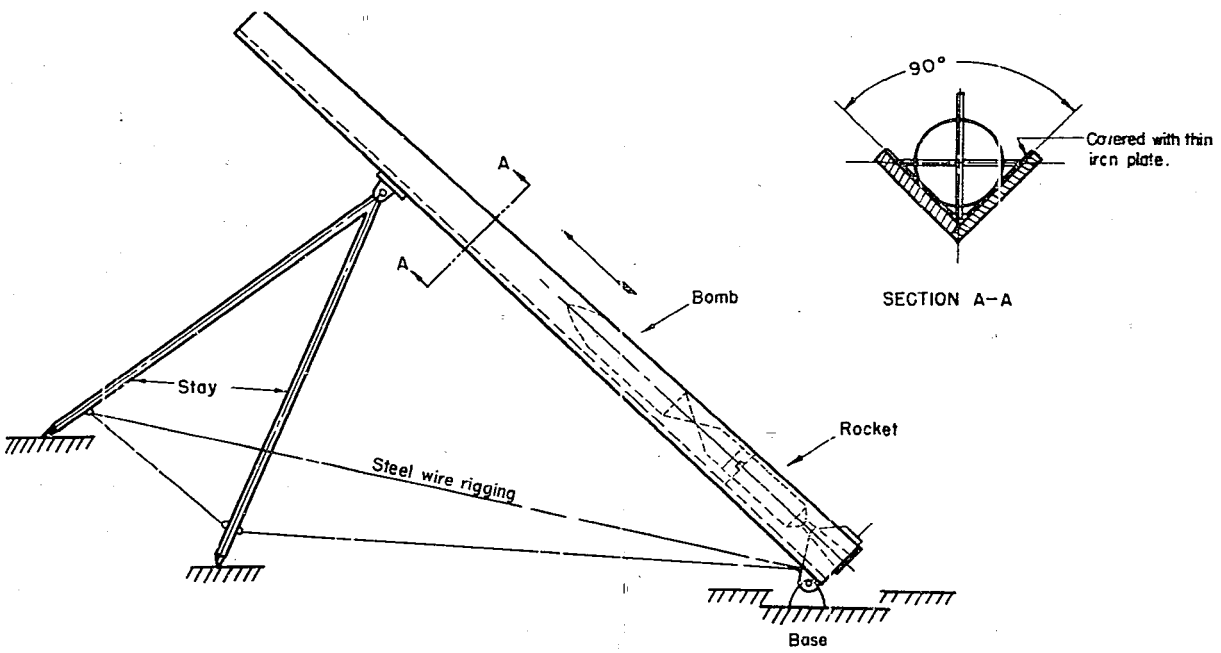


*Figure 1(B)3*
*ROCKET-BOMB LAUNCHING STAND*

*ENCLOSURE (B)3, continued*

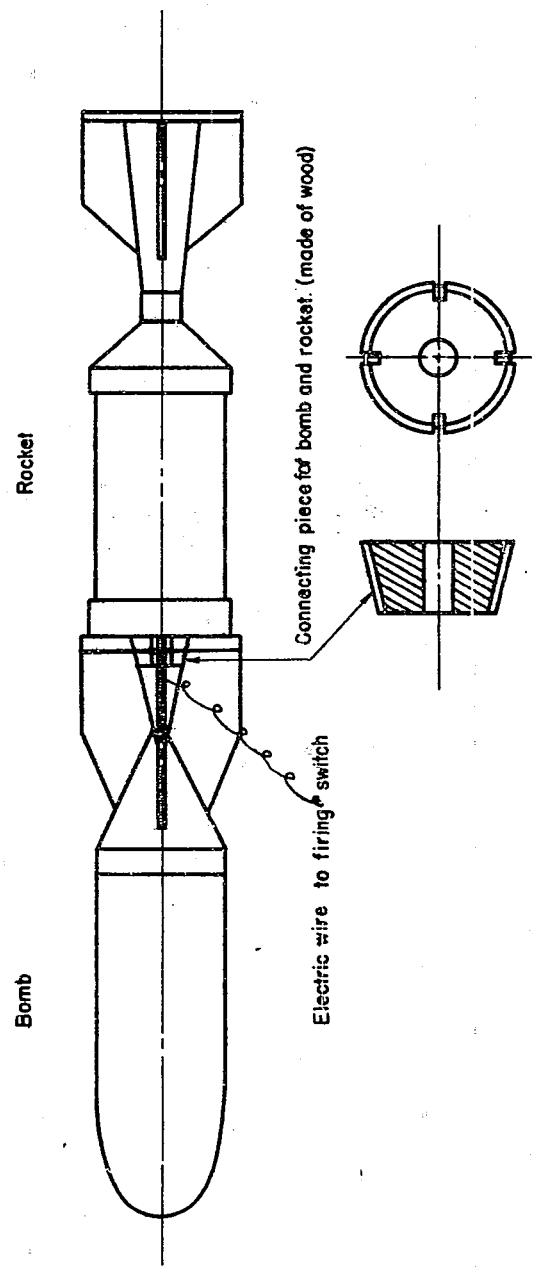


*Figure 2(B)3*
*CONNECTION OF BOMB AND ROCKET*

# ENCLOSURE (B) 4

## THE THEORY OF COMBUSTION OF PROPELLANTS AND ROCKET PROPELLING BALLISTICS

By Lieutenant Commander K. MATSUSHITA
(Member of the First Naval Technical Depot)

11 February 1946

### PREFACE

It was very difficult for me to make a complete report, because I burned all my reports and experimental data at the time of the end of the War by wrong command. I have described as well as possible the outline of my researches. Therefore, you cannot expect factual completeness in this report, but I have intended to describe the directions of my research and some theoretically interesting problems in their details.

In addition I wish to point out that this report is based on my own practical experiments and research, though there are many other reports of researches on propellants by Mr. SENDO, Mr. HINO and Mr. IWAI, who were the members of the research division of the Second Naval Explosive Depot.

*ENCLOSURE (B)-4, continued*

## CHAPTER 1 - INTRODUCTION

My research on powder rockets began in August 1944. Since then I have been trying to make practical applications, to continue theoretical research on this problem which had many matters as yet not solved, and to conduct practical experiments because it was urgently required to put the powder rocket into practical use (as an accelerating method at the time of take-off and during flight for airplanes, or as the main or auxiliary power of the "OKA" and many other special attack planes).

In this research the most theoretically interesting problem is consideration of the solution of the "Peak-pressure Reducing Method".

To this problem I have been able to find at last a possible solution, but when it was found the war had ended. As this problem is the most important item in the practical application of the powder rocket, then I will describe it in detail as well as I can.

I would like to begin this report with the general theory of gas flow and gradually enter into many particular theories.

## CHAPTER 2 - THERMODYNAMICS OF JET FLOW

### 2-1 Notations

Now I will define the notations used in this chapter.

| | | |
|---|---|---|
| P: | $kg/cm^2$ | absolute pressure |
| v: | $cm^3/kg$ | specific volume |
| γ: | Cp/Cv | ratio of specific heats |
| i: | K cal/kg | total heat |
| Q: | K cal/kg | heat gain from outside (heat from friction is not included) |
| f: | K gm/kg | work done by friction |
| E: | K gm/kg | potential energy |
| w: | m/s | velocity of flow |
| a: | $m^2$ | sectional area of flow |
| G: | kg/s | flowing quantity |

### 2-2 General Fundamental Equations of Flow

As a general fundamental equation of flow we have equation (1) or (2) considering friction and external heat interchange.

$$d(w^2/2g) = -vdp - dE - df \quad \text{.....(1)}$$

$$d(w^2/2g) = -Jdi + JdQ - dE \quad \text{.....(2)}$$

*ENCLOSURE (B)4, continued*

For a gas we can take $dE = 0$, and, if considering no friction, we have $df = 0$; hence, the fundamental equation is:

$$d(w^2/2g) = -vdp \quad \ldots\ldots(3)$$

$$d(w^2/2g) = -Jdi + JdQ \quad \ldots\ldots(4)$$

In the general case we have equation (5) as the equation of continuity which is necessary to solve the problem of flow.

$$\frac{d(aw/v)}{dl} = \frac{d(a/v)}{dt} \quad \ldots\ldots(5)$$

where $l$ = length of flow passage in meters
$t$ = time in seconds

In special cases of flow, we have in every section of the flow passage:

$$aw/v = G = \text{constant} \quad \ldots\ldots(6)$$

## 2-3 Adiabatic Jet Flow

In the case of adiabatic change we have $df = 0$, and $dQ = 0$; therefore, the change of flow velocity from equation (3) becomes:

$$(w_2^2 - w_1^2)/2g = -\int_1^2 vdp \quad \ldots\ldots(7)$$

with the relation $Pv^\gamma = P_1v_1^\gamma = \text{constant}$

Also, from the total heat equation (4), we have

$$(w_2^2 - w_1^2)/2g = J(i_1 - i_2)_{ad} \quad \ldots\ldots(8)$$

and $w_1^2/2g + Ji_1 = w_2^2/2g + Ji_2 = \text{constant} \quad \ldots\ldots(9)$

We put here $(i_1 - i_2)_{ad} = H_{ad}$

In the case when $w_1$ is small, $(P_1 - P_2)$ is large and $H_{ad}$ is large and we can neglect $w_1$ in equations (7), (8) and (9).

We can generally establish the next relation in adiabatic flow from the equations (3) and (6), because these equations can exist in either case, whether the flow is accelerating or retarding.

$$\gamma Pw^2da = a(w_s^2 - w)\,dp \quad \ldots\ldots(10)$$

where $w_s = \sqrt{g\gamma pv} = \sqrt{g(dp/d\rho)_{ad}}$ = sound velocity

and $p$ = gas density.

This equation means that in a convergent passage ($da<0$) there will be a pressure drop if $w < w_s$, i.e. $dP < 0$ and flowing velocity will increase; or if $w > w_s$ there will be a pressure rise and flow velocity will decrease. In the

case of a divergent passage ( $da>0$ ) with $w<w_s$ , pressure will rise and velocity decrease; with $w>w_s$ , pressure will drop and velocity rise.

In adiabatic change we obtain the next equation for $w_2$ by means of integration from equation (3).

$$w_2 = \sqrt{2g \frac{\gamma}{\gamma - 1} P_1 v_1 \{ 1 - (\frac{P_2}{P_1})^{(\gamma-1)/\gamma} \} + w_1^2} \quad \ldots\ldots(11)$$

## 2-4 Jet From a Convergent Nozzle, Critical Pressure

If the initial velocity $w_1$ is negligible, we have the next equation for adiabatic jet flow from a convergent nozzle.

$$w_2 = \sqrt{2g \frac{\gamma}{\gamma - 1} P_1 v_1 \{ 1 - (\frac{P_2}{P_1})^{(\gamma-1)/\gamma} \}} \quad \ldots\ldots(12)$$

Putting $a_0$ for the sectional area of the nozzle, we have:

$$G = a_0 w_2 / v_2 \quad \text{and} \quad P_1 v_1^{\gamma} = P_2 v_2^{\gamma} \quad \text{or} \quad v_2 = v_1 (\frac{P_1}{P_2})^{1/\gamma}$$

therefore

$$G = a_0 \sqrt{2g \frac{\gamma}{\gamma - 1} \frac{P_1}{v_1} \{ (\frac{P_2}{P_1})^{2/\gamma} - (\frac{P_2}{P_1})^{(\gamma+1)/\gamma} \}} \quad \ldots\ldots(13)$$

or

$$a_0 = G \left[ 2g \frac{\gamma}{\gamma - 1} \frac{P_1}{v_1} \{ (\frac{P_2}{P_1})^{2/\gamma} - (\frac{P_2}{P_1})^{(\gamma+1)/\gamma} \} \right]^{-\frac{1}{2}} \quad \ldots\ldots(14)$$

As the condition for the minimum value of $a_0$ , we have obviously from equation (10) $da/dP = 0$ , so in this case it becomes $w_c = w_7 = w_s$ , i.e. when $da/dp = 0$ , flow velocity is equal to the velocity of sound.

In order to get the condition for the minimum value of $a_0$ we have:

$$\frac{d}{d(P_2/P_1)} \{ (\frac{P_2}{P_1})^{2/\gamma} - (\frac{P_2}{P_1})^{(\gamma+1)/\gamma} \} = 0 \quad \ldots\ldots(15)$$

so that we may consider the maximum value of

$$\{ (\frac{P_2}{P_1})^{2/\gamma} - (\frac{P_2}{P_1})^{(\gamma+1)/\gamma} \}.$$

We can get $P_c$ , i.e. $P_2$ , for the minimum value of $a_0$ in

$$(\frac{P_c}{P_1}) = \{ \frac{2}{\gamma + 1} \}^{\gamma/(\gamma-1)} \quad \ldots\ldots(16)$$

where $P_c$ = the critical pressure for initial pressure $P_1$
and $w_c = w_2$ for the case of $P_2 = P_c$.

Putting $P_2$ for the pressure out of the nozzle, the equations of jet velocity and quantity are different according to whether $P_2 \gtreqless P_c$

*ENCLOSURE (B)4, continued*

a) $P_2 > P_c$.

The total energy from $P_1$ to $P_2$ changes to velocity, and jet velocity becomes:

$$w_2 = \sqrt{2g \frac{\gamma}{\gamma - 1} \{ 1 - (\frac{P_2}{P_1})^{(\gamma+1)/\gamma} \} P_1 v_1}$$

or $$w_2 = \sqrt{2gJ (i_1 - i_2)_{ad}} = 91.51 \sqrt{H_{ad}}$$

Putting $a_o$ for the minimum sectional area of the mouth of nozzle, the flow quantity G becomes:

$$G = a_o \sqrt{2g \frac{\gamma}{\gamma - 1} \{(\frac{P_2}{P_1})^{2/\gamma} - (\frac{P_2}{P_1})^{(\gamma+1)/\gamma} \} (\frac{P_1}{v_1})} \quad \text{in Kg/s}$$

Letting $$\Phi = \sqrt{2g \frac{\gamma}{\gamma - 1} \{ 1 - (\frac{P_2}{P_1})^{(\gamma-1)/\gamma} \}}$$

$$\Psi = \sqrt{2g \frac{\gamma}{\gamma - 1} \{(\frac{P_2}{P_1})^{2/\gamma} - (\frac{P_2}{P_1})^{(\gamma+1)/\gamma} \}} = \Phi (\frac{P_2}{P_1})^{1/\gamma}$$

we have $$w_2 = \Phi \sqrt{P_1 v_1} \qquad G = \Psi a_o \sqrt{\frac{P_1}{v_1}}$$

b) $P_2 = P_c$.

$P_2/P_1 = P_c/P_1$ then $w_2 = w_c$, $\Phi = \Phi_c$ and the values of G and $\Psi$ reach their maximun, i.e.

$$w_c = \sqrt{2g \frac{\gamma}{\gamma + 1} P_1 v_1} = \Phi \sqrt{P_1 v_1} \quad \ldots\ldots(17)$$

$$= 91.51 \sqrt{(i_1 - i_c)_{ad}} \quad \ldots\ldots(18)$$

$$G_{max} = a_o \{\frac{2}{\gamma + 1}\}^{1/(\gamma-1)} \sqrt{2g \frac{\gamma}{\gamma + 1} \frac{P_1}{v_1}}$$

$$\Psi_{max} = \Psi_{max} a_o \sqrt{\frac{P_1}{v_1}} \quad \ldots\ldots(19)$$

c) $P_2 < P_c$.

The pressure at the section of the mouth of the nozzle cannot drop to $P_2$ and at mouth pressure becomes $P_c$, so that only the energy from $P_1$ to $P_c$ i.e. $-\int_1^c v dp = J(i_1 - i_c)_{ad}$, changes to velocity in the nozzle and expansion from $P_c$ to $P_2$ is done outside of the nozzle. Thus the energy of this part cannot change to velocity and the jet velocity becomes the same value as given by equations (17) or (18), independently of $P_2$. The flow quantity is given by equation (19). We can never get a velocity higher than the speed of scund with a convergent nozzle.

*ENCLOSURE (B)4, continued*

## 2-5 Jet Flow From a Divergent Nozzle

At the section $a_0$ (see Figure 1(B)4) pressure has the value $P_c$, the critical pressure, and velocity is $w_c$, given by equations (17) or (18), i.e. the velocity of sound. Flow velocity rises more and more from sound velocity at the constriction ($a_0$) along the divergent passage. $a_2/a_0$ is the ratio of divergency.

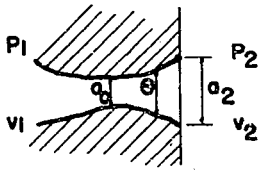


*Figure 1(B)4*
*CROSS SECTION OF DIVERGENT NOZZLE*

The ratio of divergency in the case in which all energy from $P_1$ to $P_2$ changes to velocity, is a function of $P_2/P_1$ and is given by the following equation:

$$\frac{a_2}{a_0} = \left\{\frac{2}{\gamma+1}\right\}^{1/(\gamma-1)} \sqrt{\frac{\gamma-1}{\gamma+1} \Big/ \left(\frac{P_2}{P_1}\right)^{2/\gamma} - \left(\frac{P_2}{P_1}\right)^{(\gamma+1)/\gamma}} \quad \text{.....(20)}$$

because

$$G = a_2 w_2 / v_2 = a_0 w_c / v_c$$

In this case the value of jet velocity is given as:

$$\left.\begin{aligned} w_2 &= \sqrt{2g \frac{\gamma}{\gamma-1} \left\{1 - \left(\frac{P_2}{P_1}\right)^{(\gamma-1)/\gamma}\right\} P_1 v_1} = \Phi \sqrt{P_1 v_1} \\ &= \sqrt{2gJ (i_1 - i_2)_{ad}} = 91.51 \sqrt{H_{ad}} \end{aligned}\right\} \text{.....(21)}$$

and the flow quantity is given by equation (19), that is

$$G_{max} = \Psi_{max} \, a_0 \sqrt{\frac{P_1}{v_1}} = \Psi a_2 \sqrt{\frac{P_1}{v_1}} \quad \text{.....(22)}$$

In a nozzle which has a smaller mouth sectional area than $a_2$ it is impossible to change all the energy to the extent of $P_2$ velocity and a part of it is lost.

In a nozzle which has a mouth of too large a sectional area, pressure drops a value lower than $P_2$ and velocity increases, but at the mouth, pressure is compressed again to $P_2$ and velocity is decreased to the value corresponding to $P_2$. In this case a shock wave occurs in the flow and results in an energy loss.

## 2-6 Case With Friction

The work done by friction returns to the gas in the form of heat.

Putting $\zeta$ as the coefficient of friction loss and $\phi$ as coefficient of velocity we have $H_f = \zeta H_{ad}$ $\qquad \phi = w_2/w_{2ad}$

$$H_f = \zeta H_{ad} = (1 - \phi^2) w_{2ad}^2 / 2gJ$$

$$\zeta = 1 - \phi^2 \quad \text{.....(23)}$$

*ENCLOSURE (B)4, continued*

$$H/H_{ad} = 1 - \zeta = \phi^2 = \text{nozzle efficiency}$$

If $H_f$(K cal/kg) is friction loss and H is true heat drop,

$$H_f = (w_{2ad}^2 - w_2^2) / 2gJ = H_{ad} - H$$

and $$(w_2^2 - w_1^2) / 2g = \int_1^2 vdp - \int_1^2 df = J(i_1 - i_2) = JH$$

If we neglect $w_1$, we can get the following equation for jet velocity:

$$w_2 = \phi\Phi \sqrt{(P_1v_1)} = 91.51\,\phi \sqrt{H_{ad}} = 91.51 \sqrt{H} \quad \text{.....(24)}$$

For a convergent nozzle, if $P_2 > P_c$, we have

$$G = w_2 a_0 / v_2 = \phi\Phi a_0 \sqrt{P_1 v_1 / v_2} \quad \text{.....(25)}$$

For a divergent nozzle, if the ratio of divergency is compatible with $P_2/P_1$, we have

$$G = w_2 a_2 / v_2 = \phi\Phi a_2 \sqrt{P_1 v_1 / v_2} \quad \text{.....(26)}$$

With $\mu$ the coefficient of flow-out, we have

$$\left.\begin{aligned} G &= \mu G_{ad} = \mu w_{2ad} a_0 / v_{2ad} \quad \text{for convergent nozzle} \\ &= \mu w_{2ad} a_2 / v_{2ad} \quad \text{for divergent nozzle} \end{aligned}\right\} \quad \text{.....(27)}$$

For a nozzle: $$\mu = \phi v_{2ad} / v_2 \cong \phi \quad \text{.....(28)}$$

For an orifice, putting $\alpha$ as the coefficient of vena contracta:

$$G = w_2 \alpha a_0 / v_2 = \mu w_{2ad} a_0 / v_{2ad}$$

$$\mu = \alpha\phi v_{2ad} / v_2 \cong \alpha\phi \cong \alpha \quad \text{.....(29)}$$

## CHAPTER 3
## THEORETICAL EQUATIONS OF JET FLOW IN THE CASE OF "EXPLOSIVE GAS"

### 3-1 Notations

In this chapter we use several different notations as follows:

$\tau_0$: $^oK$ = Temperature of explosion

$\tau_1$: $^oK$ = Temperature of combustion gas of rocket

f: $kg/cm^2$ . liter/kg = Force of explosive or specific energy,

$v_0$: liter/kg = Gas volume i.e. volume of 1 kg of gas at $0^oC$ and 1 atm.

*ENCLOSURE (B)4, continued*

$\omega$: Kg = Weight of charge

T: Kg = Thrust

t: sec = Combustion time of propellant

$P_1$, $P_2$, $P_c$, etc., have the same meaning as before so that suffix 1 means the pressure in combustion chamber and suffix 2 shows the pressure at the mouth of nozzle i.e. the back pressure. Pressures are absolute.

## 3-2 Relations Among Characteristic Values of Explosives

The characteristic values f, $\tau_0$, $v_0$, etc. are defined by the composition of an explosive and it is possible to calculate these values from the reaction formulae by means of heat calculations. It is also possible to get these values experimentally with any closed explosion chamber.

"f" represents the energy of one kilogram of combustion gas at its explosion temperature, $\tau_0$, and its unit are kg/cm$^2$ . liters/kg or atm . liters/kg.

$$f = \frac{1 \text{ (atmosphere)} \times v_0 \text{ (liter)}}{273.2} \qquad \tau_0 = \eta R \tau_0 \quad \text{(atmosphere-liter/Kg)}$$

$$= 1.033\, v_0 \tau_0 / 273.2 \quad \text{Kg/cm}^2 \times \text{liter/Kg} \qquad \ldots\ldots\ldots\ldots\ldots\ldots\ldots\ldots\ldots\ldots (30)$$

and $P_1 v_1 / \tau_1 = 1 \times v_0 / 273.2$

We may consider this equation approximately true. It cannot be strictly substantiated, because the combustion gas is not a complete gas and it is considered that the composition of this combustion gas will be a little different from that resulting from a complete combustion because the explosive burns incompletely if $\tau_1$ is considerably smaller than $\tau_0$.

Therefore, $P_1 v_1 = v_0 \tau_1 / 273.2$

$$v_0 = \frac{f}{1.033} \frac{273.2}{\tau_0}$$

$$\therefore P_1 v_1 = \frac{f}{1.033} \frac{\tau_1}{\tau_0} \quad \text{or} \quad v_1 = \frac{1}{P_1} \frac{f}{1.033} \frac{\tau_1}{\tau_0} \qquad \ldots\ldots\ldots\ldots\ldots\ldots\ldots\ldots (31)$$

Here the unit of f is kg/cm$^2$ • liter/kg.

## 3-3 The Values $P_c$ and $w_c$

From the last chapter we have

$$\frac{P_c}{P_1} = \left\{\frac{2}{\gamma + 1}\right\}^{\gamma/(\gamma-1)}$$

$$w_c = \phi \sqrt{2g \frac{\gamma}{\gamma + 1} P_1 v_1} = \phi \sqrt{g \gamma P_c v_c} = \phi \times \text{sound velocity}$$

*ENCLOSURE (B)4, continued*

From equation (31) we have

$$w_c = \phi \sqrt{2g \frac{\gamma}{\gamma+1} \frac{f}{1.033} \frac{\tau_1}{\tau_0}} \quad \cdots\cdots(32)$$

Namely, $w_c$ will be a function of combustion temperature, $\tau_1$, only because f, $\tau_0$ and $\gamma$ are constant for a certain explosive. However, we must investigate theoretically and experimentally the relation between $P_1$ and $\tau_1$ because it may be considered that $\tau_1$ changes with $P_1$.

## 3-4 Flow Velocity, $w_2$ of Jet

From equation (21) and (24) of the last chapter

$$w_2 = \phi \sqrt{2g \frac{\gamma}{\gamma-1} \left\{ 1 - \left(\frac{P_2}{P_1}\right)^{(\gamma-1)/\gamma} \right\} P_1 v_1}$$

Here the ratio of divergency $a_2/a_0$ is suitable for the value of $P_1$ and $P_2$.

From the equation (31) it follows that:

$$w_2 = \phi \sqrt{2g \frac{\gamma}{\gamma-1} \left\{ 1 - \left(\frac{P_2}{P_1}\right)^{(\gamma-1)/\gamma} \right\} \frac{f}{1.033} \frac{\tau_1}{\tau_0}} \quad \cdots\cdots(33)$$

Namely, $w_2$ becomes a function of $P_1$ and $\tau_1$

## 3-5 Relation of Flow Quantity G

From equation (27)

$$G = \mu G_{ad} = \mu w_{c\,(ad)}\, a_0 / v_{c(ad)}$$

$$\mu = \phi\, v_{c(ad)}/v_c \cong \phi \quad \text{and from} \quad P_1 v_1^{\gamma} = P_c v_{c(ad)}^{\gamma}$$

$$1/v_{c\,(ad)} = \left(\frac{P_c}{P_1}\right)^{1/\gamma} \frac{1}{v_1}$$

Therefore

$$G = \phi a_0 \left\{ \frac{2}{\gamma+1} \right\}^{1/(\gamma-1)} \sqrt{2g \frac{\gamma}{\gamma+1} \left(\frac{P_1}{V_1}\right)}$$

But from

$$\sqrt{P_1/v_1} = P_1 \sqrt{1/P_1 v_1}$$

We have

$$G/a_0 = \phi \left\{ \frac{2}{\gamma+1} \right\}^{1/(\gamma-1)} P_1 \sqrt{2g \frac{\gamma}{\gamma+1} \cdot \frac{1}{P_1 v_1}}$$

Namely

$$= \phi \left\{ \frac{2}{\gamma+1} \right\}^{1/(\gamma-1)} P_1 \sqrt{2g \frac{\gamma}{\gamma+1} \cdot \frac{1.033}{f} \cdot \frac{\tau_0}{\tau_1}} \quad \cdots\cdots(34)$$

Therefore, we can show $G/a_0$ as a function of $P_1$ and $\tau_1$.

*ENCLOSURE (B)4, continued*

3-6 Relation Between Mean Thrust, $T_m$, Combustion Time, t, and Weight of Charge, $\omega$.

If the charge $\omega$ completes its combustion in time, t, the mean quantity of gas generated in every second is given as $\omega/t/kg/s$, and if we neglect the weight of gas which remains in the combustion chamber after the end of combustion (for it is very small), we may consider that the mean quantity of gas flow per second is equal to the mean quantity of gas generated per second, so that it may be written as follows:

$\omega/t$ - mean quantity of gas flow and its mass is $\omega/(t \cdot g)$

Then as the mean thrust $T_m$ is given as the product of mean flow quantity and flow velocity, we have

$$T_m = \frac{\omega}{t} \cdot \frac{w_2}{g} \quad \cdots\cdots(35)$$

$$T_m \cdot t/\omega = w_2/g$$

$$\frac{T_m \cdot t}{\omega} = \phi \sqrt{\frac{2}{g} \cdot \frac{\gamma}{\gamma - 1} \left\{ 1 - \left(\frac{P_2}{P_1}\right)^{(\gamma-1)/\gamma} \right\}} \frac{f}{1.033} \cdot \frac{\tau_1}{\tau_0} \quad \cdots\cdots(36)$$

Thus, obviously from equation (36), the value which is given with $T_m \times t$ or impulse $T_m \times t$ in time t, divided by the weight of charge, namely, the value of impulse per kilogram of explosive, becomes a function of $P_1$ and $\tau_1$, and when inner pressure $P_1$ and combustion temperature $\tau_1$ are constant, it is proportional to $\phi$, if $a_2/a_0$ is compatible with $P_1/P_2$. Here we consider, of course, that $P_2$ is constant. Further, in a nozzle whose $a_2/a_0$ is not compatible with $P_1/P_2$, this value is smaller than that obtained from equation (36).

3-7 Relation Between Thrust, T, and Inner Pressure, $P_1$

$$T = G/g \cdot w_2$$

$$\frac{T}{a_0} = \phi \left\{ \frac{2}{\gamma + 1} \right\}^{1/(\gamma-1)} \sqrt{\frac{2}{g} \frac{\gamma}{\gamma + 1} \frac{P_1}{v_1}} \quad \phi \sqrt{2g \frac{\gamma}{\gamma - 1} \left\{ 1 - \left(\frac{P_2}{P_1}\right)^{(\gamma-1)/\gamma} \right\} P_1 v_1}$$

$$\frac{T}{a_0} = 2\gamma\phi^2 \left\{ \frac{2}{\gamma + 1} \right\}^{1/(\gamma-1)} P_1 \sqrt{\frac{1}{\gamma^2 - 1} \left\{ 1 - \left(\frac{P_2}{P_1}\right)^{(\gamma-1)/\gamma} \right\}} \quad \cdots\cdots(37)$$

and so $T/a_0$ is a function of $P_1$ and, if $P_2/P_1$ is small, it is nearly proportional to $\beta$.

3-8 Change in Thrust With Variation of $P_2$

Now we put T' as the value of thrust in the case in which $P_1$ is constant and $P_2$ changes its value, and putting T as the value of thrust in the case in which $P_1$ is constant and $P_2 = 1\ kg/cm^2$, we have:

$$\frac{T'}{T} = \sqrt{\left\{1 - \left(\frac{P_2}{P_1}\right)^{(\gamma-1)/\gamma}\right\} / \left\{1 - \left(\frac{1}{P_1}\right)^{(\gamma-1)/\gamma}\right\}} \quad \cdots\cdots(38)$$

*ENCLOSURE (B)4, continued*

From equation (38) we can calculate the ratio of thrust increase in the case in which $a_2/a_0$ changes its value to suit the change of value $P_2/P_1$ according to change of altitude. We must remember that, if $a_2/a_0$ is constant, it will be different.

If we use a nozzle in which $a_2/a_0$ is compatible with $P_2 = 1$ kg/cm$^2$ on the ground, the pressure difference $(1-P_2)$ kg/cm$^2$ at high altitude does not change to velocity, because only the energy of the pressure difference, $(P_1 - 1)$ kg/cm$^2$, changes to velocity $w_2$ though the back pressure becomes $P_2 < 1$ kg/cm$^2$.

Therefore, the velocity or thrust T does not increase over the value T and we have $T = T'$. In the case in which we take the value $a_2/a_0$ greater than is consistent with $P_2 = 1$ kg/cm$^2$, and if we show the pressure meant by this value of $a_2/a_0$ as $P_2'$, then it becomes $T'>T$ at the altitude in which $P_1<1$. In an altitude whose back pressure $P_2$ is greater than $P_2'$ there is some loss of energy; therefore, in an altitude whose back pressure $P_2<P_2'$ the value of $T'/T$ will be obviously greater than the value which is given by equation (38).

Of course, $T = T'$ if we take the value $a_2/a_0$ smaller. However, we assumed that $P_1$ is constant.

## CHAPTER 4
## GENERAL CALCULATION CURVES IN A KIND OF PROPELLANT, "TOKU FDT$_6$"

### 4-1 Characteristic Values of "TOKU FDT$_6$"

$f = 10{,}060$ kg/cm$^2$ · liter/kg

$\tau_0 = 2720^\circ$ K

$\gamma = 1.25$ (assumed)

### 4-2 General Calculation Curves

With the propellant "Toku FDT$_6$" as an example, I have obtained several curves by means of calculation with the equations which were developed in the preceding chapter. The relationships on which the curves are produced are outlined below, and in Figures 2(B)4 through 10(B)4.

| | | | |
|---|---|---|---|
| Figure 2(B)4 | Relation between $P_1$, $V_1$, $\tau_1$, | from equation (31) | |
| Figure 3(B)4 | Relation between $P_1$ and $P_c$ | from equation (16) | |
| Figure 4(B)4 | Relation between $w_c$ and $\tau_1$ | from equation (32) | $\phi = 1$ |
| Figure 5(B)4 | Relation between $a_2/a_0$ and $P_1/P_2$ | from equation (20) | $\gamma = 1.25$ |
| Figure 6(B)4 | Relation between $w_2$, $P_1$, $\tau_1$ | from equation (33) | $\phi=1$, $P_2=1$ kg/cm$^2$ |
| Figure 7(B)4 | Relation between $G/a_0$, $P_1$, $\tau_1$ | from equation (34) | $\phi = 1$ |
| Figure 8(B)4 | Relation between $(T_m \times t)/\omega$, $P_1$, $\tau_1$ | from equation (36) | $\phi=1$, $P_2=1$ kg/cm$^2$ |
| Figure 9(B)4 | Relation between $T/a_0$, $P_1$ | from equation (37) | $\phi=1$, $P_2=1$ |
| Figure 10(B)4 | Relation between $\tau/\tau_1$, $P_2$, $P_1$ | from equation (38) | |

*ENCLOSURE (B)4, continued*

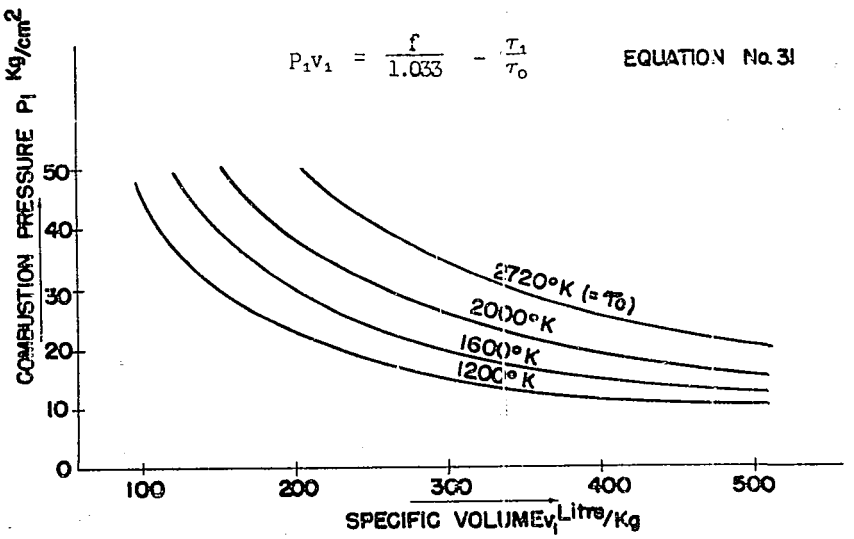


*Figure 2(B)4*
*RELATION BETWEEN $P_1$, $V_1$, AND $\tau_1$*

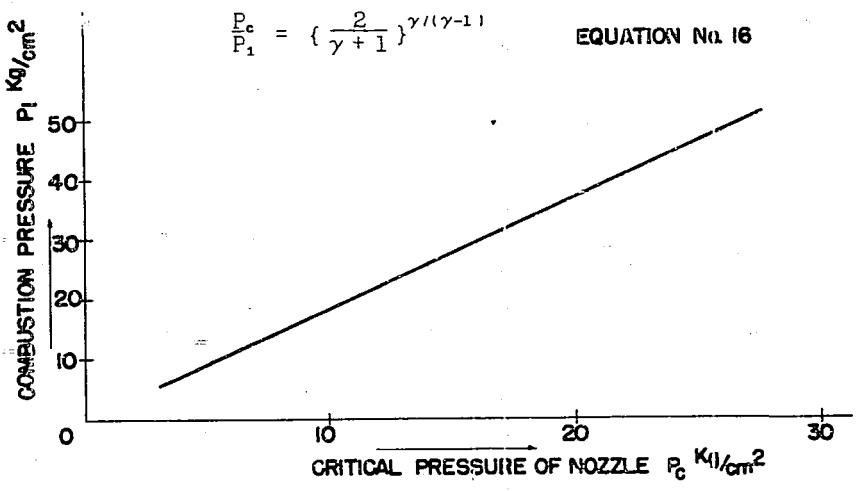


*Figure 3(B)4*
*RELATION BETWEEN $P_c$ AND $P_1$*

*ENCLOSURE (B)4, continued*

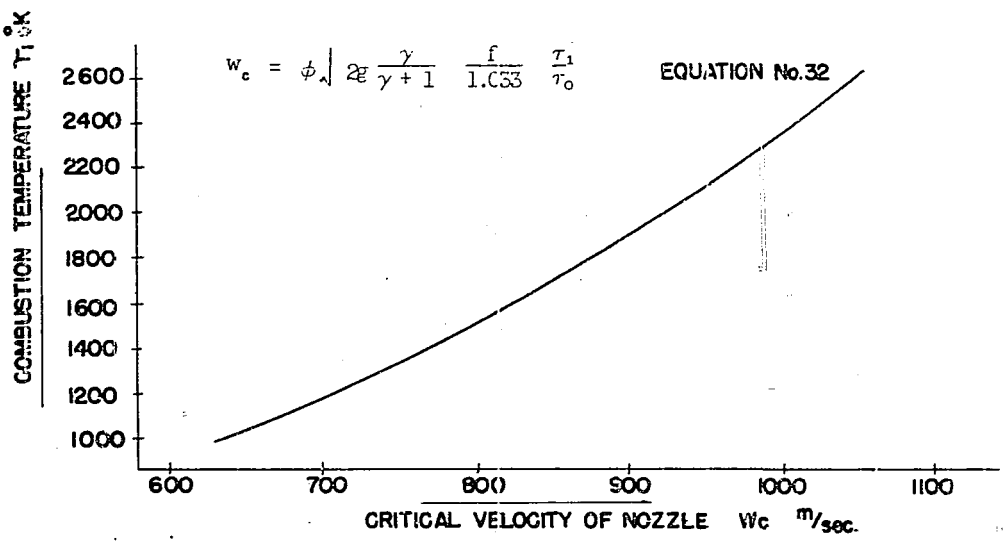


*Figure 4(B)4*
*RELATION BETWEEN $W_c$ AND $\tau_1(\phi = 1)$ FOR "TOKU FDT$_6$"*

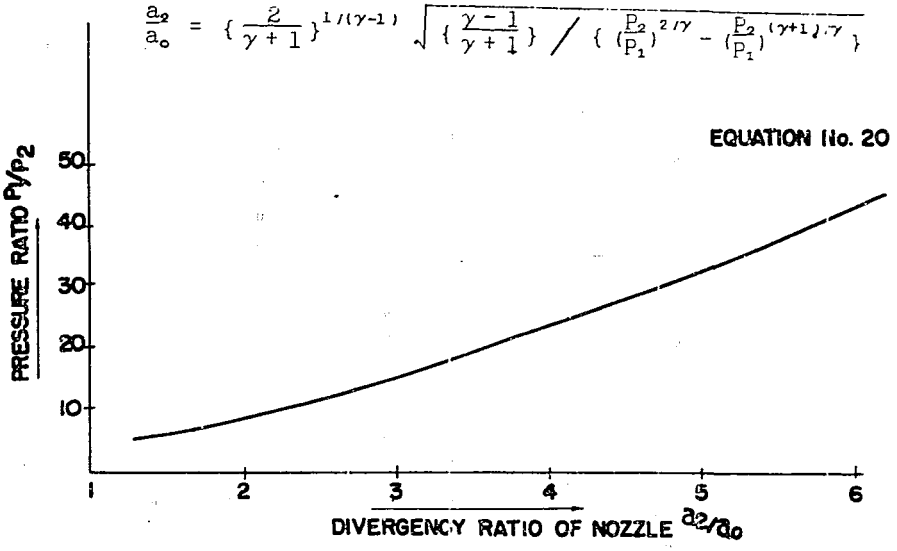


*Figure 5(B)4*
*RELATION BETWEEN $a_2/a_0$ AND $P_1/P_2$ (FOR $\gamma = 1.25$)*

*ENCLOSURE (B)4, continued*

$$W_2 = \phi \sqrt{2g \frac{\gamma}{\gamma - 1} \{1 - (\frac{P_2}{P_1})^{(\gamma-1)/\gamma}\} \frac{f}{1.033} \frac{\tau_1}{\tau_0}}$$ EQUATION No.33

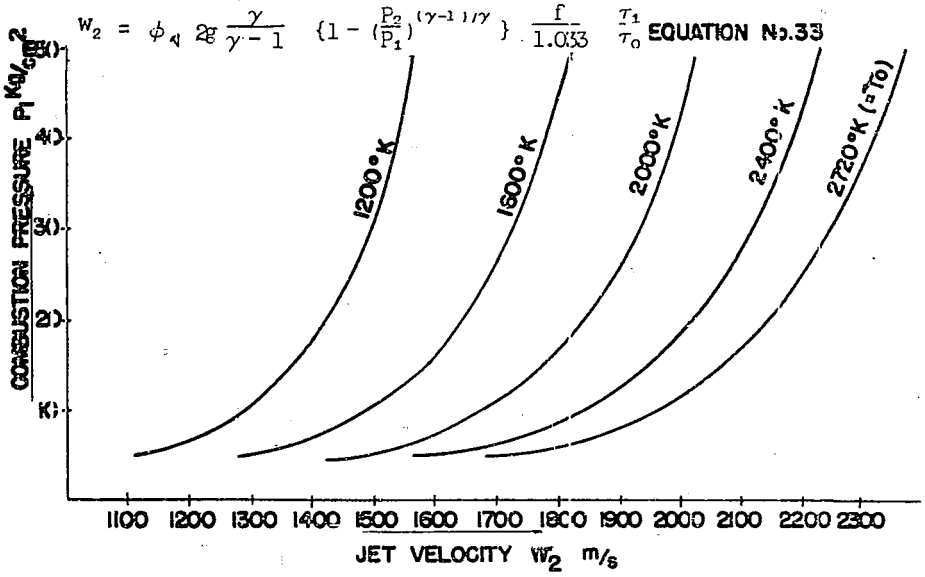


*Figure 6(B)4*
*RELATION BETWEEN $w_2$, $P_1$ AND $\tau_1$ FOR "TOKU FDT$_6$"*

$$\frac{G}{a_0} = \phi \{\frac{2}{\gamma + 1}\}^{1/(\gamma-1)} P_1 \sqrt{2g \{\frac{\gamma}{\gamma + 1}\} \frac{1.033}{f} \frac{\tau_0}{\tau_1}}$$ EQUATION No.34

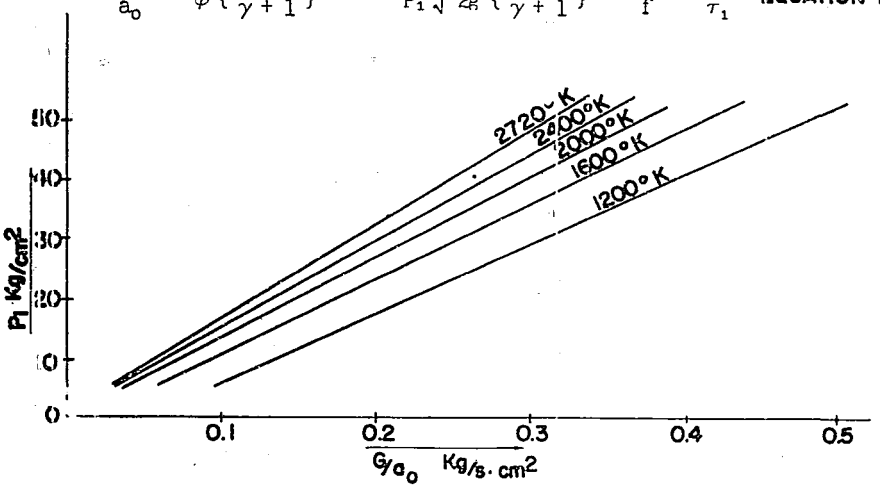


*Figure 7(B)4*
*RELATION BETWEEN $G/a_0$, $P_1$, $\tau_1$ [$\phi$ = 1] FOR "TOKU FDT$_6$"*

*ENCLOSURE (B)4, continued*

$$\frac{T_m \cdot t}{\omega} = \phi\sqrt{\left[\frac{2}{g}\left\{\frac{\gamma}{\gamma-1}\right\}\left\{1-\left(\frac{P_2}{P_1}\right)^{(\gamma-1)/\gamma}\right\}\frac{f}{1.033}\frac{\tau_1}{\tau_0}\right]} \quad \text{EQUATION No. 36}$$

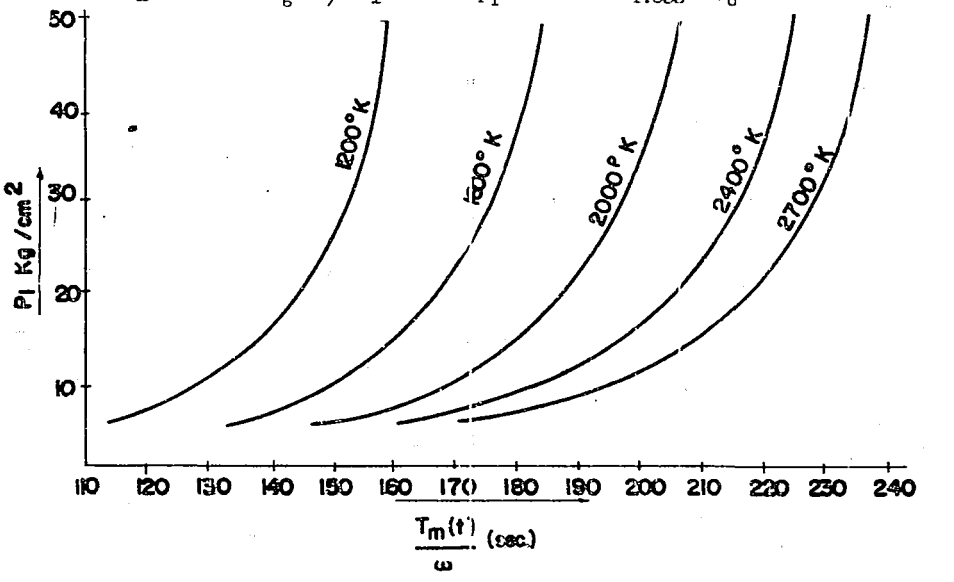


*Figure 8(B)4*

*RELATION BETWEEN* $\frac{Tm\ (t)}{\omega}$, $P_1$ *AND* $\tau_1$ *(*$\phi = 1$, $P_2 = .1$ kg/cm$^2$

*FOR "TOKU FDT$_6$"*

$$\frac{T}{a_0} = 2\gamma\phi^2\left\{\frac{2}{\gamma+1}\right\}^{1/(\gamma-1)} P_1\sqrt{\frac{1}{\gamma^2-1}\left\{1-\left(\frac{P_2}{P_1}\right)^{(\gamma-1)/\gamma}\right\}} \quad \text{EQUATION No. 37}$$

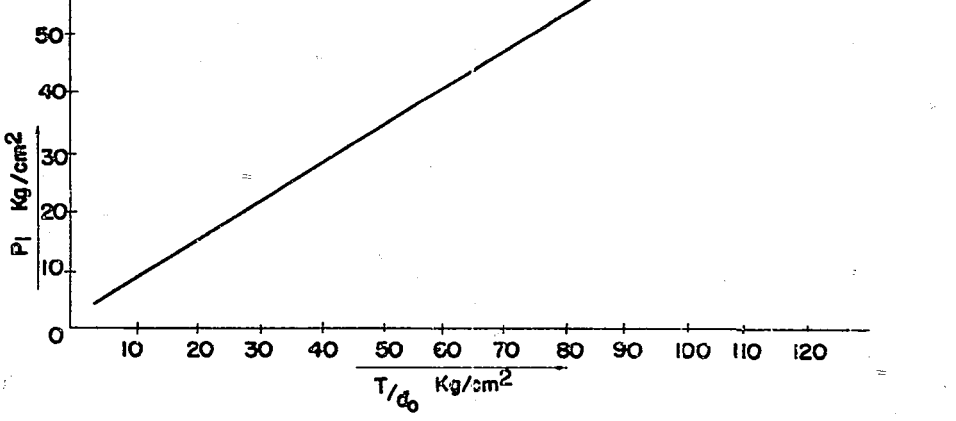


*Figure 9(B)4*

*RELATION BETWEEN* $T/a_0$ *AND* $P_1$ *(*$\phi = 1_2$, $P_2 = 1$)

*ENCLOSURE (B)4, continued*

$$\frac{T'}{T} = \sqrt{\{1 - (\frac{P_2}{P_1})^{(\gamma-1)/\gamma}\}} \Big/ \{1 - (\frac{1}{P_1})^{(\gamma-1)/\gamma}\}$$

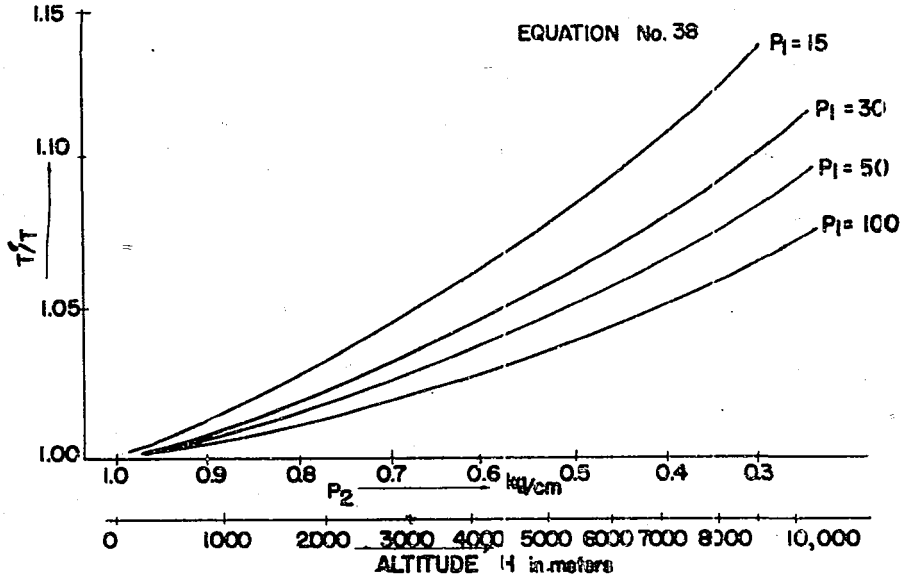


*Figure 10(B)4*

*RELATION BETWEEN* T /T, $P_2$ *AND* $P_1$

## CHAPTER 5
## INTRODUCTION TO ROCKET PROPELLING BALLISTICS

For the theory of combustion of propellants in rockets there are many researches and in the report "Research On Rocket Ballistics" which was published by the Second Naval Explosive Depot on 20 January 1938, it is concluded that:

The pressure equation in combustion is:

$$P = P_0 + (P_1 - P_0)\ z[\xi] \quad \text{.....(39)}$$

The relation between ratio of combustion and combustion time is:

$$\int_0^z \frac{1}{dz\{\phi\ z\ \{P_0 + z\ \xi\ (P_1 - P_2)\}} = A^*t \quad \text{.....(40)}$$

This equation is based on equations (41) and (42),

$$\frac{dz}{dt} = A P \phi z \quad \text{.....(41)}$$

$$P = f \frac{\int_0^z \omega dz - a_0 \zeta \int_0^t Pdt}{c_0 - \frac{\omega}{\gamma}(1 - z) - \eta\{\int_0^z \omega dz - a_0 \zeta \int_0^t Pdt\}} \quad \text{.....(42)}$$

in which A is vibercity and $\phi(Z)$ is a function of form. Here P is the inner

pressure corresponding to $Z = 1$ ($Z$ = ratio of combustion), $P_0$ is the pressure induced by the initiator powder and $\zeta$ is a function of $Z$, $A_0$, $W$, $C_0$, $\phi(Z)$, etc.

$$\zeta = \phi \left\{ \frac{2}{\gamma + 1} \right\}^{1/(\gamma-1)} \sqrt{2g \frac{\gamma}{\gamma + 1} \kappa_\tau}$$

$C_0$: volume of powder chamber in liters

$\eta$ : covolume in liter/kg

$Z$ : ratio of combustion

$\phi$ : coefficient of velocity

$\phi(Z)$ : function of form

But this equation is subject to discussion and if we had some theoretical information about the pressure induced by initiator powder, $P_0$, and about the peak pressure which occurs at the beginning of combustion and so on, then we would have an accurate solution for the combustion theory.

## CHAPTER 6
## GENERAL CONSIDERATION ABOUT THE PRESSURE TIME CURVE DURING COMBUSTION OF PROPELLANTS

### 6-1 The Range of Pressure in Use

The pressure in the combustion chamber of a powder rocket has a very wide range depending on its use and the physical characteristics of the propellant. In general, it is used as follows:

(1) Propelling power of rocket gun, rocket bomb, etc.,
(2) Accelerating airplanes.
(3) Auxiliary power for take-off and main power for rocket-catapulting of planes.

In case (1) it is required to complete combustion and exert a thrust in a very short time, in order to make accurate the trajectory of shot and to make the effective range as long as possible. To utilize the propellant most effectively the thrust must be exerted in a very short time and before the shot will be influenced by the force of gravity. Therefore, it becomes necessary to make combustion velocity as large as possible, namely to use high pressures for a given weight of charge. For this purpose we use a mean combustion pressure of about 50 to 3000 kg/cm$^2$ depending on the thickness and composition of the propellant.

In case (2) the process is controllable and we need not consider the effect of gravity. However, it is required to continue the thrust for as long a time as possible within the allowed range of acceleration value. This is especially true in the case of speed increase aloft. At the same time it is necessary that the rocket be as light as possible. Therefore, the propellant for this use must have slow combustion and be able to maintain combustion at a very low pressure. For this we use pressures of about 5 to 30 kg/cm$^2$.

In case (3) in order to use the rockets effectively as an auxiliary thrust at the time of taking off, it must complete its combustion just before completion of take-off. This time is about three to four seconds for a small plane, ten seconds for a medium sized plane, and about twenty seconds for a large plane. Besides, in the case of a rocket catapult it is necessary to finish the combustion effectively within a limited rail length; it, therefore,

has a time limit and must be very light in weight. In order to pack a certain constant weight of explosive compactly, the proper thickness of propellant must be used. For this purpose we use pressures of about 30 to 50 $kg/cm^2$ depending on composition and the mutual relations between powder thickness, combustion velocity, pressure, and combustion time.

Thus the pressure used has so wide a range that the pressure curves of rockets are naturally different from each other, but generally the forms of the curves have a common tendency.

## 6-2 Form of Pressure-Time Curve

When we begin combustion with a suitable quantity of black powder as the initiator, we obtain pressure-time curves for propellants as shown in Figure 11(B)4 for cordite, tubite and a propellant which maintains a constant surface area.

1. Cordite

In this case a peak pressure occurs at the beginning of combustion. Pressure drops rapidly because the surface area of combustion decreases at once.

2. Tubite

(a) Rapid combustion

In this case the curve will resemble that of case (1), but its slope is less.

(b) Slow combustion

After dropping from the peak value, pressure keeps nearly constant, decreasing slowly.

3. Constant surface area

After the peak is passed, the curve becomes completely flat and it maintains a constant value to the end.

## 6-3 Notations on the Pressure-Time Curve

Hereafter, we will consider the case of tubite and will use the following notations (see Figure 12(B)4):

$P_{max}$: Peak pressure

$P_e$: Pressure at end of combustion

$t_e$: Combustion time

$P_i$: Pressure at the point in which the effect of peak disappears.

$P_i'$: Pressure value traced back along the curve to $t = 0$, assuming no peak.

$P_{mo}$: Theoretical mean pressure $= \int_0^{t_e} P dt / t_e$

$P_m$: Approximate mean pressure. If $t_e$ is large, then

$$P_m = \frac{P_i + P_e}{2}$$

*ENCLOSURE (B)4, continued*

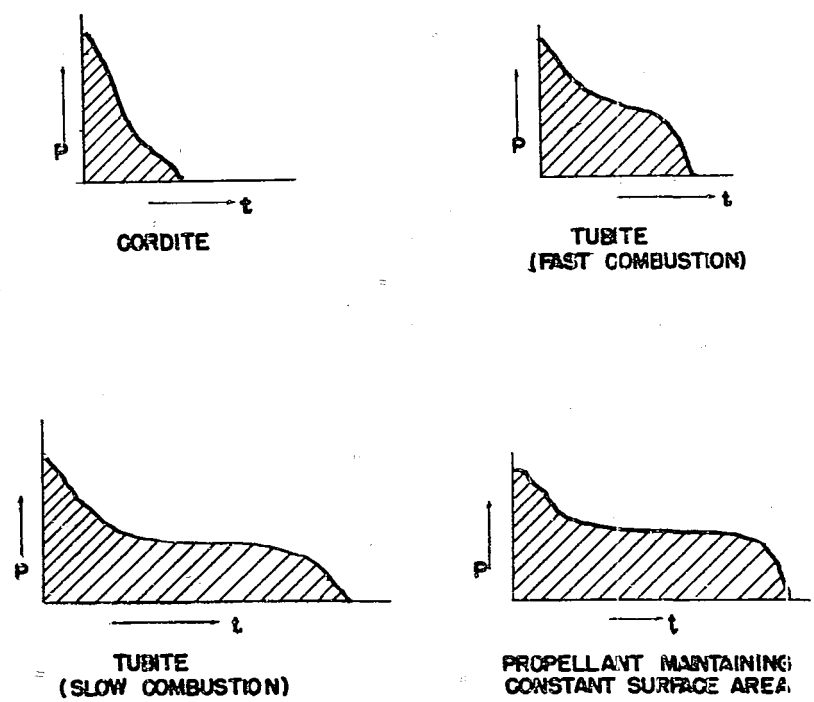


*Figure 11(B)4*
*PRESSURE-TIME CURVES FOR PROPELLANTS*

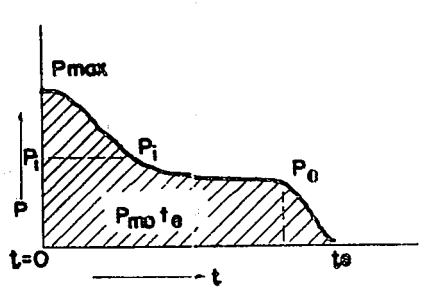


*Figure 12(B)4*
*NOTATIONS ON PRESSURE-TIME CURVE*

*ENCLOSURE (B)4, continued*

## CHAPTER 7
## LEADING TO AN EQUATION FOR PRACTICAL APPROXIMATE CALCULATION BY MEANS OF THE COMBUSTION THEORY OF PROPELLANTS

### 7-1 The Case Considering Loading Density ($\Delta$) and covolume($\eta$)

At a certain time t, a small weight of the gaseous products of combustion remains in the combustion chamber, though almost all has flowed out from the nozzle. If we neglect the weight of black powder ($\omega_s$) and the weight of air which was in the chamber before combustion, then we have the next equation, because the total weight of the gaseous products is equal to the sum of the weight of gas which has flowed out and the weight of remaining gas.

$$\omega\int_0^t dz = \int_0^t a_0\zeta P dt + \rho\{c_0 - V_t - \eta(\omega\int_0^z dz - \int_0^t a_0\zeta P dt)\} \quad \{\omega\int_0^z dz - \int_0^t a_0\zeta P dt\} \quad \{1 + \eta\rho\}$$

$$= \rho\,(c_0 - V_t) \qquad \cdots\cdots(43)$$

where
$$\rho = \frac{1}{v} = P\frac{1.033}{f} - \frac{\tau_0}{T} = \kappa_\tau P \qquad \cdots\cdots(44)$$

We use the same notations as those in the equation (42). This equation is Abel Noble's equation. Then, considering equation (43) at the time $t_e$ or Z = 1, we have

$$\{\omega\int_0^1 dz - \int_0^{t_e} a_0\zeta P dt\}\{1 + \eta\rho_e\} = \rho_e c_0 \qquad (\because V_{t_e} = 0)$$

$$\{\omega - a_0\zeta\int_0^{t_e} P dt\}\{1 + \eta P_e\} = \rho_e c_0$$

Putting $\int_0^{t_e} P dt = P_{mo} t_e$ (absolute pressure)

We have:

$$\{\omega - a_0\zeta P_{mo} t_e\}\{1 + \eta\kappa_\tau P_e\} = \kappa_\tau P_e c_0 \qquad \cdots\cdots(45)$$

In this equation, if we describe $t_e$ as a function of mean combustion velocity $W_m$, we have:

$$\{\omega - a_0\zeta P_{mo}\frac{d}{2w_m}\}\{1 + \eta\kappa_\tau P_e\} = \kappa_\tau P_e c_0$$

where $w_m = d/2t_e$, $t_e = d/2w_m$ (d = thickness)

Dividing both terms by $\omega$ we have:

$$\{1 - \frac{a_0}{\omega}\zeta P_{mo}\frac{d}{2w_m}\}\{1 + \eta\kappa_\tau P_e\} = \kappa_\tau P_e \frac{1}{\omega/c_0} \qquad \cdots\cdots(46)$$

Thus we can obtain experimentally the reaction among these elements, as we are able to get the difference of $P_{mo}$ and $P_e$ as an effect of the end surfaces of the propellant and varying with the ratio of the length of explosive, l, and thickness, d.

*ENCLOSURE (B)4, continued*

If we can consider in the case of slow combustion that $P_{mo} = P_e$ , then we have a practical approximate equation as follows:

$$\left\{ 1 - \frac{a_0}{\omega} \zeta P_{mo} \frac{d}{2W_m} \right\} \left\{ 1 + \eta \kappa_\tau P_{mo} \right\} \cong \kappa_\tau P_{mo} \frac{1}{\omega / c_0} \quad \text{.....(47)}$$

Thus we have an approximate relation among the elements $P_{mo}$, mean combustion velocity $W_m$, nozzle sectional area $a_0$, weight of charge $\omega$, thickness d, loading density $(\Delta = \omega/c_0)$ combustion temperature, etc. From equation (47)

$$X \equiv \kappa_\tau P_{mo} 1/\Delta , \quad Y \equiv 1 + \kappa_\tau \eta P_{mo} , \quad Z \equiv 1 - \frac{a_0}{\omega} \zeta P_{mo} \frac{d}{2W_m}$$

then we have $Z = X/Y$ .....(48)

Here X can be calculated, if $\Delta$ and $P_{mo}$ are given. Y will be possible to calculate too, if $P_{mo}$ is given. Z will become a function of $a_0$ and $\tau$ if $P_{mo}$, $\omega$ and d are given, because $W_m$ is given from the experimental relation between $P_{mo}$ and $W_m$. (See Figure 13(B)4.)

Therefore, if $\tau$ is given, $Z = X/Y$ , where X and Y are constants and Z is a function of $a_0$ . From this relation we can calculate $a_0$ or, if $a_0$ is given, we can get $\tau$.

7-2 The Approximate Equation In the Case In Which the Terms of the Loading Density $\Delta$ and of Covolume $\eta$ Are Neglected.

In equations (47) and (48) we have

$$\kappa_\tau = \frac{1.033}{f} \cdot \frac{\tau_0}{\tau}$$

From experimental data we have $\tau / \tau_0 = 0.5$ to 0.6 or $\tau_0 / \tau = 1.67$ to 2.0, when $f \cong 10{,}000$. Then we can consider $\kappa_\tau = 0$. Therefore, when $P_{mo}$ is small and $\Delta$ is large, we can consider $X \cong 0$, $Y \cong 1$ and, finally, $Z = 0$.
We get, therefore:

$$1 - \frac{a_0}{\omega} \zeta P_{mo} \frac{d}{2W_m} = 0 \quad \text{.....(49)}$$

From this we have the next equation as an approximation for the case in which $P_{mo}$ is small and $\Delta$ is large.

$$\zeta \frac{d}{2W_m} P_{mo} \frac{a_0}{\omega} = 1 \quad \text{.....(50)}$$

We must use this equation with caution since the error will become greater when $P_{mo}$ is large and $\Delta$ is small.

*ENCLOSURE (B)4, continued*

For example, putting $f = 10{,}000$, $\tau_0/\tau = 1.5$, then $\kappa_T = 1/6500$; therefore putting $\Delta = 0.5$ we have as follows:

$X = (2/6500)\, P_{mo}$ (putting $P_{mo} = 50$)

$X = 1/65 = 0.0154$

$Y = 1 + (1/6500)\eta\, P_{mo}$, ($\eta = 1$, $P_{mo} = 50$)

$Y = 1/130 + 1 = 1.007$

$X/Y \cong 0.015$

$Z \cong 0.015$ (In equation (49) we have $Z = 0$)

If $P_{mo} = 50$ and $\Delta = 0.5$, then the error in Z becomes about 1.5%. Therefore, in calculating of $a_0/\omega$ from equation

$$\frac{a_0}{\omega} = \frac{1}{[\zeta\, P_{mo} \cdot \frac{d}{2}\, W_M]}$$

the error becomes about 1.5%.

To calculate the value of $\tau$ from equation (50) given $a_0$, $\omega$ and $P_{mo}$ we have:

$\zeta = \text{constant}/\sqrt{\tau}$ i.e. $\sqrt{\tau} = \text{constant "C"}$

From equation (48) we have

$(1 - \alpha)\sqrt{\tau} = \text{constant "C"}$ where $\alpha = 0.015$ but $P_{mo} = 50$, $\Delta = 0.5$)

$$\tau\,(48) = \frac{C^2}{(1-\alpha)^2} = C^2 \times 1.031$$

$$\tau\,(50) = C^2$$

Therefore, the temperature error due to equation (50) compared to (48) will be about 3% in this case.

The above description of error, of course, depends on the values $P_{mo}$ and $\Delta$. In the case of short combustion time, namely, $P_{mo} \neq P_e$, it will naturally be different.

## 7-3 Consideration Due to Experimental Data About the Approximate Equation

Making practical application of this approximate equation, it might be better first to calculate the rough value of an unknown element using the simple equation (50) and then to settle experimentally its correct value by means of a trial and error method. It is remarkable that the values of mean combustion velocity $W_m$ will only be scattered a little depending on the temperature of the propellant, its gluey grade, etc., though the propellant compositions are the same. Therefore, values of $P_{mo}$ will also scatter a little, so we must consider the values of $P_{mo}$ and $W_m$ referring to an experimental relation between $P_{mo}$ and $W_m$. For example, the author has obtained the following experimental formulae for the propellants "Toku $FDT_6$" and "Toku $DT_2$" by means of his own experiments (see Figures 13 (B)4 and 14(B)4.)

*ENCLOSURE (3)4, continued*

$$W_m = a + b P_{mo} \quad \text{or} \quad \frac{d}{2t_e} = a + b \int_0^{t_e} \frac{Pdt}{t_e} \qquad \text{.....(51)}$$

$$P_{mo} = \frac{d}{2bt_e} - \frac{a}{b}$$

(a and b are constant; d is the thickness of propellant). For "Toku $DT_2$",

$$a = 1.60, \quad b = 0.113$$

For "Toku $FDT_6$" a = 1.55, b = 0.082 ($P_{mo}$ is gauge pressure)

It is very difficult to solve theoretically and mathematically the effect which is given to the value of $W_m$ by the temperature of propellant, its gluey grade, etc., and we must solve this problem by means of much experimental data. This will probably be very difficult.

As for the value of $\tau$, it is influenced considerably by the degree of incomplete combustion, and it is recognized experimentally that the value of $\tau$ will rise, decreasing the amount of black smoke when the value of $P_{mo}$ increases. The composition of the propellant will also enter into the problem. When $\Delta$ is small, the condition of combustion improves and black smoke decreases and it is easily recognized by means of experiment that the value of $\tau$ rises. Therefore, we must calculate $\tau$ from the approximate equation. The value of $\tau$ should be somewhat different from the calculated value, varying with changes of $P_{mo}$ for a constant value of $\Delta$; also $\tau$ should be scattered in accordance with any difference of $\Delta$ for the same value of $P_{mo}$, because in this equation we do not consider the condition of combustion.

The value of $\tau$ given in accordance with the ratio of the heat loss against the heat of combustion of the rocket, should be dependant on the magnitude of heat loss due to radiation and transmission from the wall of the combustion chamber, if the inner pressure and the quantity of flow are essentially constant. It is easily recognized experimentally that the value of $\tau$ decreases in the case in which the heat loss, which is absorbed by the rocket material and lost externally, is larger. Besides, this heat loss inevitably becomes greater when the temperature of the rocket wall or of the outside is lowered; therefore, it is recognized in cold climates that $\tau$ becomes lower and thereby the values of $P_{mo}$, etc. change for the same rocket.

In such a case, if $\tau$ is different for a rocket of the same design, using the same kind of propellant, or if $\tau$ is different, using another propellant, the value of $P_{mo}/W_m$ must become greater for a constant value of $a_0/\omega$ when $\tau$ increases or $\tau/\tau_0$ becomes greater. Since from equation $W_m = a + b P_{mo}$ we have

$$\frac{P_{mo}}{W_m} = \frac{1}{a/P_{mo} + b}$$

the value of $P_{mo}$ becomes greater. Therefore, if $\tau$ or $\tau/\tau_0$ becomes greater, the value of $P_{mo}$ becomes greater for a constant value of $a_0/\omega$. Consequently the value of $W_m$ becomes greater, so that in the same rocket, if $\tau$ increases or in the case in which the same quantity of a different propellant is used and $\tau/\tau_0$ becomes greater, $P_{mo}$ should be greater and $t_e$ should decrease.

*ENCLOSURE (B)4, continued*

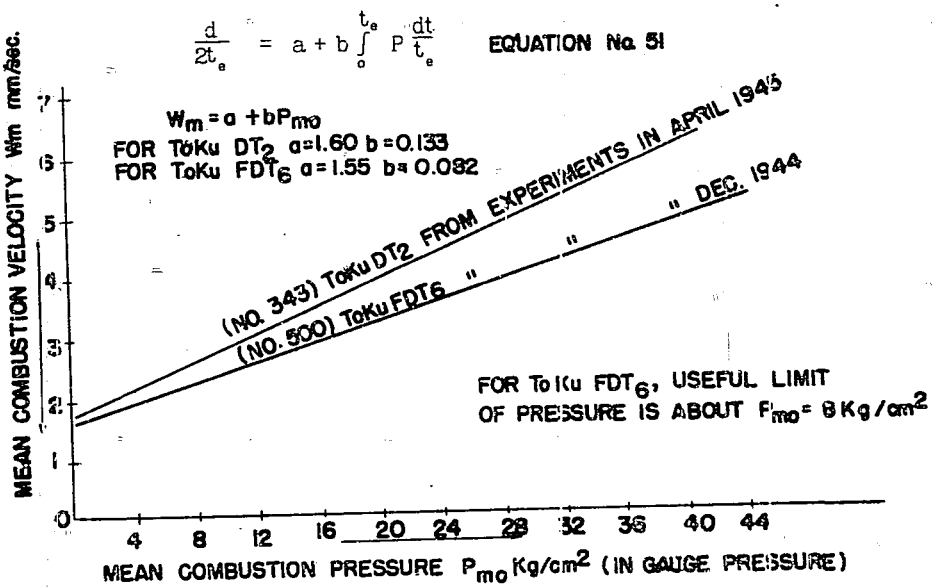


*Figure 13(B)4*
*RELATION BETWEEN $P_{mo}$ AND $W_m$*

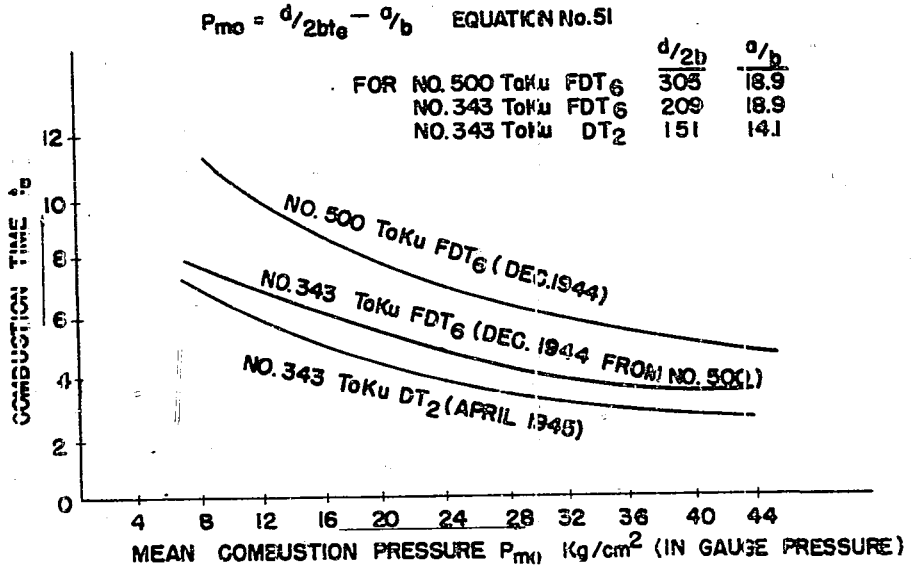


*Figure 14(B)4*
*RELATION BETWEEN $P_{mo}$ AND $t_e$*

*ENCLOSURE (B)4, continued*

## 7-4 Liquid Rockets

For a liquid rocket in equation (43) we can put $V_t = 0$. In equation (46) $f$ and $\tau_0$ are the characteristics of the explosives, so that for a liquid rocket we can get this value by measurement by the same method as for explosives but using a sample of the mixture of the liquid and fuel to be used.

Then $\tau_0$ shows the total weight of mixture jetted from

$$t = 0, \text{ to } t = t \text{ and } P_{mo} = P_e$$

in steady jet condition and, if we put $P_{mo} = P$, then $P$ = constant. Here we are not concerned with peak pressure at the beginning of combustion.

Putting $\omega = Q$ kg and with $q$ kg/s being the quantity of the liquid mixture jetted per second, then $d/2\ W_m = t_e$ and becomes $t = Q/q$.

$$\left\{ 1 - \frac{a_0}{Q} \zeta P \frac{Q}{q} \right\} \left\{ 1 + \kappa_\tau \eta P \right\} = \kappa_\tau P \frac{1}{Q/c_0}$$

$$\left\{ 1 - \frac{a_0}{q} \zeta P \right\} \left\{ 1 + \kappa_\tau \eta P \right\} = \kappa_\tau P \frac{1}{Q/c_0} \quad \text{.....(52)}$$

From this we get the relation of elements for any liquid rocket, but the relation between P and q, etc., must be obtained experimentally as in the relation between $P_{mo}$ and $W_m$ for any explosive.

# CHAPTER 8
# OUTLINE OF THE METHOD OF DESIGNING A POWDER ROCKET

## 8-1 Required Values for Design

Taking m as the mass of a body flying in the sky, v flight velocity and T thrust, and disregarding the resistance of air, we have

$$\int_{V_1}^{V_2} m dv = \int_0^t T dt$$

Therefore, the increase of velocity is proportional to the integration of T by t. Considering air resistance, it will change in accordance with velocity change, so that thisrelation should be a little more complex. We can generally estimate the degree of velocity increase with the value of impulse. There is a relation between velocity increase, thrust and time. Also, since the combustion time t is decided by the function of the powder rocket, we will be able to fix the value of $W_m$ and therefore d for a compatible value of $P_{mo}$.

## 8-2 Determination of Charge

Rocket thrust is given by

$$T = \frac{\omega}{t} \cdot \frac{W_2}{g}$$

*ENCLOSURE (B)4, continued*

Therefore, it is proportional to the product of mean gas flow per second and jet velocity, or we have

$$\frac{T \times t}{\omega} = \frac{W_2}{g} \quad \text{.....(53)}$$

where $W_2$ is possible to calculate with $P_1$, $P_2\tau$, etc. We have from experimental data:

$$\frac{T \times t}{\omega} = 180 \text{ to } 200 \quad \text{.....(54)}$$

This value is for a good nozzle efficiency, for a low nozzle efficiency it might be 140 to 160.

From equation (54) we can get $\omega$ when $\tau \cdot t$ is given.

## 8-3 Determination of Nozzle Dimensions

(1) Method for fixing $a_0$.

It should be generally satisfactory to calculate it with equation (50). There is, however, considerable dispersion in the values of force of explosives and errors due to the effects of temperature of propellant, etc.

$$\frac{a_0}{\omega} \zeta P_{mo} \frac{d}{2W_m} = 1$$

For the value of $\tau/\tau_0$ we may take about 0.55 in calculation of $\zeta$. Thus we can establish an approximate value of $a_0$.

(2) Method for fixing $a_2$

We can fix the value of $a_2$, fixing $a_2/a_0$ corresponding to the given $P_1/P_2$ from the curve of $a_2/a_0 - P_1/P_2$. This curve is based on the value of $\gamma$, and if the character of gas is given, it is possible to fix $a_2$ according to $P_1/P_2$. The question arises how to choose $P_1$ on the pressure curve. Generally, in the case of tubite, if the time developed by combustion reaches several seconds, we should take $P_e$ or less than $P_e$ rather than $P_{mo}$ as the value of $P_1$ for $a_0$, taking into consideration energy loss and thrust peak.

(3) Divergent Angle of the Divergent Part

The author did not experiment specifically on this problem. But from my experience I can say that for a rocket used for an airplane, we may take as its value about 20°. For a large rocket, if pressure is high, $a_2/a_0$ becomes greater; if the angle is small, the length of nozzle becomes great. If its surface is rough, the friction loss becomes greater and its weight is increased because of the additonal nozzle length required.

*ENCLOSURE (B)4, continued*

## CHAPTER 9
## CONSIDERATION ABOUT THE PHENOMENA OF INTERMITTENT COMBUSTION i.e. THE BREATHING PHENOMENA IN COMBUSTION

### 9-1 Explanation of Intermittent Combustion

In the summer of 1944 we succeeded in our experiments on a rocket for airplane use. It was named "4 FH 120" and used propellant "No. 500 Toku FDT6" Propellant data were about nine seconds combustion time, and about 15 kg/cm$^2$ mean pressure. While we made many practical applications from autumn to winter, we recognized that the combustion pressure gradually became lower and the combustion time increased (about 10 kg/cm$^2$ mean pressure and about 11 seconds in time for smooth combustion). When the pressure dropped from this value we often encountered intermittent combustion. These phenomena also occurred at high altitudes, though we had smooth combustion on the ground. These phenomena are characterized by unsmooth combustion and intermittent jet flow having a time interval or 1-2 seconds, 3 seconds, or more. Thus combustion is not completed in one jet and by the end of combustion it has had several rests. Therefore, thrust is exerted intermittently.

For "Toku FDT6" in this breathing phenomenon combustion develops very thick black smoke.

Combustion with barely no breathing is very unstable and oscillation in pressure in the jet often occurs. In such cases the form of the pressure curve becomes as shown in Figure 15(B)4.

It is remarkable that in case (c) the frequency of breathing varies, and that every curve before or after breathing has a similar form. Pressure drops step by step in accordance with the decrease of combustion surface (end area of propellant), but the interval of combustion is not constant.

In our experiment we found that other things being equal, the breathing phenomena have a tendency to occur easier in case of horizontal setting of the rocket than in vertical setting and upward jet.

### 9-2 Cause of Intermittent Combustion

In considering these phenomena we can give following as their causes:

(1) Combustion velocity is excessively influenced by lowering of temperature of propellant,

(2) Combustion pressure drops in correspondance with the decrease of combustion velocity for rockets of the same design.

(3) Pressure has a certain limit on its lower value, (necessary to maintain continuous combustion) in accordance with the character of propellants. For "Toku FDT6" this limit was about 5 to 8 kg/cm$^2$ gauge pressure. (It is remarkable that combustion in the rocket chamber is essentially different from combustion in open air. While combustion in the chamber has a low pressure limit, combustion of propellant in open air is possible with very slow development).

(4) Corresponding with the lowering of the temperature of propellant, specific energy declines simultaneously with pressure drop and decrease of combustion velocity. Also, the combustion temperature becomes low and it approaches the critical temperature, which is the limit of temperature possible for continuing combustion. With the pressure drop due to decrease of end area of propellant, the combustion temperature decreases gradually and reaches the limiting value.

*ENCLOSURE (B)4, continued*

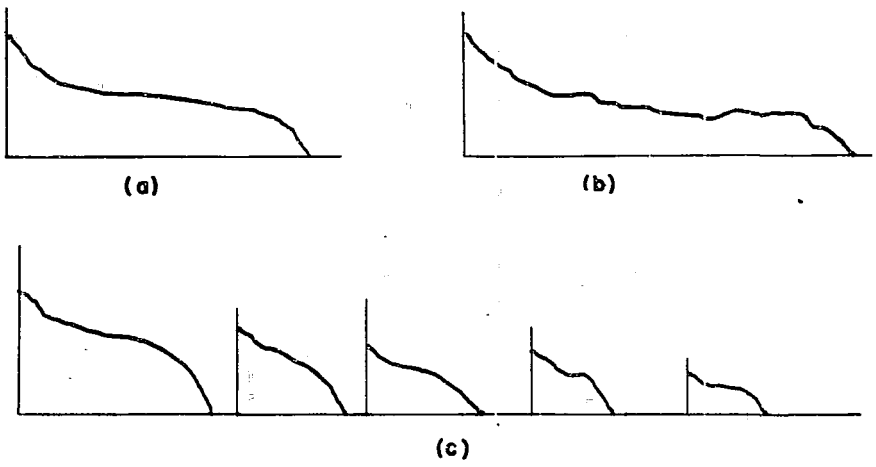


*Figure 15(B)4*
*PRESSURE CURVES FOR (a) SMOOTH, (b) UNSTABLE AND (c) INTERMITTENT COMBUSTION*

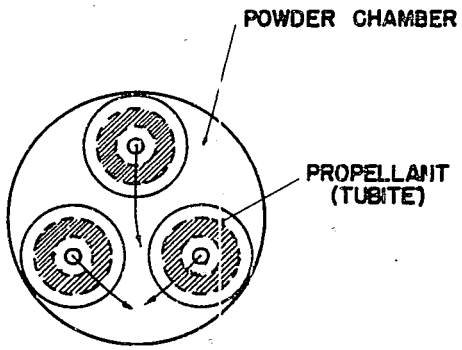


*Figure 16(B)4*
*MECHANICAL DISTURBANCE OF PROPELLANT DURING COMBUSTION*

(5) The difference of combustion between horizontal and vertical position of the rocket is as follows:

In the case of horizontal burning, propellants will fall or slip downwards perhaps with a little rotation, as they become thin. (Figure 16(B)4) Parts of their combustion surfaces may be disturbed either by friction with the chamber wall or other propellants. Therefore, generation of gaseous products becomes partially unstable and combustion pressure in chamber will tend to drop below the critical pressure, if combustion pressure is near the lower limit.

In the case of vertical burning, when propellants become thin, they do not rotate and combustion on their surfaces is not disturbed. Further, since the nozzle is situated vertically, the gas flows upwards and combustion is improved by convection, etc. Combustion temperature also increases in comparison with horizontal burning, so that in this case temperature and pressure are more difficult to decrease than in the horizontal case.

*ENCLOSURE (B)4, continued*

The relation between the critical pressure and the critical temperature is as follows:

In Figure 17(B)4 I will explain this relation. When combustion of propellant is initiated, if the difference between generated heat quantity and heat loss is large, then temperature quickly becomes greater than $\tau_K$ and pressure greater than $P_K$.

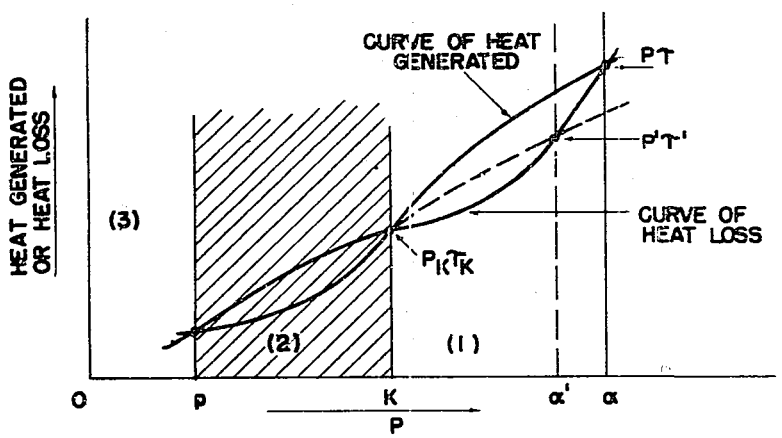


*Figure 17(B)4*

*RELATION BETWEEN CRITICAL PRESSURE AND CRITICAL TEMPERATURE*

Combustion continues at the point $P\tau$ with a balance of heat loss and heat generated. But as the surface area decreases gradually, pressure drops, generated heat decreases and the curve of generated heat quantity goes downwards while the curve of heat loss is constant for the rocket. Therefore, the point of balance $P\tau$ moves to the left, for example $P'\tau'$, and gradually approaches the critical point $P_K \tau_K$. When it reaches $P_K \tau_K$, combustion becomes unstable and the condition may enter region (2) with disturbance of combustion surface.

If generated heat becomes less than state K, the process enters completely into region (2) and in this region the heat loss is greater than the heat generated. Therefore, temperature drops suddenly, combustion cannot continue and the jet stops. In this state of rest, the propellant begins decomposition with no combustion in region (3) and heat will be generated again with scarcely any flow of gas, that is, scarcely any heat loss. Heat will then be accumulated and when the temperature reaches its ignition value, combustion will be developed again and the condition will reenter region (1).

Thus, repeating combustion and rest, the breathing phenomena occur. For this explanation it is necessary to have a little discussion, but in general I think it is good.

Mr. HINO has explained this critical point of combustion as follows: Taking combustion velocity as W:

$$w = a_1 P^n + b_1 p \qquad \text{where} \qquad n < 1 \qquad \text{and} \qquad n \cong \frac{1}{3}$$

*ENCLOSURE (B)4, continued*

He established four pressure regions: A very low pressure region where

$$W = a\,p^{1/3}$$

a lower pressure region where $W = a + bp$ with a small, b large;

a higher pressure region where $W = a + bp$ with a large, b small; and

a very high pressure region where $W = bp = W_0P$.

Therefore, as in Figure 18(B)4, the relation between W and P should be suddenly changed from a linear relation near the pressure limit. This explanation may be worthy of consideration.

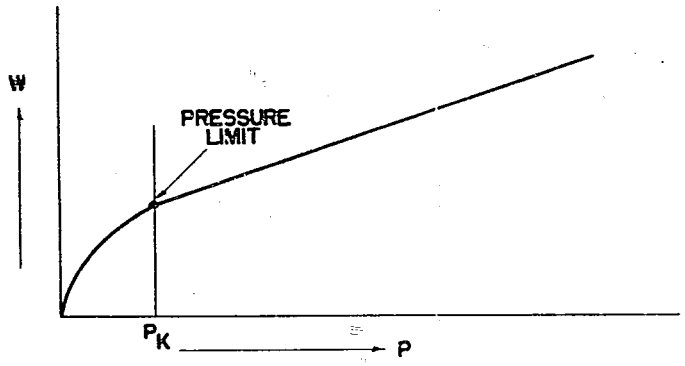


*Figure 18(B)4*
*RELATION BETWEEN COMBUSTION VELOCITY "W" AND PRESSURE "P"*

## 9-3 Elimination of Intermittent Combustion

We investigated in cold climates the effect of lowering the temperature of propellants on combustion velocity. As a result we made the nozzle area smaller and increased the pressure in use to keep the pressure and temperature of combustion over their limiting values.

We maintained smooth combustion without unstable disturbances of combustion surface by preventing movement of the propellants. We used a wire frame for propellants to prevent touching the chamber wall though the propellants were free to rotate during combustion.

# CHAPTER 10
# CONSIDERATION ABOUT THE PEAK PRESSURE IN THE PRESSURE-TIME CURVE OF COMBUSTION

## 10-1 Form of Peak Pressure Curve and Its Duration

The most troublesome problem in the design of a powder rocket is the question of the peaks in pressure and thrust.

The peak influences the strength of the combustion chamber and of parts receiving thrust. Especially in the case of a rocket catapult we cannot increase the mean acceleration with regard to this peak, therefore, its rail-length becomes long and it incurs many troubles.

*ENCLOSURE (B)4, continued*

If we have a solution for this peak, then we may avoid these troubles. It is very important in the case of powder rockets. Therefore, I have had a great interest in this question.

If we took black powder as an initiator in quantities experimentally necessary and sufficiently small, and the ratio of the weight of black powder to the volume in the chamber, i.e. $\omega_g/c_0 - V_0$ was very small, and if the charge $\omega >> \omega_g$, the pressure rise due to combustion of only the initiator itself at the instant of ignition should be very small. It is very small in comparison with that of the propellant. But there always occurs a high pressure peak at the beginning of combustion of propellants as shown in Figure 19(B)4. In case of bad ignition of the propellants, that is, when the propellants begin their combustion several seconds after the combustion of initiator powder and after the gas of initiator has flowed out of the chamber, a peak pressure occurs as shown in Figure 19(B)4.

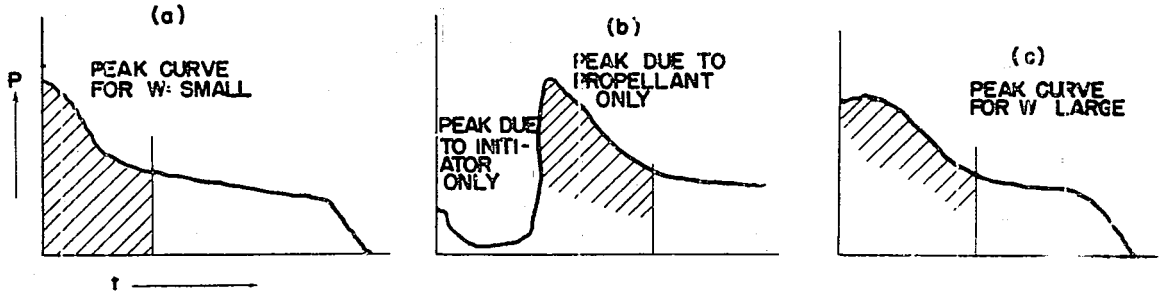


*Figure 19(B)*
*EXPERIMENTAL PRESSURE CURVES SHOWING PEAKS*

The form of the peak curve is different, of course, varying with the kind of propellant. The larger the combustion velocity, the more roundish is the curve, and the smaller the combustion velocity, the sharper is the curve. Now we will consider the meaning of peak curve or of its slope. From equation (43) in paragraph 7-1 we have the following, if we neglect $\omega_g$:

$$\{ \omega \int_0^z dz - \int_0^t a_0 \zeta P \, dt \} \{ 1 + \eta\rho \} = \rho(c_0 - V_t) \quad \ldots\ldots\ldots\ldots\ldots\ldots\ldots\ldots\ldots\ldots (43)$$

$$\rho = 1/v = P \frac{1.033}{f} \cdot \frac{\tau_0}{\tau} = \kappa_\tau P$$

$$\tau/\tau_0 \cong 0.5 \text{ to } 0.6$$

$$\zeta = \phi \left( \frac{2}{\gamma + 1} \right)^{1/(\gamma-1)} \sqrt{2g \frac{\gamma}{\gamma + 1} \kappa_\tau}$$

($\eta$ = covolume, liter/kg)

Substituting dt for dz, we have

$$\{ \frac{\omega}{V_0} \int_0^t S w \, dt - \int_0^t a_0 \zeta P \, dt \} \{ 1 + \eta \kappa_\tau P \} = \kappa_\tau P (c_0 - V_t) \quad \ldots\ldots\ldots\ldots\ldots\ldots\ldots\ldots (54)$$

*ENCLOSURE (B)4, continued*

If we neglect $\kappa_\tau$ because it is very small, we get

$$\frac{\omega}{V_o}\int_0^t S\,w\,dt \cong \int_0^t a_o \zeta P\,dt \qquad \text{.....(55)}$$

Here, if we consider $\zeta$, P and W constant, we get

$$\omega/V_o S\,w \cong a_o \zeta P$$

This formula means that the gaseous products per second are approximately equal to the quantity of flow out per second if surface area in combustion is constant, and therefore pressure and combustion velocity are also constant.

Now if P is constant, in order to get $dP/dt$, we differentiate equation (54), because if we got it from the equation (55), $\kappa_\tau$ is neglected and the value would never be true, since $V_t$, $V_o$ and $V_t$ are functions of t, though we assume $\zeta$ is constant. Here we may consider

$$w = a + bP, \qquad \tau/\tau_o \cong \text{constant}, \qquad \text{so that} \qquad \zeta \cong \text{constant}$$

Therefore, if we put any value of P, in the descending part of the peak curve, into this equation of $dP/dt$ which is obtained from equation (54), then $dP/dt$ has a negative value and we get the slope at that point.

Here I will abridge practical calculations. Now I will consider simply the descending part of the peak curve while the slope at any point in this curve can be given mathematically. From equation (55) in which $\kappa_\tau$ is neglected, we had:

$$\frac{\omega}{V_o}\int_0^t S\,w\,dt = \int_0^t a_o \zeta P\,dt$$

This equation means that the quantity of gaseous products generated in time t from the beginning is equal to the total flow out quantity of the gas at that time. This relation is approximate.

Differentiating this equation, we have

$$\frac{\omega}{V_o} S\,w = a_o \zeta P \qquad \text{.....(56)}$$

But if we consider $P \geq P_o$, and equation (56) exists only in the case of $P = P_o$, namely

$$P_o \equiv \frac{\omega}{V_o} S w_{P_o}/a_o\zeta$$

so that

$$P \neq \frac{\omega}{V_o} S w_P/a_o\zeta$$

From $W = a + bp$ we have the next relation:

$$\frac{\omega}{V_o} S(a + bP) \neq a_o \zeta P$$

The right term becomes greater than the left, namely, the flow out quantity per second becomes greater than the generated quantity per second. The values of a and b are given below from my experiments.

*ENCLOSURE (B)4, continued*

| | | |
|---|---|---|
| "Toku FDT6" | a = 1.55 | b = 0.082 |
| "Toku DT2" | a = 1.60 | b = 0.113 |

and, in general, a is nearly 1.5, b is nearly 0.1. $P_0$ is the constant pressure in steady combustion with the constant surface area S.

In this case in order to keep P constant or to equalize the left and the right sides, we must make the sectional area of the nozzle smaller than $a_0$. In other words, in order to keep pressure $P_0$, the nozzle area must be $a_0$, but to keep pressure P, the nozzle area must be $(a_0 - \Delta a_0)$, namely it must be smaller by as much as $\Delta a_0$. Therefore, pressure should drop gradually from P to $P_0$ and $\partial P/\partial t < 0$ if nozzle area kept as just $a_0$ $\partial P/\partial t$ is obtained by means of differentiation of equation (54) as a function of P as previously mentioned, but clearly it is also a function of a and b.

From equation (56) we have:

$$\frac{a_0 \zeta}{S \omega / V_0} = \frac{a + bP}{P} \qquad \text{.....(57)}$$

Therefore, in equation (56), if P is large, then the left term will be less than the right side, so that in equation (57) the left term is constant while the right side becomes smaller if P becomes greater than $P_0$.

Namely $\frac{a}{P} + b = c \qquad (P = P_0,\ c = \text{constant})$

$$\frac{a}{P} + b < c \qquad (P > P_0) \qquad \text{.....(58)}$$

Thus $\partial P/\partial t$ is a function of P, a and b. In order to discuss the influence of a and b with respect to $\partial P/\partial t$, we may consider a and b in equation (58) where a appears as a/P. Generally P is large but a is very small. Therefore, the term a/P is very small in comparison with the second term b and its value scarcely changes with a change of a.

Therefore, any change of the second term, or value of b, directly affects the value of the left side of equation (58); in other words, the value of $\partial P/\partial t$ depends more directly upon b than a. If we consider $\partial P/\partial t$ for a certain pressure P for various propellants with different combustion velocities, the larger the value of b, the slower is the pressure drop.

If P is comparatively small, (but $P > P_0$) and the value of a/P is comparable to the value of b, then the value of a will influence $\partial P/\partial t$ comparably to b. We are able to say that the slope of the curve of pressure drop after the peak depends mainly on P and b for sufficiently large values of P and depends on P, a and b for small values of P.

The larger the values of a and b in the formula $w = a + bP$, the more convex, roundish or flatter becomes the form of the peak curve, and the smaller are a and b, the more concave or sharper becomes the form, and the influence of b is great (see Figure 20(B)4). The time required to go from $P_{max}$ to $P_c$ is longer for larger values of a and b than for their smaller values. For example, for "No. 500 Toku FDT " time $t_e$ continues about 9-11 seconds against $P_{m_0}$ = 10 to 15 kg/cm$^2$. In this case the time of the peak curve is about 1 second. The larger the value of $P_{max}$ becomes, the longer is the time of the peak curve for the same value of $P_0$. Therefore, $P_{max}/P_0$ depends mainly on b and $P_{max}$. In order to bring its value near to one, $P_0$ and b are made larger. This value of $P_{max}/P_{m_0}$ will be nearer to one, of course, for thin propellants, namely, those of short combustion time, than for those of long combustion time, because

*ENCLOSURE (B)4, continued*

the time pressure $P_0$ is acting becomes shorter for a constant time of the peak part. In other words, we are able to say that for the same thickness of propellant, the larger becomes the ratio of the time of peak duration against $t_e$ or the larger becomes $P_{mo}$ against $P_1$ or $P_0$, the nearer to one becomes $P_{max}/P_{mc}$.

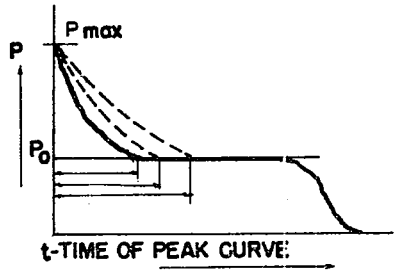


*Figure 20(B)4*

*VARIATIONS IN DURATION OF PEAK PRESSURE*

10-2 General Characteristics of the Value of $P_{max}$

I will enumerate in this section the general characteristics of $P_{max}$ mainly basing my discussion on theoretical considerations gained from our experiments.

(1) If we put $P_{max}/P_1$ or $P_0 \equiv \lambda_p$ and say this is the "peak ratio", then $\lambda_p$ has the relation with $P_1$ or $P_0$ shown in Figure 21(B)4, where $P_0$ represents the pressure in steady combustion with a constant surface area $S = S_0$. For tubite we take $P_1$ instead of $P_0$ but here we consider $P_0 = P_1$.

$\lambda_p$ is about 2 to 3 for a comparatively small value of $P_0$ ; if the volume of the chamber is comparatively small and the value of $s/(C_0 - V_0)$ is comparatively large. For example, with "Toku FDT6" and "Toku $DT_2$" with $\lambda_p$ = 2 to 3 and $P_1 \cong 40$ kg/cm$^2$, $\lambda_p$ becomes 1.5 to 2 and, in general, for large values of $P_1$, $\lambda_p$ approaches one.

Considering the value of $P_{max}/P_{mo}$, we are able to say there is a similar relation for a certain value of $t_e$. For different values of $t_e$ this must not be discussed as a general property, because the influence given to $P_{mo}$ with any difference of time after peak part is rather large.

(2) The value of $P_{max}$ never depends upon loading density, but upon the value of $S\ \omega/(C_0 - V_0)$, where $C_0$ is the volume of combustion chamber and is the initial volume of the propellants in the chamber.

Peak due to excess of initiator powder is another question. The higher the combustion velocity of propellant and the larger the ratio of initial surface area of propellant against volume of combustion chamber, the higher is the value of the peak pressure $P_{max}$ due to the combustion of the propellant itself.

Comparing propellant "Toku $DT_2$" with "Toku $FDT_6$" with regard to their value of combustion velocity W, we find the higher value in the former. Their pressure curves $P_0$ or $P_{mo}$ and $P_{max}$ show the higher value for the former.

Finally, it has been recognized experimentally that according to (1) above $\lambda_p$ has a constant value for a certain value of $P_0$ in almost all kinds of propellants. Therefore, the larger W becomes, the larger is the absolute value of $P_{max}$ for the different kinds of propellants.

*ENCLOSURE (B)4, continued*

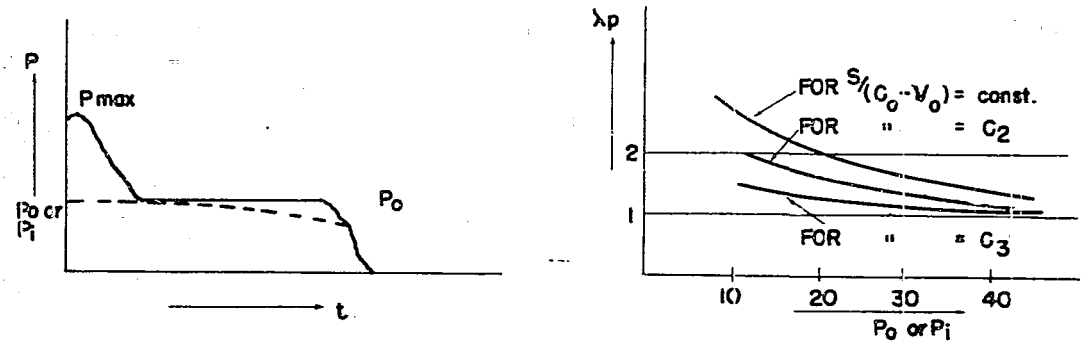


*Figure 21(B)4*

*CHARACTERISTICS OF $P_{max}$*

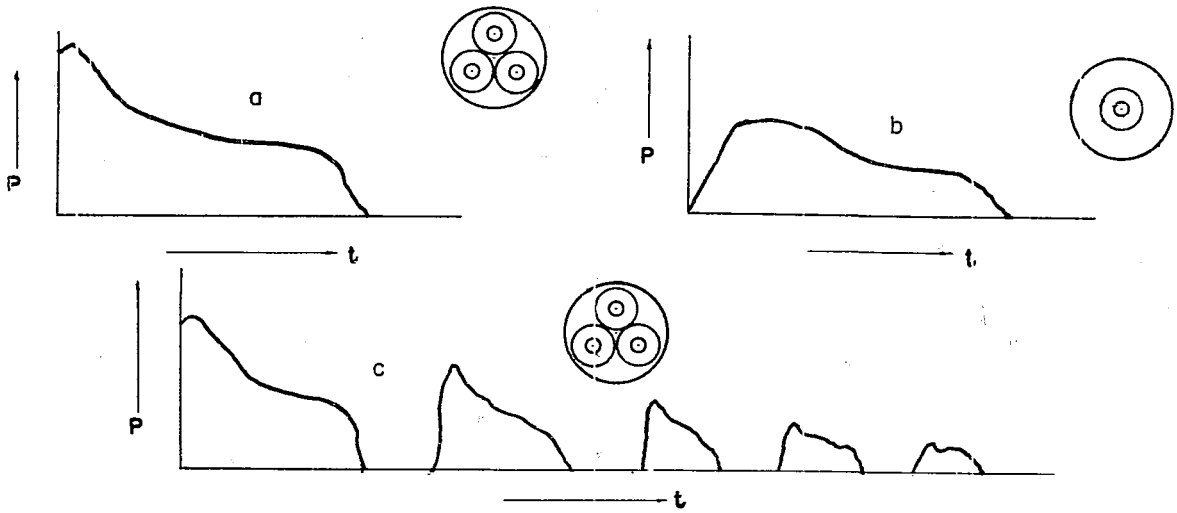


*Figure 22(B)4*

*EXPERIMENTAL PRESSURE CURVES*

$S/(C_0 - V_0)$ we find experimentally has a great effect on the value of $P_{max}$, as shown in Figure 22(B)4.

In case (a), Figure 22(B)4, we put three tubites in the chamber, in case (b) we put only one tubite in the same chamber, in case (c), the case of intermittent combustion, we put three tubites. In all cases $\omega/a_0$ is a constant and the volume of the powder chamber $C_0$ is constant. Propellant "Toku FDT6 No. 500" was used. Now I will explain (a) and (b).

For (a) $$S_0/(c_0 - V_0) \equiv \gamma_a$$

Loading density $\Delta a_0$.

For (b) $$\frac{1/3\ S_0}{c_0 - 1/3\ V_0} \equiv \gamma_b$$

$$\gamma_b < 1/3\ \gamma_a , \quad \Delta_b = 1/3\ \Delta_a$$

*ENCLOSURE (B)4, continued*

In Figure 22(B)4 (b) the value of $P_{max}$ is very small in comparison with $P_{max}$ in Figure 22(B)4 (a). The relation of the loading density is not of direct concern in this connection. It is obviously proved in Figure 22(B)4 (c) that in every breathing curve the form of the peak curve is almost the same, but the ratio $\lambda_p$ is gradually decreasing. While the value of loading density decreases, S is always nearly constant and V decreases. The value of $S/(C_0 - V)$ changes only a little and in this case the changes of the peak curves develop according to the value of $S/(C_0 - V)$. It is found that $\lambda_p$ in every peak of this case can be plotted upon the curve in Figure 21(B)4 for a constant value of $S/(C_0 - V)$.

From the results of my experiments in high altitude there is a certain relation between the change of altitude, or of back-pressure, and the peak ratio $\lambda_p$, i.e. $P_{max}$ becomes lower and $\lambda_p$ approaches unity with a drop of back-pressure.

For this item we had some experimental data in which $\lambda_p$ became very small at altitudes of about 6000 or 700m. We did not perform these experiments accurately enough and I cannot argue forcefully for this relation. We must make further experiments on this problem.

(4) The value of $P_{max}$ is also influenced by the charge of the initiator, pressure of initiator's gaseous products, relative situation of initiator against propellant and nozzle, etc.

For this item we must make many experiments in all possible cases. We can surmise, however, that:

(a) In case of late or early ignition, $P_{max}$ has almost a constant value, but in the case of instantaneous ignition, $P_{max}$ becomes smaller.

(b) It seems to us that $\lambda_p$ becomes smaller with better ignitability of propellant.

(c) If the initiator charge of black powder $\omega_g$ becomes greater over a certain degree in comparison with initial surface area of the propellant $S_0$, then the pressure due to initiator will be shown as $P_{max}$. But it is no question if $\omega_g$ is comparatively small. Especially if the ignitability of propellant is bad, there are often such cases in which combustion of propellant begins after the initiator gas has almost flowed out completely and $P_g$ (pressure due to initiator gas) has dropped to almost zero. In this case $P_g$ has no influence on the value of $P_{max}$.

## 10-3 Increase of Combustion Time, $t_e$, in Case of No Peak

Now we will assume that combustion develops with no peak and we get a flat pressure curve from the beginning. In this case $t_e$ will increase longer than in the ordinary case.

We will consider theoretically the degree of increase of $t_e$.

Consider $S = S_0 =$ constant, and after the peak the pressure is always constant, $P_0$. Here $\Delta t_e$ is the time increase. If the pressure curve is flat from its beginning and its value is always $P_0$, then the difference of flow out quanti.. in time $t_e$ is shown in the following equation:

$$\int_0^{t_p} a_0 \zeta P dt - \int_0^{t_p} a_0 \zeta P_0 dt = a_0 \zeta \left\{ \int_0^{t_p} P dt - \int_0^{t_p} P_0 dt \right\} \quad \text{.....(59)}$$

*ENCLOSURE (B)4, continued*

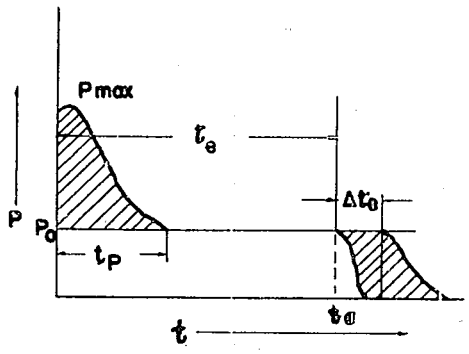


*Figure 23(B)4*
*INCREASE IN $t_e$ FOR CASE OF COMBUSTION WITH NO PEAK*

Here we assume S = constant.

Where P is a function of t we have:

$$\{ \frac{\omega}{V_0} \int_0^t S_0 w dt - \int_0^t a_0 \zeta P dt \} \{ 1 + \eta \kappa_\tau P \} = \kappa_\tau P (c_0 - v_t) \quad \ldots\ldots\ldots\ldots\ldots\ldots (54)$$

but $t = o$, $P = P_{max}$, $t = tp$, $P = P_0$ and we must put in these conditions.

Equation (59) shows the product of $a_0\zeta$ and the shaded area of the peak part. (See Figure 23(B)4.) Therefore we have for $\Delta t_e$:

$$a_0\zeta \{ \int_0^{P_t} P dt - P_0 t_p \} / a_0 \zeta P_0 = \Delta t_e \quad \ldots\ldots\ldots\ldots\ldots\ldots\ldots\ldots\ldots\ldots\ldots (60)$$

If we assume, no peak occurs, the time increase will become $\Delta t_e$ as shown in the above equation and as shown in the shaded area of Figure 23(B)4.

But this value of $\Delta t_e$ is not strictly accurate, being only approximate.

It is useful to estimate its accurate value, because in these calculations we assumed that $\zeta$ is constant or the value of $\gamma$ and $\tau/\tau_0$ are constants independently of P.

## 10-4 Theoretical Consideration About the Causes of Peak

Considering the causes whereby a peak occurs in the pressure curve, I will enumerate below theoretically possible explanations.

(1) Excess quantity of black powder used as an initiator; i.e. excess of pressure due to initiator.

(2) Increase of the initial surface area of propellant with unevenness of its initial surface.

(3) The value of combustion velocity at the initial surface of propellant might be very large because the glueyness of the propellant near the initial surface might be softer than the inner part.

*ENCLOSURE (B)4, continued*

(4) Sudden rise of combustion velocity at the instant of ignition because of ignition mechanism of propellant.

(5) Pressure rise at the instant of gas generation due to the plug effect of air which occurs at the open mouth of nozzle.

Items (1), (2), and (3) are not worth considering except in some special cases, but (4) and (5) are of general interest.

Hereafter I will discuss each of the above items.

(1) Excess of black powder.

If the quantity of black powder $\omega_g$ is large in comparison with the charge of propellant $\omega$, the pressure $P_g$ due to the black powder should reach a rather high value. If the total surface area of the black powder is taken as $S_g$ and its combustion velocity as $W_g$, then $P_g$ depends on $S_g \times W_g$ and $(C_0 - V_0)$.

For example, we are able to find far larger values of $P_g$ than $P_0$ in cases of rocket bullets for rocket guns of small size in which the charge of propellant is comparatively small. In this case $P$ is shown as $P_{max}$. For rockets of large size in which $\omega_g$ is negligibly small in comparison with $\omega$, $P_g$ scarcely affects $P_{max}$ but we must make mention of the fact that a part of $P_g$ must be added to the initial pressure due to the propellant itself, if combustion of the propellant begins before all of the black powder gas has flowed out.

(2) Excess of surface area because of unevenness.

If there is such fine unevenness on the surface of the propellant, the surface area should be very large in comparison with its apparent area.

In that case $a_0 \zeta P' = \frac{\omega}{V_0} S_0' w$ (where $S_0'$ is true area).

We can get a higher $P'$ than $P_0$ and, if $S_0 >> S_0$, it may be $P_{max}$.

In this consideration it is assumed that the burning surface will become smooth and the unevenness of initial surface will disappear, but practically the unevenness of the surface is very small and it is of no importance. Though there is a little unevenness, it is not worth considering that the surface will become smooth after its ignition, and therefore this item can be, in general, ignored.

(3) Less glueyness of propellant's surface.

When any very thick tubite is formed by a press and die, its glueyness may become softer near its surface and harder in its inner part because, depending on the shape of die, pressure in the die will be lower in parts near the surface than near its center. It is considered that combustion velocity will be greater for softer glueyness.

But if we consider that this effect may occur practically, then the pressure curve must gradually drop and there will be, in general, no peak pressure.

Also in the case of intermittent combustion it is shown practically that in later curves there occur also peak pressures; therefore, in the inner part of the propellant, too, the peak occurs in form similar with the one of the initial surface. It is not worth considering that this action is a main cause of peak pressure.

*ENCLOSURE (B)4, continued*

(4) Sudden rise of combustion velocity due to ignition mechanism of propellant.

It is very interesting in considering this that the peak pressure can occur also in vacuum.

The ignition temperature of a gas mixture is the temperature from which reaction will develop naturally in that mixture, but it is not a physical constant and it will be different depending on methods of heating and other conditions. This ignition point does not always correspond to the temperature at which flame will occur in the gas mixture (so called constant "preflame period") during which reaction is already developing. Therefore, for propellants as for solid explosives it may also be considered that the surface of the propellant does not ignite directly with the initiator gas in a moment and develop to steady combustion. During the short preflame period a small amount of gas will be generated and the propellant will begin its decomposing reaction prior to its ignition. With this decomposing reaction the temperature rises suddenly and explosion therefore occurs later in the gas near the suface of the propellant with temperature rising more suddenly and successively as the propellant begins its combustion. But it would not be correct to consider that the peak pressure may be the pressure rise due to this explosion wave. This pressure rise is defined only by the composition of the propellant and it is very difficult to believe that the pressure in the entire combustion chamber rises to this value, because this phenomenon occurs in a very thin layer around the surface of the propellant. This explosion pressure should be very high and it is not considered likely that the pressure drops from $P_{max}$ in a continuous curve.

With the following considerations about $P_{max}$ we may be able to explain its cause.

In the combustion and explosion of a gas the chemical reaction developing at the flame plane and at the explosion wave plane is accelerated by the temperature rise, by absorption ions of radiation of each molecule or by activation of molecules due to collision with electrons or ions. The temperature rise is accelerated by collision and adiabatic compression and absorption of infra-red rays and flame will be developed by heat transmission, or in other words, by the collision of molecules.

Therefore, as a first phenomenon, the gas surrounding the surface of propellant explodes with a certain reaction velocity and reaction temperature defined by the composition of gaseous product generated in the preflame period. But this layer may be considered very thin. By this explosion a compression wave occurs in that part, and at this instant there occurs a pressure rise at the surface of propellant. Therefore, at the beginning of combustion, the propellant begins its combustion in a very high pressure as the second phenomenon. We may consider that the combustion velocity will be $W' = a + bP'$ at this instant, where $P'$ is the pressure in the layer very near to the surface of propellant at the instant of ignition (not of the entire chamber) and will disappear at once. Next, if, the propellant begins its combustion with combustion velocity $W'$, then, as a third phenomenon, the gaseous products fill up the chamber suddenly and the pressure in the chamber rises to $P_{max}$. Since the pressure reached is $P_{max}$, it begins to drop continuously in accordance with the relation between the flow out quantity and the generated quantity of gaseous products.

This consideration surely seems to be a cause of $P_{max}$ and according to this theory $P_{max}$ will depend on the first combustion velocity $W' = a + bP'$, on $S_0/(C_0 - V_0)$ and on $a_0\zeta\rho$. It may be considered that $P_{max}$ will depend on a, b, and $P'$, depending on the propellant as well as on the ratio between the

*ENCLOSURE (B)4, continued*

surface area and the initial volume of the combustion chamber and the relation of nozzle area $a_0$ to flow out quantity.

This explains why $P_{max}/P_0$ approaches unity if the usual pressure becomes higher, because if $P_0$ approaches to P' then $W = a + bP_0$ approaches W' since P' depends mainly upon the composition of gas and may be independent of the pressure intended to be used. From this theory, peak must occur even in a vacuum and $P_{max}/P_0$ approaches unity as $P_0$ increases.

P' may be calculated by the explosion theory from the following fundamental equations if the composition of the gas is defined:

$$D = v\sqrt{\frac{P' - P}{v - v'}}$$

$$W = (v - v')\sqrt{\frac{P' - P}{v - v'}}$$

$$c_v(T' - T) - Q = \frac{1}{2}(P + P')(v - v')$$

$$\gamma' P'/v' = (P' - P)/(v - v')$$

where
- D : velocity of compression wave
- P : initial pressure
- P' : explosion pressure
- v : specific volume in initial state
- v' : specific volume in explosion state
- W : velocity of gas flow due to compression wave
- Q : heat of reaction
- $\gamma'$ : Cp/Cv at temperature T'
- T : initial temperature (absolute scale)
- T' : explosion temperature (absolute scale)

(5) Pressure rise due to plug-effect of air at open mouth of nozzle

(a) Neglecting the initiator gas and considering that the plug of air in the nozzle will give a closing-effect at the instant of sudden generation of gaseous products at the instant of ignition, we may consider that the slope of the pressure curve at the beginning of the pressure rise is nearly similar to it in the case of a closed explosion chamber.

$$P = f\int_0^z \omega dz \;/\; \{c_0 - \frac{\omega}{\delta}(1 - z) - \eta\int_0^z \omega dz\}$$

From this equation we can calculate the slope $\partial P/\partial t$

But we must remark that $\partial P/\partial t$ derived from this calculation will be useful only for estimating the true value of slope.

(b) When gas is suddenly generated at the instant of ignition in the combustion chamber and it rushes with velocity $w_2$ against quiescent air at the end of nozzle, there occurs a compression wave in the air because $w_2$ is much larger than the velocity of sound. By this compression wave, pressure rise occurs in the air at the end of the nozzle and thereby $P_{max}$ may occur in the chamber.

*ENCLOSURE (B)4, continued*

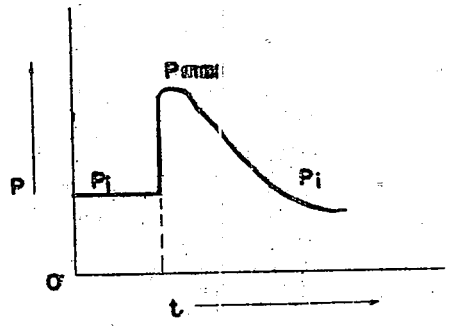


*Figure 24(B)4*
*EFFECTS OF BACK PRESSURE AT NOZZLE*

According to this theory $P_{max}$ or peak pressure cannot occur in a vacuum, because compression waves cannot occur in a vacuum. Therefore, there is no rise in a pressure curve of combustion in a vacuum.

Now we assume that a rocket is burning with a steady jet at constant combustion pressure $P_1$ which is in relation $a_0 \zeta P_1 = \delta s' \omega$ and assume this rocket to be in a vacuum (back pressure is zero).

In this case if air, whose pressure is 1 kg/cm$^2$, suddenly surrounded this rocket, a compression wave should occur at the end of the nozzle and a pressure rise would exist.

This pressure rise will be given by Rüdenberg's equation:

$$P_s' - P_1 = P_2 - P_1 = \Delta P = \frac{2\rho_1}{1+\gamma}(D^2 - w_s^2) \quad \text{.....(61)}$$

where $P_2$ or $P_s$ = absolute value of pressure rise

$P_1$ = absolute value of back pressure

$\rho_1$ = density of air in pressure $P_1$

$\gamma$ = ratio of specific heat of air in back pressure

$D$ = velocity of compression wave

$w_s$ = sound velocity in back pressure

$w_2$ = gas velocity at the end of nozzle due to combustion pressure, $P_1$ (pressure of gas at the end of nozzle is 1 kg/cm$^2$)

$w$ = velocity or air flow in pressure $P_2$ which is caused by compression wave.

If a rigid piston instead of gas dashed against the air, $w$ would be equal to the velocity of the piston $w_2$, but here, gas dashes at pressure $P_1$ and when gas dashes, it is considered that a pressure rise occurs in the gas also and the velocity of the gas will decrease. Therefore, $w_2$ will be greater than $w$.

*ENCLOSURE (B)4, continued*

Velocity of the compression wave D, should be greater than $w_2$ and, if we consider it more theoretically, we may establish the relation between D and $w_2$. For the present we will assume that $D = F(w_2)$ and then

$$w_2 = \phi \sqrt{2g \frac{\gamma}{\gamma - 1} \{1 - (\frac{P_1}{P_i})^{(\gamma-1)/\gamma}\} \frac{f}{1.033} \cdot \frac{\tau_i}{\tau_o}}$$

$w_2$ is a function of $f$, $\tau_1/\tau_o$, $P_1$, and $P_i$, and if we assume $\tau_1/\tau_o = 0.55$, and $P_1$ is constant, then $w_2$ becomes a function of $f$ and $P_i$.

From $$P_i a_o \zeta = \delta S w$$

we have $$P_i \propto Sw/a_o\zeta \propto Sw/a_c$$

where $$\zeta = \phi \{\frac{2}{\gamma + 1}\}^{1/(\gamma-1)} \sqrt{2g \frac{\gamma}{\gamma + 1} \kappa_\tau} \quad \text{and} \quad \kappa_\tau = \frac{1.033}{f} \frac{\tau_o}{\tau_i}$$

If $P_i$ increases then $w_2$ becomes larger. Therefore, D becomes larger and the value of $\Delta P$ becomes larger. Namely, the absolute value of $P_{max}$ will increase with $P_i$ as S and W become larger and it will decrease when $a_o$ becomes greater.

As above mentioned we can calculate the pressure rise of air at the end of a nozzle from equation (61) in the case of the sudden appearance of 1 kg/cm$^2$ back pressure around a steady jet in vacuum.

If $P_s > P_1$, pressure in the chamber rises to $P_s$ at the instant in which $P_s$ occurs at the nozzle end, because gas in the chamber will be compressed from the nozzle end by the compressed air whose pressure is $P_s$. Theoretically, the gas flow stops instantaneously. Just at the moment when the progress of the compression wave of air at nozzle end begins to flow the pressure might drop. Therefore, the gas begins suddenly to flow out and acquires flow velocity against the inner pressure $P_s$. The inner pressure will drop gradually from

$P_s$ and we have $(P_s - P_1)/P_i = \frac{2\rho_1}{1 + \gamma} [\{F(w_2)\}^2 - w_s^2]/P_i$

$$P_s > P_i \quad \text{.....(62)}$$

For a constant value of $w_2$, $F(w_2)$ should be constant.

In the relation between $P_1$ and $w_2$, as obviously shown by Figure 6(B)4 in Chapter 4, $w_2$ changes only a little with change of $P_1$ for comparatively high values of $P_1$ when a certain value if $\tau_1$ is constant. It is, of course, a different problem with a large increase of $\tau_1$. Here we consider that change of $\tau_1$ is negligibly small.

Therefore, if $w_2$ changes only slightly with change of $P_1$, it is considered that the increase of $P_s$ should be very small with increase of $P_1$. From this consideration it is believed that the higher $P_i$ becomes the closer $P_s/P_i$ approaches unity. If $P_1$ changes, namely, if back pressure changes, $P_s$ should change proportionally with change of $P_i$.

Now we will consider the mechanism of pressure rise at the instant of ignition using the above considerations as a basis.

Using only this theory, neglecting other causes and putting S = constant, the pressure curve should be flat from its beginning with pressure $P_i$ (as $P_i a_o \zeta = (SW)$), if combustion began and developed in a vacuum.

*ENCLOSURE (B)4, continued*

Considering a case where back pressure is atmospheric pressure, the quantity of gaseous products generated per unit time is very large at the instant of sudden ignition and it can be assumed that pressure in the chamber may suddenly rise to $P_s$. If dP/dt is very large, gas velocity at the end of the nozzle should reach $w_2$ from zero and a compression wave occur in the air. Therefore, there will occur a pressure rise $P_s$ in that part and pressure in the chamber will reach $P_s$ at once, i.e. it is possible to consider that primary pressure in the chamber reaches $P_1$ and, secondly, it rises to $P_s$ prior to the beginning of the jet, after which gas begins to flow or jet.

Depending on the value of dP/dt, the rising curve of gas velocity will vary and naturally the degree of its sudden rise with shock will be different. $P_s$ should be affected by this degree, so that it should be difficult for a compression wave to occur with a small value of dP/dt and $P_s$ should be low. It is considered that dP/dt should depend either upon the property of propellant, W, or the ratio between generated gas quantity per second $\delta SW$ and the volume of the chamber $(C_0 - V_0)$ i.e. $\delta SW/(C_0 - V_0)$. Namely, dP/dt depends upon or is proportional to $SW/(C_0 - V_0)$

On the basis of these considerations, $P_{max}$ may be written as follows: putting $\eta_1$ as a coefficient of the effect due to $SW/(C_0 - V_0)$ and $P_1$ as pressure desired for steady combustion:

$$P_{max} = \kappa\eta_1 P_s \qquad \text{with} \qquad \eta_1 < 1$$

If any preflow occurs with the flow of initiator gas, it is considered that $w_2$ should be relatively small and $P_s$ should be lower. Therefore, putting $\eta_2$ as a coefficient of this effect, we have

$$P_{max} = \kappa'\eta_1\eta_2 P_s \qquad \text{where} \qquad \eta_2 < 1$$

The combustion temperature $\tau_1$ should be $T_{max}$ for pressure $P_{max}$ and $T_{max} \neq \tau_1$; therefore we must consider this effect too. It is considered that $T_{max} \geq \tau_1$ so putting $\eta_3$ as the coefficient of this effect, we have

$$P_{max} = \eta_1\eta_2\eta_3 P_s \qquad \text{where} \qquad \eta_3 \geq 1$$

From all these relations we have

$$P_{max} = \eta_1\eta_2\eta_3 P_s = \eta P_s$$

The value of $\eta$ will be obtained experimentally.

By these considerations we can calculate the value of $P_{max}$ as a function of S, W, $a_0$, s, $\tau_0$, f, $C_0$, $V_0$ etc., theoretically and with the help of experimental data.

However, we must further develop our research on this theory with respect to the following items:

(a) Theoretical development is required for the form of the function $D = F(w_2)$.

*ENCLOSURE (B)4, continued*

(b) We must confirm with experimental research that $P_s$ will be proportional to $P_1$. The author once made experiments on this question with jet combustion in higher altitudes (1000, 5000, 6000, 7500m) and measured the pressure in the chamber and determined the pressure curve, but he did not get exact data. These experiments will be described later.

(c) We considered that $P_{max}$ depends on $P_s$, but $P_s$ also varies with $w_2$; we should be able to get an exact solution for this theory by researching on the value of $P_{max}$, by adjusting the length of the Laval tube (or nozzle) or having only convergent parts of nozzle, etc. The author regrets, however, that he did not have time to perform such experiments.

(d) We assumed that at the instant of ignition, pressure rises primarily to $P_1$, secondarily to $P_s$ and then gas begins its flow, but this assumption requires further discussion.

## CHAPTER 11
## THRUST PEAK

Thrust T is given by equation (37):

$$T = 2\gamma\phi^2 a_0 \left\{ \frac{2}{\gamma + 1} \right\}^{1/(\gamma-1)} P_1 \sqrt{\frac{1}{\gamma^2 - 1} \left\{ 1 - \left(\frac{P_2}{P_1}\right)^{(\gamma-1)/\gamma} \right\}}$$

This relation is nearly linear with regard to $P_1$ as shown in Figure 9(B)4.

Therefore, the thrust curve should be similar in form with the pressure curve. The thrust peak occurs simultaneously with the pressure peak and naturally $dT/dt$ is almost equal to $dP/dt$.

Thrust may be adjustable to a certain degree by means of adjustment of the divergency of the nozzle. If we take $P_e$ as the basis for fixing the ratio of divergency of nozzle, then $T_{max}$ becomes smaller than the case in which we took a pressure higher than $P_e$ as a basis. Therefore, if we take $P_{max}$ as the basis, nozzle efficiency becomes 100% for peak pressure $P_{max}$ with regard only to the ratio of divergency, and $T_{max}$ has its value as 100%. In this case, however, after the peak, the loss becomes larger and then thrust decreases, so that the ratio between $T_{max}$ and mean thrust becomes larger. If we take $P_e$ as its basis then some losses occur in the value of $T_{max}$; therefore, $T_{max}$ decreases.

It is possible to calculate the loss of pressure due to incomplete expansion in the nozzle, or due to a smaller ratio of divergency of nozzle than calculated for the corresponding back pressure. Therefore, it is possible to calculate the value of $T_{max}$, but it is difficult to calculate loss of pressure due to excessive expansion resulting from an excessive divergency ratio. But it is known from experiments that the loss of pressure is much smaller in incomplete expansion than in excessive expansion, if pressures with regard to shortage and excess of expansion are equal to each other. Therefore, we should take $P_e$ or a little less than $P_e$, as the base pressure for ratio of divergency in order to decrease the peak of thrust and to reduce losses in general. Of course, hen we cannot cancel the peak of the thrust without cancellation of the peak in pressure.

*ENCLOSURE (B)4, continued*

## CHAPTER 12
## EXPERIMENTAL RESEARCH ON PEAK-REDUCING METHOD

### 12-1 Consideration on Peak-Reducing Method

The peak of thrust is due to the peak pressure, and if we can cancel or reduce the peak pressure, then we will have made a very important contribution to the application of rockets. The author has been able to cancel the peak in some experiments. He started to solve this problem. I will describe some peak-reducing methods.

(1) To prevent incontinuous sudden rise of $w_2$ because of the compression wave at the instant of ignition, caused a preflow of air through the nozzle prior to ignition of the initiator, which gradually increases velocity.

This method requires some mechanical devices, and is effective against cause (5) (see paragraph 10-4), but this is difficult for powder rockets.

(2) Method of back-pressure-drop at the nozzle end.

For a rocket which is flying with a plane, we might be able to reduce its peak pressure by means of a venturi-tube fitted at the end of nozzle, in order to decrease back pressure at that point. The effect of this method will be doubtful because we have no experimental data. This may be effective only for cause (5).

(3) Gradual increase of ignition area in order to reduce the value of dP/dt.

This method involves wrapping the surface of the propellant conically with something which has slow combustion velocity, or to coat the propellant's surface with some slow burning material in several layers, dividing its area into several parts and coating them with different thicknesses.

It is remarkable that it was never effective to coat the whole area uniformly; we must have some bare surface to ignite instantaneously.

This method may be effective for causes (2-5).

(4) Division of combustion chamber into several sections and prevention of simultaneous ignition in these sections.

This is very difficult.

### 12-2 Experiments and Results with Regard to Peak-Reducing Method

My experiments in peak-reduction were made by means of method (3) above because it is the most practicable and most reasonable of the several methods. In practice I divided the surface area of the propellant into several sections and intended to ignite the surface step by step, making the coating of different thickness with acetyl-cellulose dope and paper. First I intended to make the peak value equal to the steady combustion pressure $P_1$ and to maintain this $P_1$ through combustion. In order to make the peak value $P_1$, I planned to reduce the area of primary ignition surface and then to coat the excess area of surface with acetyl-cellulose dope and paper. Ignition of this coated area will be delayed somewhat.

We must investigate how much area we must make bare surface, in order to make the peak value $P_{max} = P_1$.

*ENCLOSURE (B)4, continued*

We will attempt a rough calculation in order to obtain this area. In the theory of cause (5), putting roughly $D = F(w_2) \equiv w_2$, in order to estimate this area, we have:

$$P_s = P_1 + \frac{2\rho_1}{1+\gamma}(w_2^2 - w_s^2) \quad \text{.....(63)}$$

$w_s = \sqrt{\gamma P_1 v_1}$ $P_1$ = back pressure. $P_1$, $P_s$ are in absolute value

Putting $P_{max}$ as the peak value when the entire surface area S is bare, and if we have $P_{max}/P_1 = 2.5$, we may calculate the area by which $P_s$ is reduced to 1/25 of its value.

Therefore

$$\frac{1}{2.5}(w_2^2 - w_s^2) = w_x^2 - w_s^2$$

$$w_x^2 = \frac{1.5}{2.5} w_s^2 + \frac{w_2^2}{2.5}$$

$$\therefore w_x = \sqrt{0.6 w_s^2 + 0.4 w_2^2}$$

If we assume that

$$\left\{ \begin{array}{l} w_2 = 1600 \text{ m/s} \\ w_s = 340 \text{ m/s} \\ P_1 = 15 \text{ kg/cm}^2 \end{array} \right\}$$

We have $w_x = 1044$ m/s

$$\frac{\omega}{V_o} S_x w_x = a_o \zeta P_x, \quad \text{if } P \to 1/3 \quad \text{we have } S_x = \frac{1}{3} \cdot \frac{2.8}{2} S = 0.47S$$

If $w_x = 1044$, we have from Figure 13(B)4 $P_x = 4$ to 5 kg/cm$^2$ (for "Toku FDT$_6$"). Since $W/V_o S_x W_x = a_o \zeta P_x$ if $P \to 1/3$, we have $S_x = 1/3 \cdot 2.8/2 \; S = 0.47S$ because from the P and W relation we have $W_x = 2/2.8$.

Therefore, we may take about one-half of the area as bare surface, in order to reduce the peak value to 1/2.5, namely, to make $P_x = 1/3 P_1$ or $P_{max} = P_1$. Having as a basis the theory above mentioned, I have tried several experiments. As paint I used acetyl-cellulose dope as previously mentioned, applied it heavily and used paper (blue print paper) for coating.

I will describe the most successful experiment, in which I used six propellants (length 500mm) of "No. 500 Toku FDT$_6$". Loading density was about 0.7 and nozzle diameter was 74mm.

No. 1. All surface bare

No. 2. All surface bare

No. 3. $\frac{1}{4}$ of area bare, $\frac{1}{4}$ of area painted with dope and coated with paper, $\frac{1}{2}$ of area painted and coated with double thickness of paper.

No. 4. 1/3 of area bare, 1/3 of area painted and coated with single layer of paper, 1/3 of area painted and coated with doubled layers of paper.

No. 5. $\frac{1}{4}$ of area bare, $\frac{1}{4}$ of area painted and coated with doubled layers, $\frac{1}{4}$ of area painted and coated with four layers.

*ENCLOSURE (B)4, continued*

No. 6 ½ of area bare, ¼ of area painted, ¼ of area painted and coated with doubled layers.

I was able to plot a curve in which the peak part was completely cancelled as in Figure 25(B)4. Though the number of experiments was too small to confirm this result, we were able to confirm by this example that by means of such a method it is possible to cancel the peak.

After this experiment, in a research on a "rocket catapult", I was able to lower the peak value with acetyl-cellulose dope painted on one-half the area of the propellants. Its use decreased $P_{max}/P_1$ from 2.5 to 1.4.

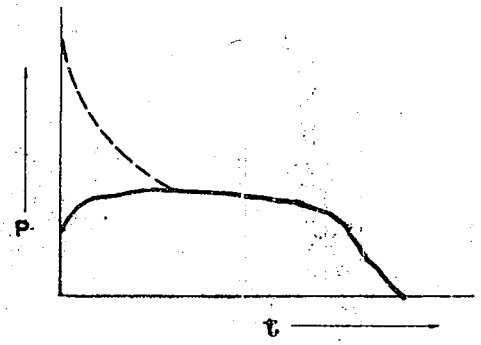


*Figure 25(B)4*
*EXPERIMENT ON CANCELLATION OF PEAK BY INCREASE OF IGNITION AREA*

## CHAPTER 13
## OUTLINE OF OTHER IMPORTANT EXPERIMENT

### 13-1 Influence on Combustion of Propellant's Temperature and Atmospheric Temperature

On this problem we conducted some experiments at Chitose Air Base in HOKKAIDO in February 1945 in order to solve the question of intermittent combustion. In these experiments we investigated the pressure drop due to temperature drop or decrease of combustion velocity and the occasion of intermittent combustion. We could only investigate rockets "4 FH 120" and "4 FR 110", but not systematically.

### 13-2 Influence on Pressure Curve of Change of Altitude or of Back-Pressure

On this question I made experiments at altitudes of 1000, 3000, 5000, 6000, and near 7000m. The conclusion of the results of these experiments is as follows:

(1) No difference is recognized in the value of steady combustion pressure (in gauge) with change of back pressure.

(2) I had a few examples in which $P_{max}$ decreased at high altitude, but I could not confirm that $P_{max}$ is proportional to $\rho$. For this question I could not get an exact conclusion, because the number of experiments was insufficient and data measured in flying planes were not accurate enough.

(3) The duration time of jet is not different in high altitudes. But it was recognized definitely that the velocity increase and its duration time becomes very large in airplanes at high altitude.

13-3 Influence of Humidity on Combustion Curve

For "Toku FDT6" we found no influence of humidity on pressure curves because its composition percentage of water is about 2.4 to 3%; therefore, it is already saturated with water. We found no difference in pressure curve even in an experiment in which we used propellants which were steeped in water for about 24 hours.

## CHAPTER 14
## CONCLUSION

I have described my researches, and I am very glad to think that these research might be useful for the further development of rockets. Powder rockets as auxiliary power for airplanes, especially as a substitute for catapults of plane carriers and as a rocket-catapult, etc. are very interesting problems and they will develop further in the future. In addition, it would be very interesting to research on problems of (1) divergency angle of nozzles of powder rockets, (2) loss of pressure due to unfitness of divergency ratio, and (3) stripes due to compression wave in jet of gas etc.

# ENCLOSURE (C) 1

## TESTS OF LIGNUM-VITAE BEARINGS AND SUBSTITUTES

Tests of lignum vitae bearing materials were conducted to find some suitable materials as substitutes for lignum vitae and to clear up the reason for the abnormal wear in lignum vitae used in strut bearings of naval ships.

### 1. Test of Substitutes for Lignum Vitae

In view of the difficulties of importing lignum vitae, tests were planned to find some home grown materials as substitutes for lignum vitae.

The test was performed by holding specimens on a rotating bronze disc under some definite pressure. The wear and friction between the specimens and the disc were measured.

We found that bakelite or phenol-resin was the best and showed excellent possibilities as underwater bearing material, and "Kaba" and "Mizumesakura," which penetrated ceresin oil, showed results as good as lignum vitae.

Bakelite has not been employed in practice, because of lack of composing materials, although "Kaba" and "Mizumesakura" are used for naval and merchant ships.

### 2. Tests on Wear of Lignum Vitae in Strut Bearings

Since the outbreak of the War of Greater East Asia, many naval ships which sailed the Southern Sea suffered from wear of the lignum vitae in their strut bearings. The wear was so abnormally large and it proceeded so much more rapidly than the Navy had ever met before, that a test was planned to clear up the reason for it and to take measures to meet the situation.

The test was conducted with a model strut bearing (100mm diameter and 400mm length) with shafting submerged under water.

The test was performed by changing bearing load, bearing speed, quantity and temperature of lubricating water, etc. Effects of the above, effect of misalignement of shaft center and effect of quality of lignum vitae upon wear were investigated.

With respect to the reason for abnormal wear, no conclusion was reached, except that an insufficient supply of lubricating water caused comparatively large wear.

At present, from information from No. Four Navy Repair Yard on Truk Island, it is assumed that the abnormal wear was caused by attached microbes of some shell existing in the Southern Sea.

To prevent the attachment of microbes described above, research regarding solutions to be applied to bearing material was planned at Yokosuka Naval Engineering Experiment Station. but was abandoned with the conclusion of the war.

# ENCLOSURE (C) 2

## SUBSTITUTE MATERIAL FOR NICKEL ALLOY STEEL

### 1. General Remarks

This memoir is based mainly on the report "Investigation on Substitute Materials for Nickel Alloy Steels Applying to Diesel Engines" which was published by Yokosuka Naval Arsenal No. 10 in 1942. This study was undertaken with the object of investigating non-Ni steels for vital parts of many types of diesel engines which were used in Navy at that time. In those days many kinds of Ni free steels had been used in constructing airplanes, airplane engines and other machines; but due to the relative massiveness and consequent difficulty of making diesel engine parts, substitute materials had not been earnestly investigated nor utilized. With the progress of war, nickle became gradually more scarce in Japan and it was necessary to reduce its consumption, so this investigation was rapidly executed. Fundamental and practical tests were performed almost satisfactorily. Some of them, however, showed by no means good results, and their practical applications were hardly realized because the types of diesel engines needed varied one after another. Apart from this investigation, substitute materials for Ni and also Mo and W containing alloys had been widely adopted in aircraft construction from the beginning of 1943. Owing to the actual results of the work on aircraft, substitute materials could be applied to the production of small type diesel engines from about 1944 to the end of the war.

### 2. Counterpart of the Investigation

The counterpart of this investigation consisted of investigating substitute materials for Ni steels used in vital parts of diesel engines, conducting fundamental and practical use tests, and gaining useful data for design and production of diesel engines.

### 3. Results of Investigation

Suitable substitutes for 80 kg/mm$^2$ Ni-Cr steel are Mn-Cr steel and 80 kg/mm$^2$ Cr steel, but NANIWA steel is not suitable because of the difficulty in heat treatment of gaining the required mechanical properties.

As a substitute for 90 kg/mm$^2$ Ni-Cr steel, 90 kg/mm$^2$ Cr-Mo steel is almost suitable.

As a substitute for 80 kg/mm$^2$ Ni-Cr case-hardened steel, Cr-Mo nitrided steel is almost suitable; Cr-Mo case-hardened steel also has good properties except that it lacks shock resisting ability. The 50 kg/mm$^2$ non-Ni case-hardened steel is available in place of Ni-Cr case-hardened steel for parts where high strength is not needed, because its wear resisting property has proved as good as Ni-Cr case-hardened steel.

Tests of practical use were also made on these substitute steels. Although the tests were conducted imperfectly, almost all of them showed good results. Cr-Mo case-hardened steel for the plunger of fuel injection pump and cam and roller has a tendency toward burning or seizure, and Cr-Mo nitrided steel was found unsuitable for the cam and roller.

### 4. Materials used in the Investigation

The following seven kinds of non-Ni steels were selected and used in this investigation:

*ENCLOSURE (C)2, continued*

| Steel No. | Type of Steel | Substitute for | Make |
|---|---|---|---|
| 1 | 80 kg/mm$^2$ | 80 kg/mm$^2$ Ni-Cr steel | D* |
| 2 | Mn-Cr | 80 kg/mm$^2$ Ni-Cr steel | N** |
| 3 | Naniwa | 80 kg/mm$^2$ Ni-Cr steel | A# |
| 4 | 90 kg/mm$^2$ Cr-Mo | 90 kg/mm$^2$ Ni-Cr steel | D |
| 5 | Cr-Mo case-hardened | 80 kg/mm$^2$ case-hardened steel | D |
| 6 | Cr-Mo nitriding | 80 kg/mm$^2$ case-hardened steel | D |
| 7 | 50 kg/mm$^2$ case-hardened | 80 kg/mm$^2$ case-hardened steel | K## |

*D-Daido Seiko Co. (Daido Steel Making Co.) NAGOYA.
**N-Nippon Tokushuko Co. (Nippon Special Steel Co.) Omori, TOKYO.
#A-Amagasaki Seiko Co. (Amagasaki Steel Making Co.) Amagasaki, HYOGO.
(NANIWA is trade name for this steel.)
##K-Kure Naval Arsenal.

These steels were selected from various kinds of non-Ni steel taking the following three points into consideration: first, tensile strength similar to original steels; second, existence of practical data from airplane and motor car production, etc.; third, composition containing elements which are home products and easy to use in making steel. Components of these steels and their mechanical properties compare with the original steels as shown in Table I(C)2 and II(C)2.

5. Experimental Procedure

The experiments were generally divided into three parts; viz. fundamental test (tests conducted with test pieces), test of full size engine parts, and test of practical use (running test).

a. Fundamental tests included the following:

(1) Heat treatment test.
(2) Chemical analysis.
(3) Fatigue test of alternate bending load.
(4) Notch sensibility test.
(5) Microscopic test.
(6) Wear test.
(7) Mechanical properties test.

Table I(C)2
STANDARD COMPOSITION OF STEELS STUDIED

| Steel No. | Type of Steel | Composition (%) | | | | | | | |
|---|---|---|---|---|---|---|---|---|---|
| | | C | Si | Mn | P | S | Cr | Ni | Mo |
| 1 | 80 kg/mm$^2$ Cr | 0.40-0.50 | <0.35 | <0.60 | <0.03 | <0.03 | 1.5-2.0 | —— | —— |
| 2 | Mn-Cr | (0.35) | (0.31) | (0.83) | (0.021) | (0.014) | (1.04) | —— | —— |
| 3 | NANIWA | (0.23) | (0.30) | (1.23) | (0.017) | (0.017) | (1.68) | W, V, 0.14 | Mo, Ti |
| - | 80 kg/mm$^2$ Ni-Cr (Original) | 0.25-0.40 | <0.35 | 0.35-0.65 | <0.035 | <0.035 | 0.3-0.9 | 2.5-3.5 | —— |
| 4 | 90 kg/mm$^2$ Cr-Mo | 0.27-0.37 | <0.35 | <0.65 | <0.03 | <0.03 | 1.0-1.5 | —— | 0.3-0.6 |
| - | 90 kg/mm$^2$ Ni-Cr (Original) | 0.25-0.40 | <0.35 | 0.35-0.65 | <0.035 | <0.035 | 0.5-1.0 | 3.0-4.0 | —— |
| 5 | Cr-Mo case-hardened | 0.17-0.23 | <0.35 | 0.7-1.0 | <0.03 | <0.03 | 1.0-1.5 | —— | 0.2-0.4 |
| 6 | Cr-Mo Nitrided | 0.24-0.34 | <0.40 | 0.6-1.0 | <0.03 | <0.03 | 2.3-2.7 | 0.15-0.35 | 0.2-0.4 |
| 7 | 50 kg/mm$^2$ case-hardened | <0.18 | <0.35 | 0.6 | <0.03 | <0.03 | —— | —— | —— |
| - | 80 kg/mm$^2$ case-hardened (Original) | <0.18 | <0.35 | 0.60 | <0.03 | <0.03 | <0.3 | 2.0-3.0 | —— |

*ENCLOSURE (C)2, continued*

Table II(C)2
REQUIRED MECHANICAL PROPERTIES OF STEELS

| Steel No. | Type of Steel | Y.P. ($kg/mm^2$) | T.S. ($kg/mm^2$) | Elon. (%) | R.A. (%) | Izod (kg-m) | BHN |
|---|---|---|---|---|---|---|---|
| 1 | 80 $kg/mm^2$ Cr | >65 | >80 | >15 | >40 | Charpy >710 | 241-293 |
| 2 | Mn-Cr | -- | -- | -- | -- | -- | -- |
| 3 | NANIWA | -- | -- | -- | -- | -- | -- |
| - | 80 $kg/mm^2$ Ni-Cr (Original) | >65 | >80 | 18 | >45 | >7.5 | >230 |
| 4 | 90 $kg/mm^2$ Cr-Mo | >75 | >90 | >15 | >50 | >Charpy 9.0 | 262-321 |
| - | 90 $kg/mm^2$ Ni-Cr (Original) | >75 | >90 | >15 | >40 | >6.0 | >260 |
| 5 | Cr-Mo case-hardened | >90 | >110 | >10 | >35 | Charpy 6.0 | -- |
| 6 | Cr-Mo Nitrided | >80 | >100 | >17 | >40 | >Charpy 7.0 | -- |
| 7 | 50 $kg/mm^2$ case-hardened | >30 | >50 | >20 | >50 | 7.5 | -- |
| - | 80 $kg/mm^2$ case-hardened (Original) | >55 | >80 | 17 | >45 | >6.0 | -- |

b. Tests of full size parts included the following:

(1) Investigation of forgeability.
(2) Investigation of difficulty of heat treatment.
(3) Investigation of machinability.
(4) Investigation of mechanical properties and mass effect of full size engine parts.

c. Test of practical use (running test) included:

(1) Test with No. 22 type diesel engine (medium size, single-acting, 4-cycle).
(2) Test with No. 2 type diesel engine (large, double-acting, 2-cycle).
(3) Test with so-called "YV" type diesel engine (small, single-acting, 2-cycle, high-speed).

In these tests, fundamental and full size parts tests were completed, but the tests of practical use were not entirely finished.

*ENCLOSURE (C)2, continued*

6. Results of Each Experiment

Results of this whole investigation are described in Paragraph 3. Here we will take up the result of the individual tests.

a. Fundamental test (test conducted with test pieces) was as follows:

(1) Heat treatment test: This test is to obtain a suitable heat treatment temperature for each steel by observing austenite transformation points and measuring tensile strength.

Steel No. 1 (80 kg/mm$^2$Cr): Suitable heat treatment temperature; quenching at 870°C, tempering at 600-650°C.

Steel No. 2 (Mn-Cr): Suitable heat treatment temperature; quenching at 870°C, tempering at 630-650°C.

Steel No. 3 (NANIWA): Suitable heat treatment temperature could not be reached because this steel is very sensitive to heat and stable mechanical properties could not be obtained. This steel was, therefore, omitted from other tests.

Steel No. 4 (90 kg/mm$^2$ Cr-Mo): Suitable heat treatment temperature; quenching at 850°C, tempering at about 600°C. It shows rather small values of tensile strength.

Steel No. 5 (Cr-Mo case-hardened): This steel has a very low value in impact load test, and after repeated experiments, an almost suitable heat treatment temperature could be obtained - first quenching at 850°C, second quenching at 800°C, tempering at 150°C for 15 hours. Case-hardening is rather easy as compared with original Ni-Cr case-hardened steel. After carburization and heat treatment, the hardness of the case comes up to about 84 Shore

Steel No. 6 (Cr-Mo, Nitrided): Suitable heat treatment temperature - quenching at 850°C, tempering at 650°C. Suitable nitriding temperature was 520-530°C for 50-60 hours with dissociation degree of ammonia gas, 30-32%. With this condition, the maximum hardness reaches 800 Vickers.

Steel No. 7 (50 kg/mm$^2$, case-hardened): Test of this steel was omitted because its properties are well known and there is no difficulty in heat treatment.

(2) Chemical analysis: Results of chemical analysis of each steel are shown in Table III(C)2.

(3) Fatigue test by alternate bending load: Steels No. 1, 2, 4, and Original 80 kg/mm$^2$ Ni-Cr steel were tested with the so-called ONO Fatigue Testing Machine for alternate bending by rotation. The results follow:

| Steel | Fatigue Limit |
|---|---|
| No. 1, 80 kg/mm$^2$ Cr | 40 kg/mm$^2$ |
| No. 2, Mn-Cr | 42 kg/mm$^2$ |
| No. 4, 90 kg/mm$^2$ Cr-Mo | 46 kg/mm$^2$ |
| Original 80 kg/mm$^2$ Ni-Cr | 43 kg/mm$^2$ |

Table III(C)2
CHEMICAL COMPOSITIONS OF STEELS TESTED
(Test Results)

| Steel No. | Type of Steel | Composition (%) | | | | | | | |
|---|---|---|---|---|---|---|---|---|---|
| | | C | Si | Mn | P | S | Cr | Ni | Mo |
| 1 | 80 kg/mm$^2$ Cr | 0.47 | 0.39 | 0.54 | 0.018 | 0.03 | 1.59 | -- | -- |
| 2 | Mn-Cr | 0.37 | 0.37 | 0.88 | 0.023 | 0.023 | 1.40 | -- | 0.31 |
| 3 | NANIWA | 0.27 | 0.10 | 1.38 | 0.023 | 0.026 | 1.52 | V=0.08 | W=0.07 |
| 4 | 90 kg/mm$^2$ Cr-Mo | 0.33 | 0.28 | 0.56 | 0.019 | 0.033 | 1.33 | -- | 0.46 |
| 5 | Cr-Mo, case-hardened | 0.15 | 0.25 | 0.88 | 0.013 | 0.028 | 1.28 | -- | 0.25 |
| 6 | Cr-Mo, nitrided | 0.24 | 0.39 | 0.74 | 0.017 | 0.036 | 2.56 | V=0.35 | 0.35 |
| 7 | 50 kg/mm$^2$, case-hardened | 0.13 | 0.24 | 0.54 | 0.021 | 0.017 | -- | -- | -- |

*ENCLOSURE (C)2, continued*

(4) Notch sensitivity test: Steels No. 2, 4, and Original 80 kg/mm$^2$ Ni-Cr were tested. This test was carried out by measuring fatigue limits of tension and compression with Haigh's Testing Machine.

NOTCH SENSITIVITY

| Steel | Specimen | | |
|---|---|---|---|
| | Unnotched (kg/mm2) | Notched (kg/mm2) | Notch Sensitivity |
| Steel No. 2, Mn-Cr | 46 | 23 | 2.00 |
| Steel No. 4, 90 kg/mm$^2$ Cr-Mo | 52 | 24 | 2.17 |
| Original 80 kg/mm$^2$ Ni-Cr | 52 | 22 | 2.36 |

(5) Microscopic test: Every steel was examined under a microscope to ascertain grain size and slag inclusions. Almost all steels were satisfactory but Steel No. 4 had too much slag.

(6) Wear test: Steels No. 1, 2, 5, 6, 7, Original Ni-Cr steel and Original Ni-Cr case-hardened steel were tested by a wear testing machine specially made. No substitute steel was inferior to the original steel. Steel No. 7 (50 kg/mm$^2$ case-hardened) showed especially good wear resisting properties, and so it would be an adequate substitute steel for parts in which too much strength is not needed.

(7) Mechanical property test: Every steel was tested under the condition of adequate heat treatment. The results are shown in Table IV(C)2.

b. Test of full size engine parts:

(1) Investigation of forgeability: (Steel No. 3 was omitted from the tests).

Forgeability of no substitute steel was inferior to the original Ni-Cr steels.

(2) Investigation of difficulty of heat treatment: Heat treatment of every steel was satisfactory.

(3) Investigation of machinability: Machinability of Steels No. 2, 4, 6, and 7 was equal to that of original steels. To secure a smooth finish on Steel No. 1 (80 kg/mm$^2$ Cr) a fine turning method utilizing a spring tool was recommended. In grinding Steel No. 5 (Cr-Mo, case-hardened), we must be careful of fractures in grinding cracks.

(4) Investigation of mechanical properties and mass effect of full size engine parts: Shock resisting property of Steel No. 1 was rather small and its mass effect was tolerably remarkable.

Mass effect of Steel No. 2 was better than that of Steel No. 1, but inferior to Original 80 kg/mm$^2$ Ni-Cr steel.

Mass effect of Steel No. 4 was better than that of Steel No. 1, but inferior to Steel No. 2.

*ENCLOSURE (C)2, continued*

In the case of testing full size parts, Steel No. 5 showed too low a value in the shock resisting test, but if we revise its standard required, it will be possible to put it to practical use.

c. Test of practical use (running test).

The results of this test are already described in Paragraph 3, as results of practical experiments. A number of tests were planned, but only few of them were finished.

7. References

This investigation was carried out on the basis of practically used data in airplane and automobile construction, and J.E.S. (Japanese Engineering Standard), S.A.E. and D.I.N. data.

Table IV(C)2
MECHANICAL PROPERTIES OF STEELS STUDIED
(Test Results)

| Steel No. | Type of Steel | Y.P. ($kg/mm^2$) | T.S. ($kg/mm^2$) | Elong. (%) | R.A. (%) | Izod (kg-m) | BHN |
|---|---|---|---|---|---|---|---|
| 1 | 80 $kg/mm^2$ Cr | 67.6 | 85.6 | 24.0 | 67.8 | 10.8 | 257 |
| 2 | Mn-Cr | 72.0 | 89.0 | 22.0 | 66.2 | 9.3 | 250 |
| 3 | NANIWA | 78.9 | 87.0 | 20.0 | 56.8 | 5.7 | not measured |
| 4 | 90 $kg/mm^2$ Cr-Mo | 77.0 | 91.4 | 23.0 | 67.3 | 10.9 | 293 |
| 5 | Cr-Mo, case-hardened | 71.3 | 93.0 | 20.0 | 51.5 | 2.7 | 304 |
| 6 | Cr-Mo, nitrided | 76.6 | 87.4 | 25.5 | 72.5 | 12.6 | 267 |
| 7 | 50 $kg/mm^2$ case-hardened | 38.2 | 58.2 | 33.0 | 75.0 | 15.9 | 189 |